2015

Synthesis and fate of oligonucleotides containing the oxidative damage product 3'-oxothymidine

Fernand Mel Bedi

A Dissertation

entitled

Synthesis and Fate of Oligonucleotides Containing the Oxidative Damage Product 3′-Oxothymidine

by

Fernand Mel Bedi

Submitted to the Graduate Faculty as partial fulfillment of the requirements for the

Doctor of Philosophy Degree in

Medicinal Chemistry

_____

Amanda Bryant-Friedrich, PhD., Committee Chair

_____

Viranga Tillekeratne, PhD., Committee Member

_____

Paul Erhardt, PhD., Committee Member

_____

Ming-Cheh Liu, PhD., Committee Member

_____

Patricia R. Komuniecki, PhD, Dean
College of Graduate Studies

The University of Toledo

May 2015

An Abstract of

Synthesis and Fate of Oligonucleotides Containing the Oxidative Damage Product 3′-Oxothymidine

By

Fernand Mel Bedi

Submitted to the Graduate Faculty as partial fulfillment of the requirements for the Doctor of Philosophy Degree in
Medicinal Chemistry

The University of Toledo
May 2015

Oxidative events that take place during normal oxygen metabolism can lead to the formation of organic or inorganic radicals. Unchecked, the interaction of these radicals with macromolecules in the organism and with DNA in particular can to lead to DNA lesions, cell damage and apoptosis. Independent generation of DNA lesions resulting from oxidative damage can be used to promote the study of their effects on biological systems.

Here we report the synthesis and characterization of a DNA damage product emanating from hydrogen abstraction at the 3′-carbon of thymidine. A phosphoramidite building block was chemically synthesized and incorporated into a DNA single strand using "reverse" oligonucleotide synthesis. The DNA lesion was then successfully generated by oxidative cleavage using sodium periodate.

Our studies indicate that although the lesion is observed it quickly degrades. Alternative conditions for oligomer isolation are warranted for full characterization of the lesion. Such studies will allow us to determine the effect that this damage product has on biological systems.

I dedicate this dissertation to my wife Eiffey Anne-Andree and my daughter Aliza Marie-Christiane.

Acknowledgements

This work would not have been possible without the support of Drs. Amanda Bryant-Friedrich and Klaus Friedrich. Thanks for believing in me.

Sincere gratitude to Dr. Wayne Hoss, Dr. Christine Hinko, and Dean Early of the College of Pharmacy and Pharmaceutical Sciences for their continuous support. Thanks for creating a culture in which students are allowed to be the architect of their own success.

To my committee members, Dr. Paul Erhardt, Dr. Ming-Cheh Liu and Dr. Tillekeratne Viranga, I am grateful for the time and intellectual investment you have made in my professional development.

To Dr. Suaad Audat Abdallah and Dr. Buthina Abdallah, I am forever indebted to you for the incredible scientific contributions you have made to my life. Thanks for making my beginning steps in the lab easy, thanks for training me, helping me be a better scientist.

To Dr. Raziyah Shaik, smart yet humble, quiet yet strong, it was a delight working with you.

To my Father Dr. Samuel Mel Bedi my inspiration, thanks for never allowing me to settle for less. To my mother Meliane Bedi, thanks for being my unwavering support.

Table of Contents

List of Tables

List of Figures

List of Schemes

List of Abbreviations

A	Adenine
C	Cytosine
^{13}C NMR	Carbon-13 Nuclear Magnetic Resonance Spectroscopy
CPG	Controlled Pore Glass
dA	Deoxyadenosine
dC	Deoxycytidine
dG	Deoxyguanosine
DNA	Deoxyribonucleic Acid
DSB	Double Strand Breaks
dsDNA	Double Strand Deoxyribonucleic Acid
ESI-MS	Electrospray Ionization Mass Spectrometry
G	Guanine
HPLC	High Performance Liquid Chromatography
^{1}H NMR	Proton Nuclear Magnetic Resonance Spectroscopy
IR	Ionizing Radiation
MALDI-TOF MS	Matrix-Assisted Laser Desorption Ionization Time-of-Flight Mass Spectrometry
NMR	Nuclear Magnetic Resonance Spectroscopy
nm	Nanometer
ODN	Oligodeoxynucleotide

ROS	Reactive Oxygen Species
SSB	Single Strand Breaks
ssDNA	Single Strand Deoxyribonucleic Acid
T	Thymine
TBAF	TetraButylammonium Fluoride
TBDMSCl	*tert*-Butyldimethylsilyl Chloride
TEAA	Triethylammonium Acetate Buffer
THF	Tetrahydrofuran
UV	Ultraviolet

List of Symbols and Formulas

Ar	Argon
CH_2Cl_2	Dichloromethane
CH_3CN	Acetonitrile
CH_3CO_2H	Acetic acid
DCM	Dichloromethane
DMF	*N,N′*-Dimethylformamide
DMTrCl	Dimethoxytrityl chloride
E	Energy
Et_3N	Triethylamine
eV	Electron volts
GSH	Glutathione reduced
H	Hydrogen atom
H^+	Proton
H_3O^+	Hydronium ion
H_2O	Water molecule
KeV	Kiloelectro volts
M	Molar
MeOH	Methanol
MeV	Mega electron volts
mL	Mililiter
NH4OH	Ammonium hydroxide
O_2	Oxygen
TBDMSCl	*Tert*-butyldimethyl silyl chloride
TFA	Trifluoroacetic acid

µL	Microliter

Chapter 1

1 Introduction

Nucleic acids, proteins, carbohydrates and lipids, are important macromolecules present in living organisms. Proteins are involved in regulating most cellular processes; carbohydrates and lipids serve as a means of energy storage. Additionally, lipids play a role in ensuring membrane integrity and cell signaling. Nucleic acids contain the genetic information of living organisms. They ensure the transfer of information from one generation to another. Of all the macromolecules, nucleic acids are considered to be the most important because of the role they play in preserving hereditary information and

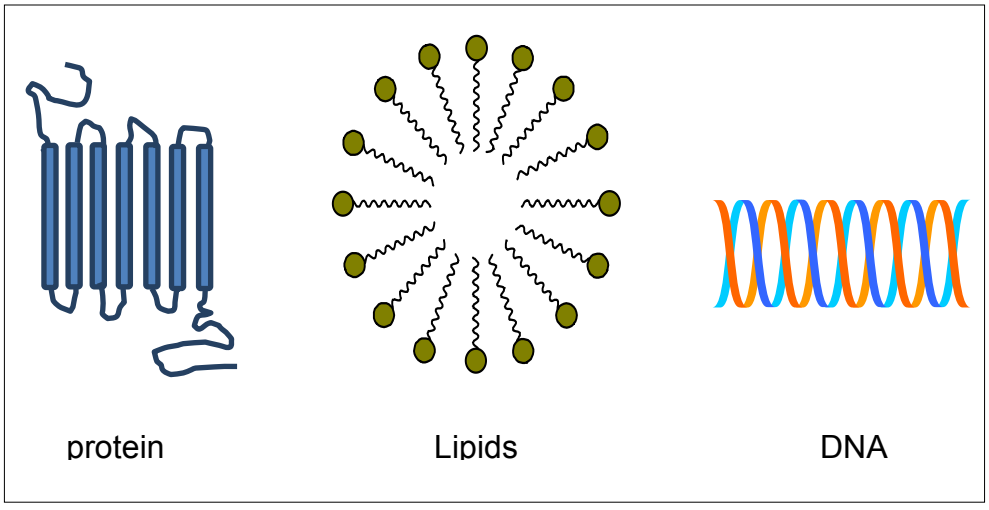

Figure 1: Generic representations of important macromolecules

maintaining cell function. Nucleic acid chemistry is a fascinating field with wide ranging applications.

1.1 DNA Structure

1.1.1 The basic unit: The deoxyribonucleotide.

The two major types of naturally occurring nucleic acids are DNA, (deoxyribonucleic acid) and RNA (ribonucleic acid). At the core, nucleic acids are composed of units called nucleotides each made up of three fundamental parts: a phosphate, a sugar and a nitrogenous base (Figure 2). In the case of DNA, the sugar portion is 2-deoxyribose whereas in RNA it is ribose. There are four nitrogenous bases in DNA: adenine (A), and guanine (G) are the two purine bases while cytosine (C) and thymidine (T) are the

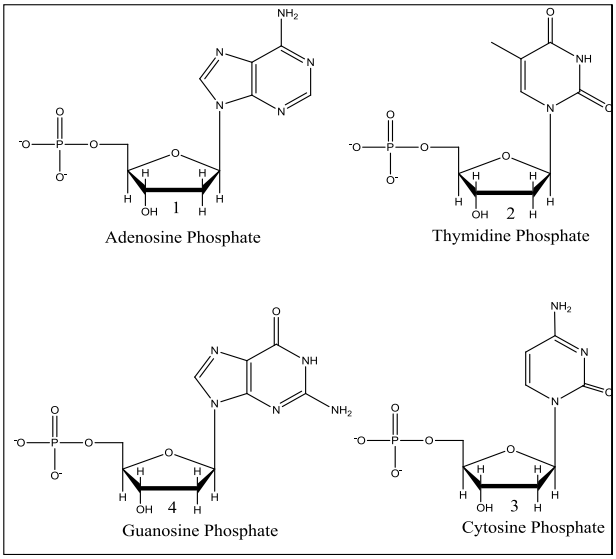

Figure 2: The Building blocks of DNA

pyrimidines. In RNA, the thymine is replaced by a uracil.[1]

1.1.2 Deoxyribonucleic acid structure

A single strand of DNA is a polymer containing the four nucleotides, each covalently bonded to the next by a phosphodiester bond. DNA primary structure is such that the backbone is formed from alternating sugars and phosphates. Although DNA can exist as a single strand, it is mainly found in nature double stranded resulting from hydrogen

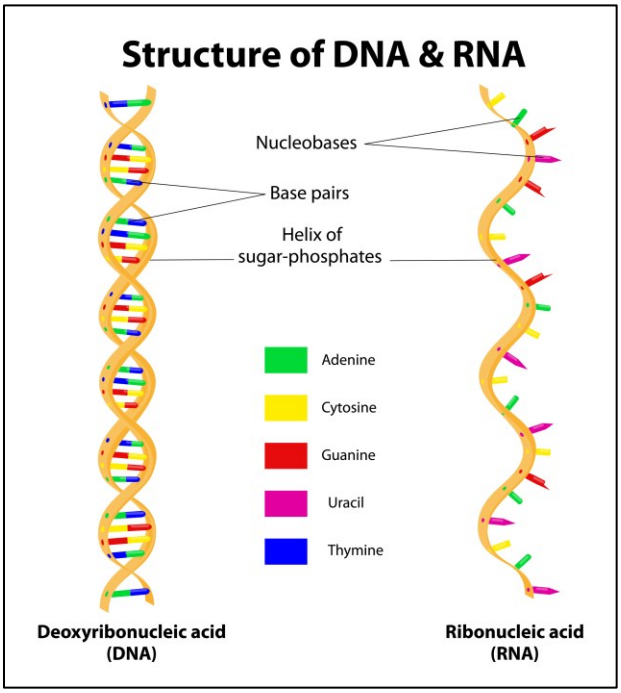

Figure 3: Structure of DNA and RNA

bonding interactions between the purine bases and their pyrimidine counterparts. Adenine preferably pairs with thymine, whereas cytosine naturally pairs with guanine conferring the observed secondary structure (**Figure 3**).

The two complementary strands of DNA are antiparallel to each other and contain the same genetic information. There are three major forms of double helical DNA. The A form of DNA is found in conditions of high osmolarity, the Z-form is a left handed helix and forms in strands containing alternating purine and pyrimidine bases. The B form is the most common. It is a right handed helix and makes a complete turn every 10 bases. It has a major groove and a minor groove where interactions with proteins and smaller diffusible species can interact with DNA.[2]

1.1.3 Function of DNA

The central dogma of biology states that DNA is transcribed to RNA, which in turn, is translated to proteins. In eukaryotic cells, DNA is encapsulated inside the cell nucleus along with other components such as DNA and RNA polymerases. DNA polymerases are responsible for the replication of DNA at the time of cell division. This process ensures the integrity of the DNA from one generation of cells to another.

The information required for the synthesis of all proteins in an organism is contained in the specific order of the nucleotides of the DNA strand. The DNA strand is transcribed into messenger RNA (mRNA) by RNA polymerase. The ribosomes in turn translate the information carried by the mRNA into proteins following the genetic code, the system by which a set of three nucleotides corresponds to a specific amino acid.

DNA is a crucial macromolecule. Damage to any of its components if not repaired impact the cells in a disastrous way.[3]

1.2 Selected applications of nucleic acid chemistry

An in depth discussion of all the applications of nucleic acid chemistry is beyond the scope of this work. Here the use of synthetic nucleoside and nucleotides currently as therapeutic agents is briefly highlighted. An introduction of independent synthesis of oligodeoxynucleotide (ODN) lesions for the study of DNA damage and repair is also included.

1.2.1 Nucleic acids as therapeutic agents

1.2.1.1 Antiviral agents

One of the most well-known applications of nucleic acid chemistry is the synthesis of modified nucleosides, nucleotides and oligonucleotides to be used as therapeutic agents. In recent history, the successful use of modified nucleotides as anti-retroviral agents has made them more relevant even to people outside the scientific community. Many lives have been impacted by the use of life saving drugs such as Azidothymidine (AZT) in the initial phases of the fight against HIV. Other antiretrovirals are currently in use to treat life threatening diseases.[4,5]

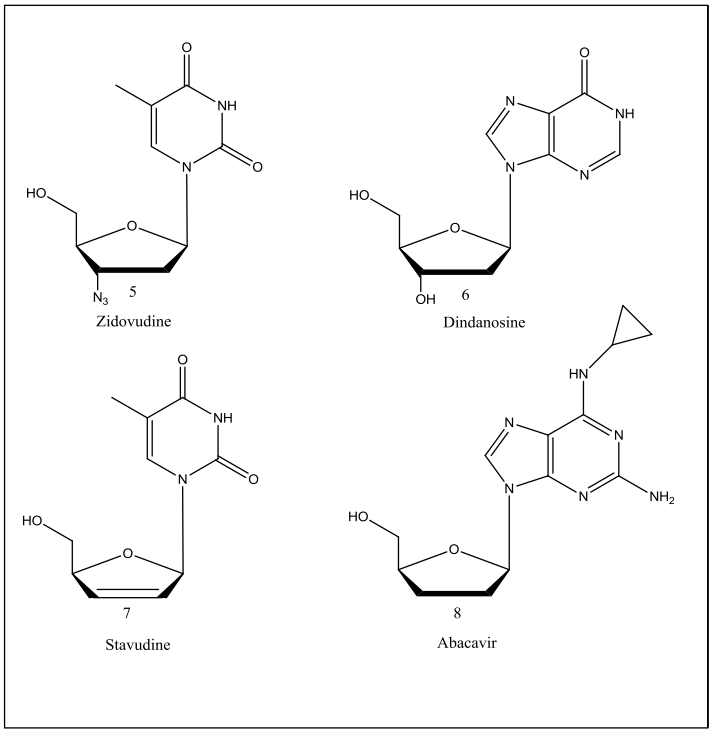

Figure 4: Synthetic nucleotides used as therapeutic agents

1.2.1.2 Immunomodulatory agent

Synthetic oligonucleotides have also been studied in their role as immunomodulatory agents. CpG oligonucleotides in particular have been intensely studied due to their stimulatory effect on the immune system. They contain a cytidine triphosphate linked to a guanosine triphosphate by a phosphodiester bond. Since the discovery of their immunostimulatory role in 1994, CPG oligonucleotides have been studied as vaccine adjuvants, antiallergenic agents and possible candidates for autoimmune disease treatments.[6,7]

1.2.2 Study of DNA damage and repair processes

Along with their application as therapeutic agents, another application of nucleic acid research has been the study of nucleotides and oligonucleotides in elucidating processes involved in DNA damage and repair. It is estimated that endogenous oxidative damage to DNA affects upward of 10,000 cells per day in the human body. Although the body is equipped with repair mechanisms to efficiently cope with such a high amount of damage, some damage lesions are not repaired.[8] One method to investigate the fate of such lesions is to independently synthesize the lesion of interest for *in vitro* studies. Such studies provide crucial information about the stability of the lesion, its effect on DNA double strand structure and stability and its reactivity with endogenous macromolecules.[9] Our group is interested in the synthesis of oligonucleotides to facilitate the study of the mechanisms involved in DNA damage and the subsequent effect on the organism.

1.3 Overview of DNA damage

Since the genetic code is contained within the sequence of the DNA nucleobases, any alteration to the integrity of DNA can have repercussions on protein synthesis and the overall functioning of the organism. As a chemical entity, DNA structure can be affected by interactions with other chemicals in the cellular environment. These interactions along with the alteration of the physical properties inside the cell can lead to DNA damage. DNA damage has been established as a key step in the process of aging, and

carcinogenesis. Causes for DNA damage can be of either exogenous or endogenous origin.

1.3.1 Exogenous causes of DNA damage

DNA damage can be caused by exogenous factors. Although these factors are numerous this section will discuss major contributors such as chemotherapeutic agents, foods that we consume in our diet and ionizing radiation.

1.3.1.1 Toxic gases

Toxic chemicals that are inhaled such as industrial gases, nitrogen mustards and cigarette smoke are all causes of DNA damage. Nitrogen mustards are known to alkylate DNA causing intrastrand cross linking. Although they can be used as chemical warfare agents, their properties have proven useful as chemotherapeutic agents.[10] Cigarette smoke contains a mixture of compounds including potential carcinogens.[11]

1.3.1.2 Chemotherapeutic agents

Many therapeutic agents also cause DNA damage. They are used in cancer chemotherapy to selectively target tumor cells. They include alkylators such as carmustine and lomustine, platinum containing crosslinkers such as cis-platin and carboplatin, antimetabolites such as methothrexate and finally topoisomerase II inhibitors including daunorubucin and doxorubucin.[12]

1.3.1.3 Diet

There are many types of foods that have been linked to DNA damage. For instance, methyl donors such as methionine, choline, vitamins B6 and B 12 are important in the process of DNA methylation. Both hypermethylation and hypomethylation have been cited as causes for human malignancies.[13] Iron rich foods have also been implicated in facilitating DNA damage through the possible production of reactive oxygen species in Fenton type reactions.[14] A lack of antioxidants in the diet has also been associated with a higher rate of DNA damage.

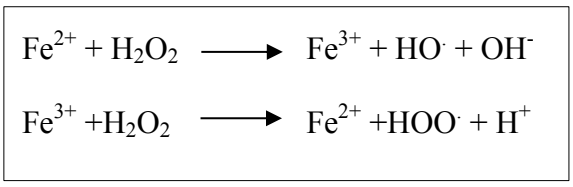

Scheme 1: Fenton type reactions

1.3.1.4 Ionizing radiation

Radiation is the emission of energy in the form of waves or particles. When radiation has enough energy (10eV) to dislodge an electron from its orbit within an atom and generate an ion, it is called ionizing radiation (IR). This type of radiation is also capable of breaking chemical bonds within a molecule. Living cells exposed to IR risk having their cellular content, including DNA, damaged. Depending on the type and the amount of IR exposure, DNA damage by IR can cause cancer. Sources of radiation exposure are multiple. They include cosmic rays that originate from outer space, radiation from natural decay of radioactive material present in the soil and the rocks on earth, and man-made

sources used in medical imaging, science and industry. We are exposed to radiation through the intake of radioactive compounds in the air we breathe, the food we consume and the water we drink.

Alpha particles (α) are positively charged radiation particles emitted during the α-decay of radioactive material. Chemically identical to a helium nucleus with two protons and two neutrons, they are usually relatively low in energy (5 MeV), slow moving and do not penetrate past the skin. They can cause local tissue damage when they are inhaled or ingested in high amounts.

Beta particles (β) are radiation particles emitted during β-decay of radioactive nuclei such as potassium 40. They can be either positively or negatively charged. They travel faster and are more penetrating than α–particles albeit without the same damaging ability.

Photon radiation is a term used to define both gamma radiation (γ) and X-rays: γ–radiation has its origin in the nucleus and X-ray is produced from outside the nucleus such as the electrons. Although the distinction is not always accurate, the term γ-radiation is reserved for photon radiation with an energy higher than 100-120 KeV while X-Rays have an energy range of 100 eV-120 KeV. X-rays are the most common man made source of IR used in medical diagnosis and imaging.

UV light, have been implicated in damaging DNA. UV radiation is made up of UVA, UVB and UVC. The depletion of the ozone layer has caused an increase in the amount of UVA and UVB that reaches the earth. Although the most dangerous type, UVC is

blocked by the ozone layer. Long exposure to UV light from the sun or from tanning beds can damage DNA and is linked to an increase in rates of skin cancer.

Of all the above mentioned forms of ionizing radiation, γ-radiation and UV light are the most likely to cause significant DNA damage through a variety of different mechanisms, resulting in single and double strand breaks, as well as base damage.

1.3.2 Endogenous causes of DNA damage

As significant as exogenous causes, endogenous factors play a role in altering DNA. Under physiological conditions, many reactions can result in breaks in the DNA strand, the generation of abasic sites, halt of cell replication and mutations. The endogenous causes of DNA damage include hydrolysis, lipid peroxidation, alkylating agents, and oxidative damage.

1.3.2.1 Damage caused by hydrolysis

Hydrolysis of DNA is the breaking of chemical bonds within the structure of DNA by the addition of water. Hydrolysis of DNA can affect the phosphodiester bond, cause deamination of the bases as well as cleave the glycosidic bond between the ribose of DNA and the bases. Although hydrolysis of the phosphodiester bond is theoretically possible and thermodynamically favored, the reaction rarely occurs in physiological conditions and most likely requires the presence of a catalyst.[15]

Hydrolytic deamination of the base is usually catalyzed by deaminases and generates uracil from cytosine, xanthine from guanine, hypoxanthine from adenine, and thymine from methylcystosine.[16,17,18,19] The base excision repair (BER) process is used to remove and replace the damaged base. When the damage is not repaired, deamination leads to point mutations in the daughter cells.

The N-glycosidic bond is the most likely to undergo hydrolytic cleavage and is reported to cause 10,000 abasic sites per cell per day.[20] The reaction occurs significantly faster with purines ($t_{1/2}$ =730 y) than with the pyrimidines ($t_{1/2}$ = 14,700 y).[21] These abasic sites are known to cause cell toxicity as they are involved in intrastrand cross links, and facilitate strand breaks through base catalyzed elimination of the phosphate. [22,23]

1.3.2.2 Alkylation

Several DNA adducts have been identified as a result of endogenous alkylation caused by small reactive molecules. Among the alkylating agents, S-adenosylmethionine (SAMe) has been studied as one of the most important. Betaine and choline have also been identified as alkylating agents. Adducts formed from alkylation have varying levels of occurrence *in vivo* and different fates as well. Some prevalent adducts include 7-methylguanine, 3-methyladenine, 3-methylthymidine and 3-methylcystosine. These lesions can stop DNA synthesis and replication. They are repaired mainly through the base excision repair pathway and give rise to an apurinic/apyrimidinic (AP) site.

O-alkylated products such as O^6-methylgunanine and O^4-methylthymine have also been detected in cells.[24] They are mutagenic, causing GC→AT and TA→CG transitions during DNA replication.[25,26] In order to repair the adducts, DNA methyl transferases remove the methyl group from the oxygen.

1.3.2.3 Oxidative damage

Oxidative damage to DNA is the most common type of DNA damage endogenously. It happens as a result of an imbalance between the generation of reactive oxygen species and the body′s ability to inactivate them.

1.3.2.3.1 Reactive oxygen species

Reactive oxygen species (ROS) are oxygen containing compounds that have a high propensity to engage in reactions with other chemical entities. ROS can be found as charged or neutral compounds. The list of ROS includes the superoxide (O^{2-}) anion, hydrogen peroxide (H_2O_2), hydroxyl radicals and ions ($OH^{\cdot}$, OH^-), nitrous oxide (NO), hypochlorite anion and the superoxide anion (O_2^-) among many others.

Table 1.1: List of Reactive Oxygen Species

List of Reactive oxygen species	
Hydroxyl radical	$OH^{\cdot}$
Hydroxyl ion	OH^-
Hydrogen peroxide	H_2O_2
Nitrous oxide	NO
Hypochlorite anion	OCl^-
Superoxide Anion	$O^{\cdot}{}_2^-$

1.3.2.3.2 Conditions resulting in the production of ROS

Reactive oxygen species are continuously generated as part of normal metabolic processes such as oxidative phosphorylation in mitochondrial respiration. However, their production is increased under certain conditions including chronic infection and/or inflammation.

In the process of oxidative phosphorylation, the mitochondria packages energy into adenosine triphosphate, the energy currency of the cell. The process involves the transport of electrons through the electron transport chain. Under normal conditions the electron is transferred to an oxygen molecule and subsequently reduced to a water molecule. In some instances the electron transport chain results in the production of a superoxide (O^{2-}) anion.

Activated neutrophils generate ROS as part of the inflammatory response. Superoxide and hydrogen peroxide are initially produced. A hydroxyl radical can then be generated through the Haber-Weiss reaction: $O_2^{-}\cdot + H_2O_2 \rightarrow O_2 + OH\cdot + OH^{-}$.[27]

Peroxynitrite (ONO^{2}-) is produced from the oxidation of the vascular relaxant nitric oxide (NO). ROS can be generated through leakage of peroxisomes as well.

1.3.2.3.3 Antioxidants and their role

A host of natural antioxidants are available to reduce and detoxify reactive oxygen species. The list of anti-oxidants includes glutathione, catalase and superoxide dismutase.

Glutathione is a tripeptide containing a sulfhydryl group. It is oxidized by ROS and regenerated by an NADPH-dependent reductase. The ratio of oxidized to reduced glutathione is a biomarker for oxidative stress. Catalase is an enzyme that catalyses the reduction of hydrogen peroxide to water and oxygen. Superoxide dismutase catalyses the reduction of superoxides into hydrogen peroxide and water. Other antioxidants are water soluble ascorbic acid (vitamin C) and lipophilic Vitamin E. Both are capable of undergoing redox reactions with ROS.

1.3.2.3.4 Oxidative stress

When the production of ROS overwhelms the antioxidant ability of the body, damage to cellular components such as lipids, protein and DNA results. Oxidative stress is more likely to occur in chronic disease states or in inflammation. The damage that occurs during oxidative stress has been linked to cancer and a host of diseases states.

1.3.2.3.5 Oxidative Damage to DNA

Oxidative damage to DNA can affect the nucleobase as well as the 2-deoxyribonucleoside. Damage to the nucleobase can result in DNA adducts and lesions whereas damage to the 2-deoxynucleobase can lead to single and double strand breaks. In addition, lesions resulting from damage can further react generating DNA cross lesions and DNA-protein adducts.

Chapter 2

2 Background

In healthy organisms, cells maintain a homeostatic balance between the amount of reactive oxygen species produced and their ability to reduce them through enzymes such as catalase and glutathione. There are some instances when the generation of ROS overwhelms the cells ability to reduce and detoxify them.[28] At that stage the cell is said to be under oxidative stress. At the cellular level, the proliferation of ROS during oxidative stress can cause damage to all the macromolecules including lipids, proteins and DNA. When ROS attack DNA, both the nucleobase and the sugar portion are subject to damage.[29] The impact of DNA damage on the bases of DNA has been abundantly reported in the literature. Ongoing research has highlighted oxidation at the deoxyribose and its implications as a major contributor to the toxicology of DNA damage leading to more investigations on the subject.

2.1 Damage to the DNA nucleobase

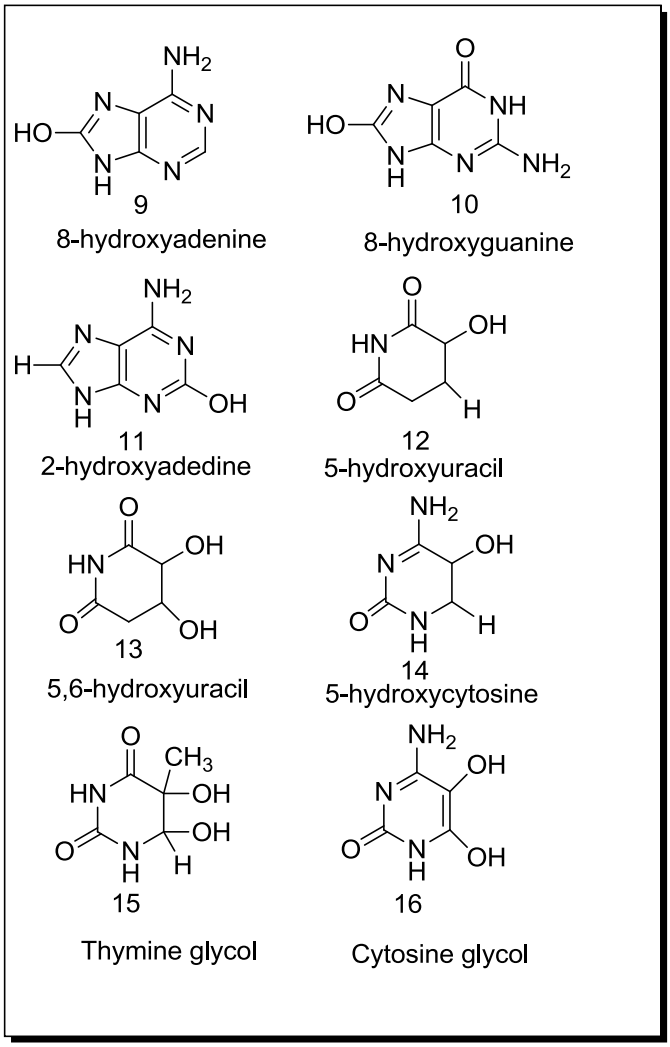

Figure 5: Oxidized bases of DNA

ROS react with DNA by addition to the double bonds of DNA bases to form oxidized DNA bases. There are numerous oxidized DNA adducts that have been identified with some more studied than others (Figure 5).

One of the well-studied adducts is 8-oxodeoxyguanosine. It appears to be the most abundant oxidative damage product.[30] 8-Oxoguanine base pairs preferably with adenine causing GC→TA transversion mutations. Other similar adducts are 8-oxoadenine, uracil glycol, cytosine glycol and thymine glycol.[31] Oxidation of methyl groups can also occur as in the case of 5-hydroxymethyuracil.[32] Most oxidized bases are repaired through the base excision repair pathway. When left unrepaired, as in the case of 8-oxoguanine, they lead to transversion mutations.

2.2 Impact of Oxidative damage on the 2-deoxyribose of DNA

ROS also interact with the 2-deoxiribose of DNA. When the 2-deoxyribose moiety of DNA reacts with a ROS, in most cases an initial hydrogen atom abstraction occurs, leading to the formation of a carbon centered radical. The carbon centered radical can either react with cellular oxygen to form a peroxyl radical or with a cellular reductant to reduce the radical. When the radical is not reduced, strand breaks and abasic sites can be generated through a variety of oxidized lesions specific to the position of the original hydrogen abstraction.[33] The sugar backbone of DNA contains seven hydrogens susceptible to abstraction by reactive oxygen species to various degrees (Figure 6).[34] Even though every hydrogen on the 2-deoxyribose is susceptible to attack by reactive oxygen species, it has previously been reported that the 4′ and 5′-hydrogen have the

highest likelihood of abstraction in B-form DNA because their location in the minor groove of DNA renders them more exposed to solvents and hence more accessible to reactive oxygen species.[35]

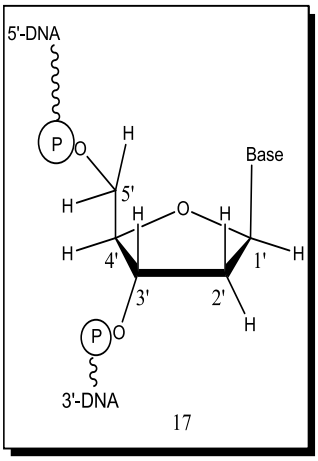

Figure 6: Seven hydrogens susceptible to abstraction by reactive oxygen species

There have been considerably more concerted efforts in synthesizing and characterizing DNA damage from the 4′ and the 5′-positions compared to studies on the DNA adducts generated from damage at the 3′ and 2′-positions. As mentioned above, a hydrogen abstraction is not only dependent on the bond energy; factors such as the accessibility of the hydrogen to the solvent and hence to oxidizing agents also play a major role. Tullius and coworkers determined using isotope labelling that the relative reactivity of hydroxyl radicals with the sugar hydrogen atoms to be: 5′ > 4′ > 3′ ≈2′ ≈ 1′. [34b]

2.2.1 Oxidation at the 5′-position

2.2.1.1 Conditions and causative agents

Oxidation at the 5′-position of the deoxyribose has been observed by Dedon and coworkers in reactions of DNA with enediyne antibiotics such as calicheamicyn and neocarzinostatin.[36] These compounds contain a 10-carbon ring with a double bond sandwiched by two triple bonds. The enediynes can undergo Bergman cyclization (Scheme 2) and generate a diradical species capable of abstracting a hydrogen atom from DNA.[37,38]

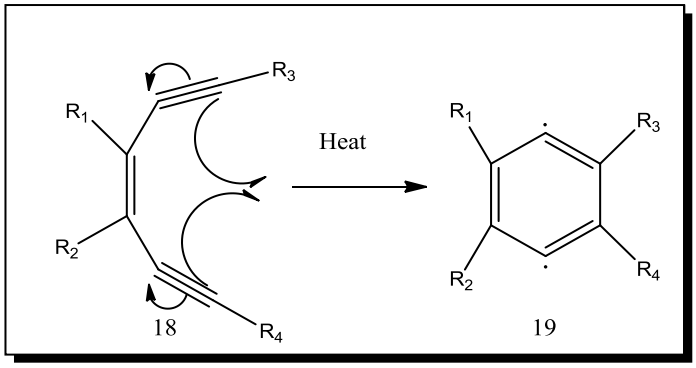

Scheme 2: Bergman Cyclization

Ionizing radiation and a host of radical species including the hydroxyl radical and the peroxyl radical have also been reported to cause oxidation at the 5′-position.

2.2.1.2 Identification and significance of lesions generated by 5′-oxidation

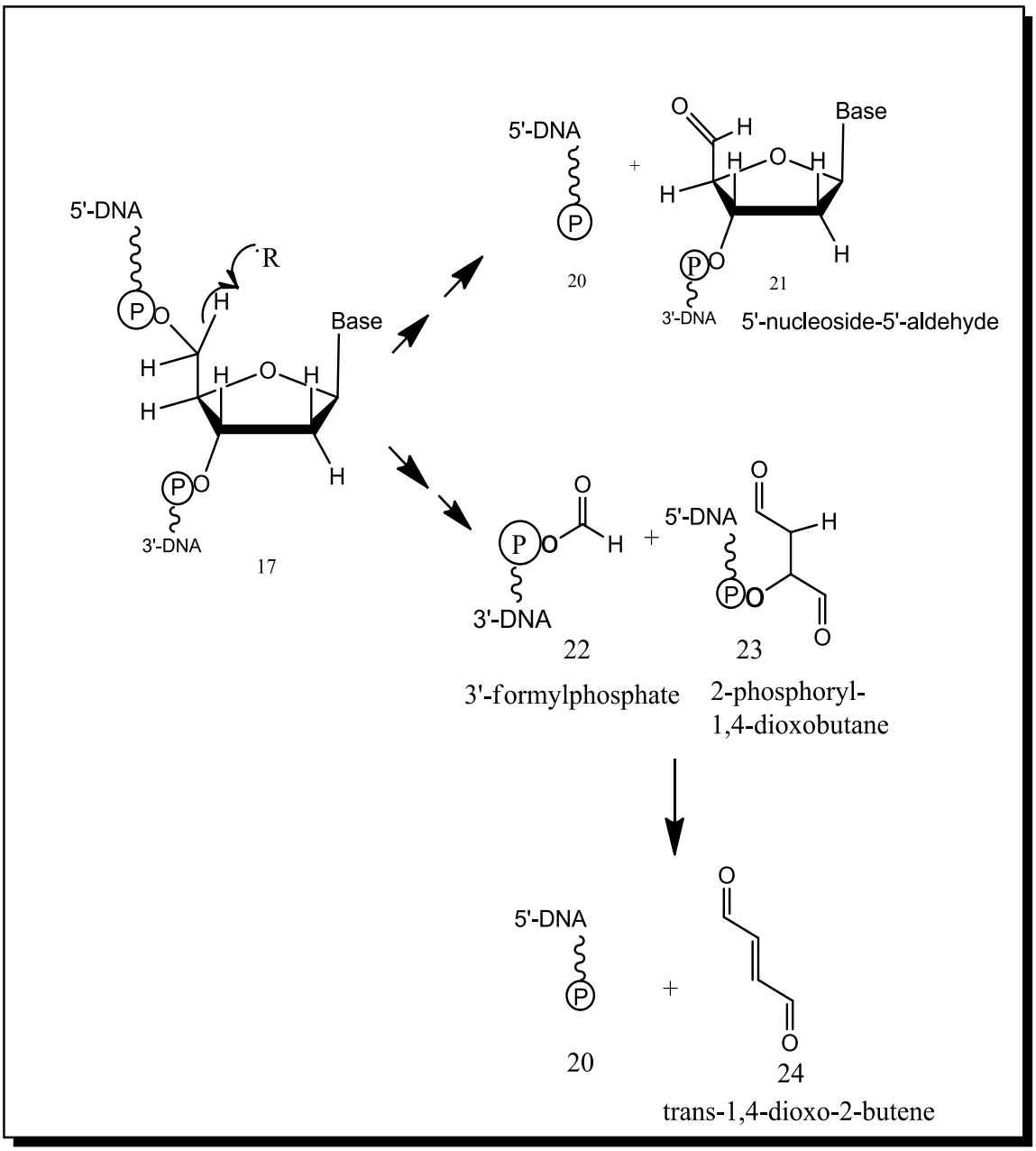

Figure 7: Products of hydrogen abstraction at the 5'-position of DNA

Hydrogen bond abstraction at the 5′-position is reported to generate two distinct sets of products along two different pathways.[39] One path leads to the generation of a strand break with a 3′-phosphate terminus and a 5′-nucleoside-5′-aldehyde terminus. The second pathway leads to the generation of trans-1,4-dioxo-2-butene, *via* the formation of a 3′-formylphosphate and 2-phosphoryl-1,4-dioxobutane. These lesions have been reported to react with DNA and proteins in cells to form various adducts due to their highly reactive nature (Figure 7).

2.2.1.3 Independent Synthesis

The independent synthesis of the damage products emanating from hydrogen abstraction at the 5′-position of DNA was completed by Greenberg and coworkers and the investigation of their chemical implication is underway.[40,41] A photolabile C-5′ tert-butyl ketone was also successfully synthesized as a precursor for the C-5′ radical.[42]

2.2.2 Oxidation at the 4′ position

2.2.2.1 Conditions and causative agents

The products of oxidation at the 4′ position have been thoroughly studied. The 4′-hydrogen has been shown to be selectively abstracted in the presence of the glycopeptide antibiotics bleomycin.[38] The bleomycin class of antibiotics is documented to bind selectively to DNA in the minor groove *via* both intercalating and non-intercalating

interactions to cause abstraction of the 4′-hydrogen. Ionizing radiation, calicheamicin and neocarzinostatin have also been reported to cause 4′-hydrogen abstraction.

2.2.2.2 Identification and significance of the lesions generated by 4′-oxidation

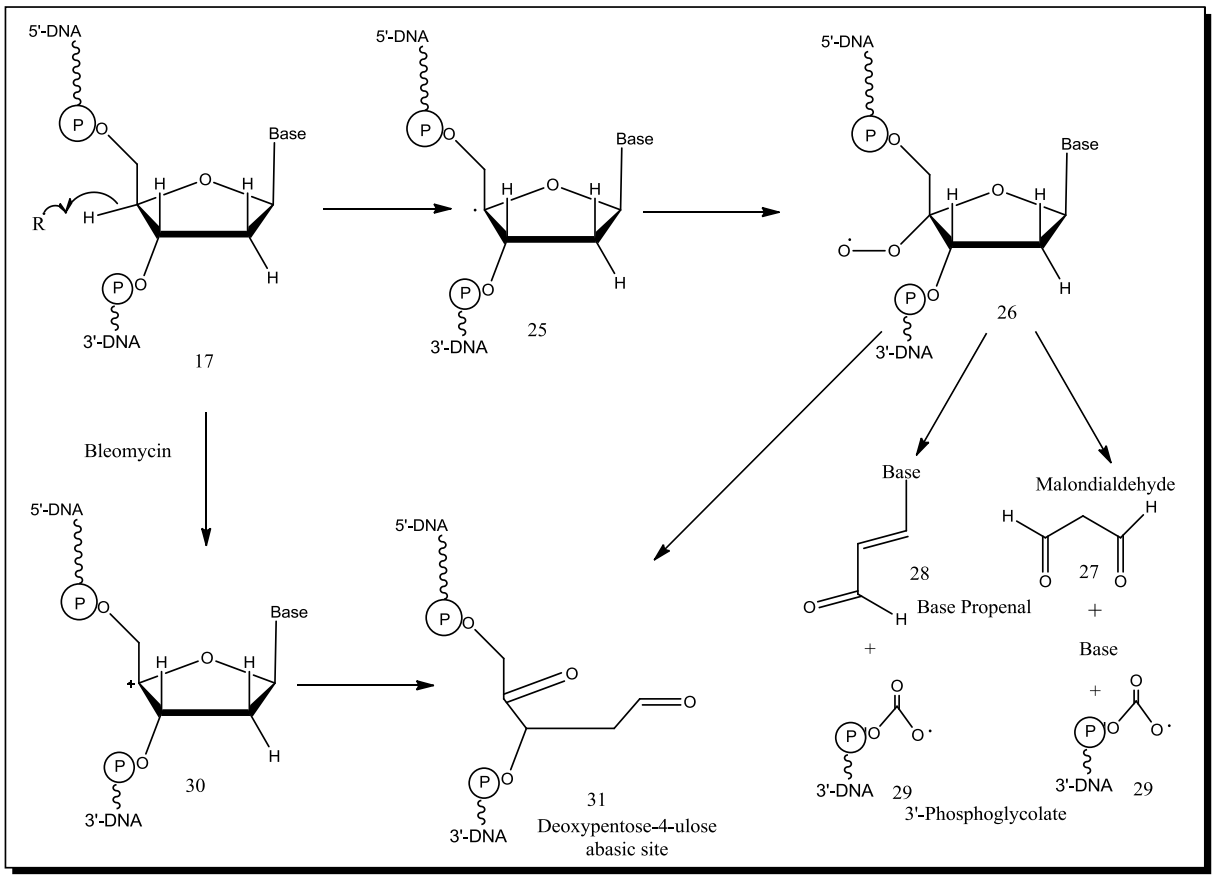

Figure 8: Products of 4'-hydrogen abstraction

The identity of the lesions emanating from damage at this position depends on both the causative agent and the reaction conditions such as pH and the presence or absence of oxygen. Following hydrogen abstraction, overall, two sets of products are generated along two possible pathways as was the case with the 5′-position. The first path leads to the generation of a 2-deoxypentose-4-ulose containing abasic site. The second path can lead to the formation of 3′-phosphoglycolate (3′-PG) plus either a base propenal or a malondialdehyde and a free base (Figure 7).[43] Oxidation with bleomycin, calicheamicin and neocarzinostatin produce 3′-PG and a base propenal, while gamma radiation produces 3′-PG, malondialdehyde and the free base (Figure 8). These lesions were identified using mass spectroscopy primarily by Giese and coworkers.[44]

Damage at the 4′-position of DNA leads to both single and double strand breaks and the formation of abasic sites with possible mutagenic effects if not repaired.[45] Some lesions, particularly the base propenal have also been reported to form adducts with DNA *in vitro*.

2.2.2.3 Independent Synthesis

Giese and coworkers developed a 4′-*C*-acyl-thymidine phosphoramidite that can be incorporated into an oligonucleotide and irradiated to produce the 4′-radical.[46] Independent synthesis of the C-4′ abasic site has been achieved by Greenberg and coworkers.[47]

2.2.3 Oxidation at the 3′-position

2.2.3.1 Conditions and causative agents

Compared to the 5′- and 4′-positions, damage at the 3′-position of the 2-deoxyribose of DNA is not as likely to be observed. One reason could be location: most DNA binding molecules responsible for hydrogen atom abstraction do so in the minor groove, while the 3′-hydrogen is located in the major groove. Another reason is the relatively low reactivity of the 3′-hydrogen compared to the two aforementioned positions.[48] A group of ROS generating species that have been shown to react at the 3′-hydrogen are photoreactive rhodium (III) complexes. Through coordination with intercalating ligands, the rhodium complexes are photochemically induced to generate a radical cation. That radical cation is believe to react with the H-3′ resulting in abstraction of the latter.[49] Damage at the C-3′ is nonetheless significant.

2.2.3.2 Identification and significance of the lesions generated by 3′-oxidation

Damage at the 3′-position of the sugar moiety generates two different sets of products depending on the presence or absence of oxygen. The first set of products, formed under aerobic conditions consists of the formation of a 3′-phosphoglycoaldehyde and a base propanoate. These products were originally proposed by Barton and coworkers.[49-50] The second set involves reactions under anaerobic conditions where the formation of a 3′-ketonucleoside on the 3′ end of the oligomer and a 5′-phosphate on the other was proposed by Joanne Stubbe.[51] In addition to the generation of a strand break, the lesions

formed through 3′-oxidation can react with other molecules to generate DNA and protein adducts.[52]

2.2.3.3 Independent synthesis

Bryant-Friedrich and coworkers developed the synthesis of a C-3′-thymidinyl radical precursor in single stranded DNA under biologically relevant conditions. Two nucleoside H-phosphonates, one bearing a C-3′ acetyl group and another a 3′-*t*-butyl-ketone were incorporated into an ODN before photoactivation generating a radical at the C-3′. The spectrum of products generated after H-3′ abstraction, including the 3′-oxolesion were observed.[53]

2.2.4 Oxidation at the 2′-position

2.2.4.1 Conditions and causative agents

The H-2′ is the other hydrogen on the 2-deoxyribose-along with the H-3′ that is accessible from the major groove of DNA.

Oxidation at the C-2′ has been reported as a result of gamma radiation of Poly Uracil as well as from the irradiation of oligonucleotides containing a halogenated uracil. The radical generated by the photolysis of the ODN at a halogenated uracil was reported to abstract the H-2′ of an adjacent adenosine.

2.2.4.2 Identification and significance of the lesions generated by 2′-oxidation

The most common lesion generated from oxidation at C-2′ is the formation of an erythrose abasic site. Heating of the lesion under alkaline conditions leads to the generation of a 3′-phosphoroglycoaldehyde.[54] Another product observed is a 3′-ketonucleoside (Figure 9).[55] Both lesions are also observed as a result of C-3′ oxidation. Abasic sites if not repaired can have potentially mutagenic effects while the 3′-ketonucleoside is essentially a strand break.

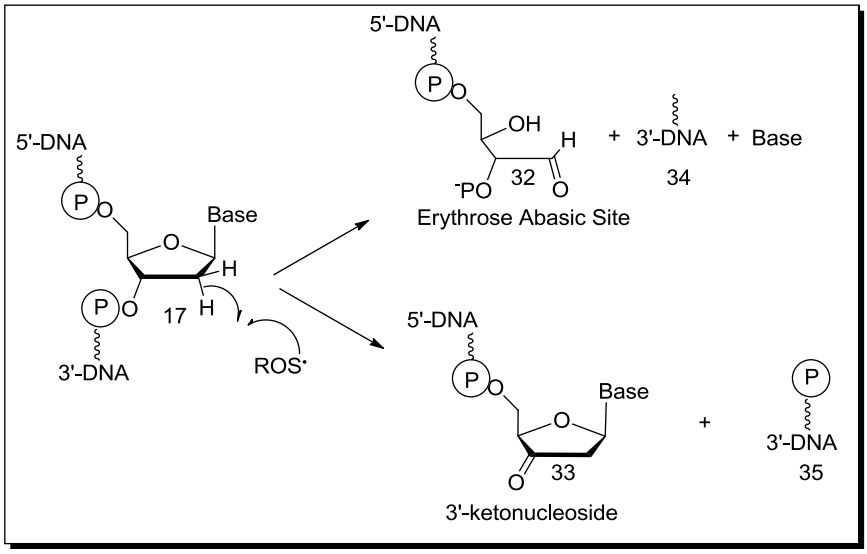

Figure 9: Lesions from C-2′ oxidation

2.2.4.3 Independent synthesis

The independent synthesis of the erythrose abasic sites was successfully completed by Greenberg and coworkers through the synthesis of a protected phosphoramidite triol,

incorporated into an oligonucleotide, then activated *via* periodate cleavage to generate the lesion.[54]

2.2.5 Oxidation at the 1′ position

2.2.5.1 Conditions and causative agents

There are many factors responsible for oxidation at the C-1′ position. Gamma radiation, UV radiation, enediyne antibiotics as well as cationic complexes such as oxoruthenium complexes, copper-phenanthroline complexes, and cationic porphyrins.[56,57,58,]

2.2.5.2 Identification and significance of lesions generated by 1′-oxidation

In the case of C-1′ oxidation the initial lesion produced is a 2-deoxyribonolactone abasic site. The lesion can further undergo β–elimination to form a butenolide then α-elimination to generate a 5-methylene-2(5H)-furanone. The 2-deoxyribonolactone abasic site has been shown to be mutagenic if not repaired. Additionally, there is evidence of the formation of DNA and protein-DNA adducts.[59,60,22, 61]

2.2.5.3 Independent synthesis

Several groups have reported the successful independent synthesis of the 2-deoxyribonolactone abasic site. Most have proceeded through the synthesis of photolabile phosphoramidite precursors that can be incorporated into an oligonucleotide. The abasic site is then generated through photoinduced cleavage.[58,]

2.3 Importance of the independent synthesis of 3′-oxothymidine

As described above, the study of the biological implications of DNA lesions is greatly facilitated by the design of synthetic pathways for the routine synthesis of monomers as well as their incorporation into oligonucleotides. These chemically generated lesions can then be studied to determine their reactivity, stability and possible toxicity in single and double stranded DNA.

3′-Oxothymidine is a DNA damage lesion that has been experimentally identified by Bryant-Friedrich and Lahoud in the study of the C3′-thymidinyl radical under both aerobic and anerobic conditions.[53] It is postulated that the lesion subsequently degrades to generate elimination products **39** and **41** as shown in Figure 10.

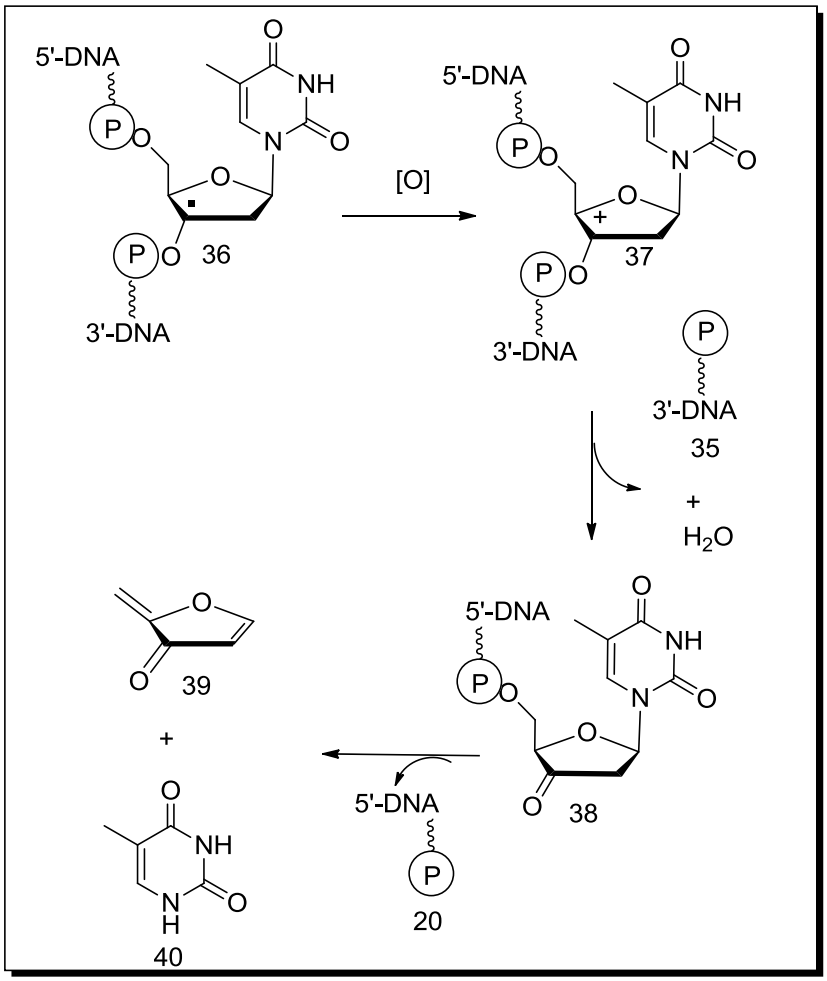

Figure 10: 3′-Oxothymidine experimentally identified by Bryant-Friedrich and Lahoud in the study of the C3′-thymidinyl radical

Saito et al. have also reported the formation of 3′-oxonucleoside analogues in their studies with uracil.[62] They reported generation of the 2′-deoxy-C2′-uracil radical **41** through the photoreaction of 2′-iododeoxyuridine under both aerobic and anaerobic conditions. Using NMR studies, it was demonstrated that 3′-ketouridine **44** was produced

from the deoxyribose C2′ radical by a 1,2 hydride shift *via* the C2′-carbocation **42** (Figure 11)**.**

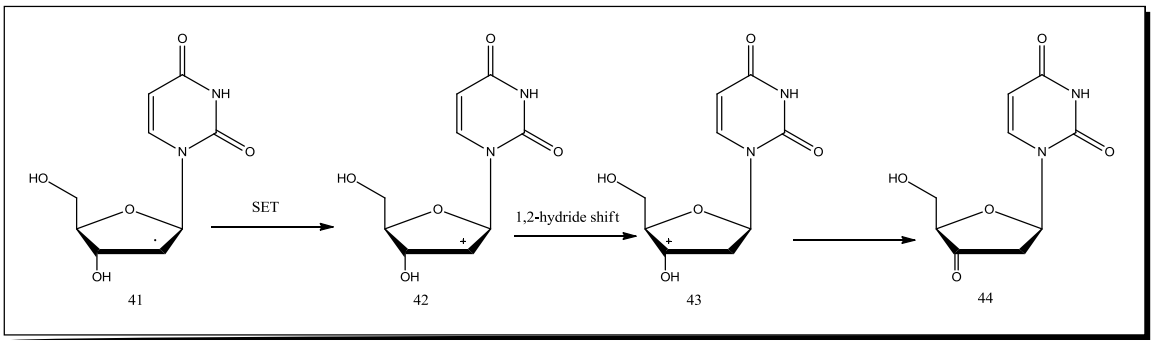

Figure 11: 3′-Ketouridine 44 produced from the deoxyribose C2′ radical by a 1,2 hydride shift via the C2′-carbocation

Greenberg et al. observed the formation of 3′-ketoadenosine in investigations into factors involved in the formation of strand breaks.[63] Following irradiation of a DNA duplex containing 5-bromodeoxyuridine, photoinduced single electron transfer (PSET) mediated generation of deoxyuridin-5-yl radical was observed. Deoxyuridin-5-yl selectively abstracts the C2′ hydrogen atom on the adjacent deoxyribose, resulting in a C2′ radical. 3′-keto-deoxynucleotide was then generated *via* oxidation of the C2′ radical to a carbocation, followed by a 1,2 hydride shift **(**see Figure 12**)**.

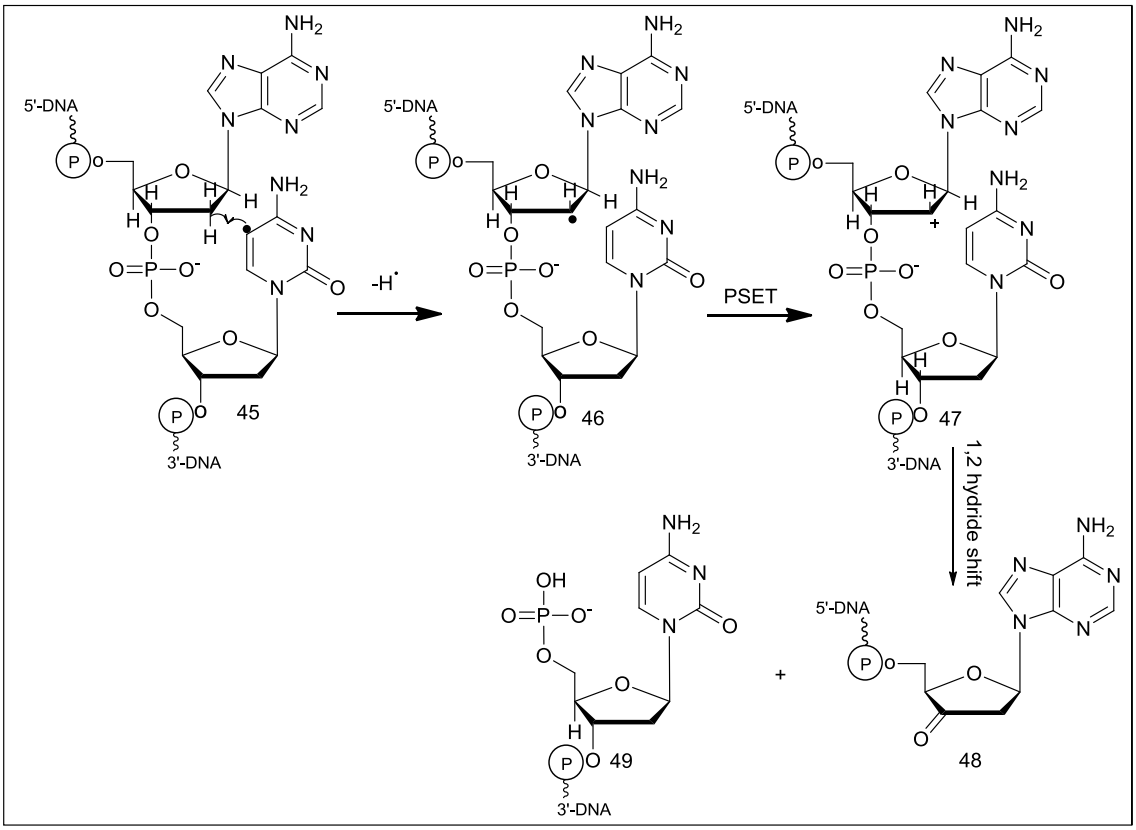

Figure 12: 3′-Ketoadeoxynucleotide generated via oxidation of the C2′ radical to a carbocation, followed by a 1,2 hydride shift

The most likely repair mechanism for the 3′-oxothymidine lesion is base excision repair. If the lesion is not repaired, a strand break remains. As seen in Figure 11, the lesion can degrade via base elimination to give rise to very reactive products such as the 2-methylene-3(2H)-furanone. These degradation products can form DNA and protein adducts.

One approach to the study of the biological implications of 3′-oxonucleotides, is to design a synthetic pathway that will allow for straightforward synthesis of 3′oxonucleotide monomers that can be included into oligonucleotides of varying length and base composition. Such oligonucleotides can serve as tools to study the stability and reactivity of 3′-oxonucleotides in single and double stranded DNA.

In previous studies focusing on oxidative damage at the C3′-position of nucleotides, our lab successfully synthesized modified nucleosides capable of generating site reactive intermediates through photololysis. These modified photocleavable moieties were incorporated in oligonucleotides and subsequently irradiated to generate the radical of interest.[53]

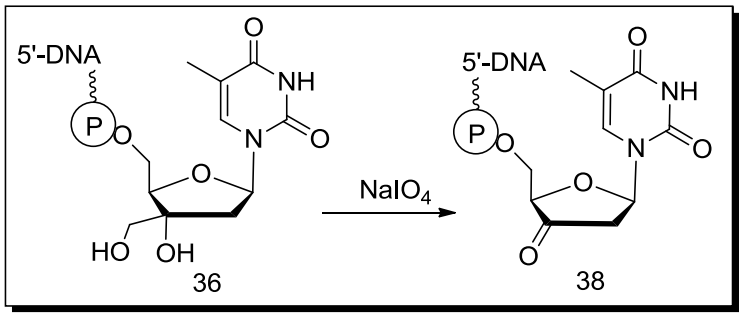

Figure 13: Post Synthetic cleavage of vicinal diols with $NaIO_4$

This study reports the synthesis of a thymidine phosphoramidite monomer, its incorporation into ODNs followed by chemical generation of the lesions of interest

through oxidative cleavage. The 3′-oxothymidine precursor was synthesized with a cis-diol at the 3′-position to allow for the generation of the ketone lesion post synthetically.

Reactive aldehydes have been successfully incorporated into ODNs through post synthetic cleavage of vicinal diols with $NaIO_4$ (Figure 13).[40] This method has demonstrated broad utility in the preparation of both base and sugar modified oligonucleotides.[40, 64] To our knowledge this approach has not been used to introduce ketone moieties into oligonucleotides.

In living organisms, enzymes synthesize DNA and RNA from the 5′ end to the 3′ end. Automated ODNs synthesis however usually proceeds from the 3′ end of the oligonucleotide to the 5′-end. Due to the desired generation of the oxo moiety at the 3′-position of the oligomer, the precursor will be incorporated into ODNs using reverse automated ODN synthesis (5′ to 3′ end) followed by the chemical generation of the lesion through oxidative cleavage with sodium periodate.

Chapter 3

3 Results and Discussions: Synthesis of 3′-hydroxymethyl Thymidine

3.1 Overview of the Synthesis of the Monomer

One strategy to study the biological implications of 3′-oxonucleotides, is to design synthetic pathways for the routine synthesis of 3′-oxonucleotide monomers as well as their incorporation into oligonucleotides of varying length and base composition. Such oligonucleotides can serve as tools to study the stability and reactivity of 3′-oxonucleotides in single and double stranded DNA.

The 3′-oxonucleotide substrates must be versatile to allow for their incorporation into a variety of sequences of varying length and their utilization in an array of biological assays. Access to these oligomers is most often accomplished through the incorporation of a versatile phosphoramidite in ODNs using automated nucleic acid synthesis.[47, 65] The amidite is appropriately protected from chemical or photochemical conversion to the damage lesion of interest until its formation is desired. This approach delivers well-defined substrates, generated at the time of use to avoid issues of lesion instability. The 3′-hydroxymethyl was chosen because it is stable to the conditions of the synthesizer and

allows for the post-synthetic chemical generation of the lesion of interest *via* periodate cleavage.

As shown in Scheme 3, the synthesis of the phosphoramidite precursor was performed starting with commercially available thymidine. The 5′-hydroxyl was protected with a *tert*-butyldimethylsilyl chloride (TBMSCl) group before the 3′-hydroxyl was oxidized to a ketone with the Dess-Martin reagent.[66] The ketone was further converted to a methylene group *via* the Lombardo reaction.[67] The resulting alkene was converted to a cis-diol by reaction with catalytic amounts of osmium tetroxide in the presence of *N*-methylmorpholine *N*-oxide (NMO) and water.

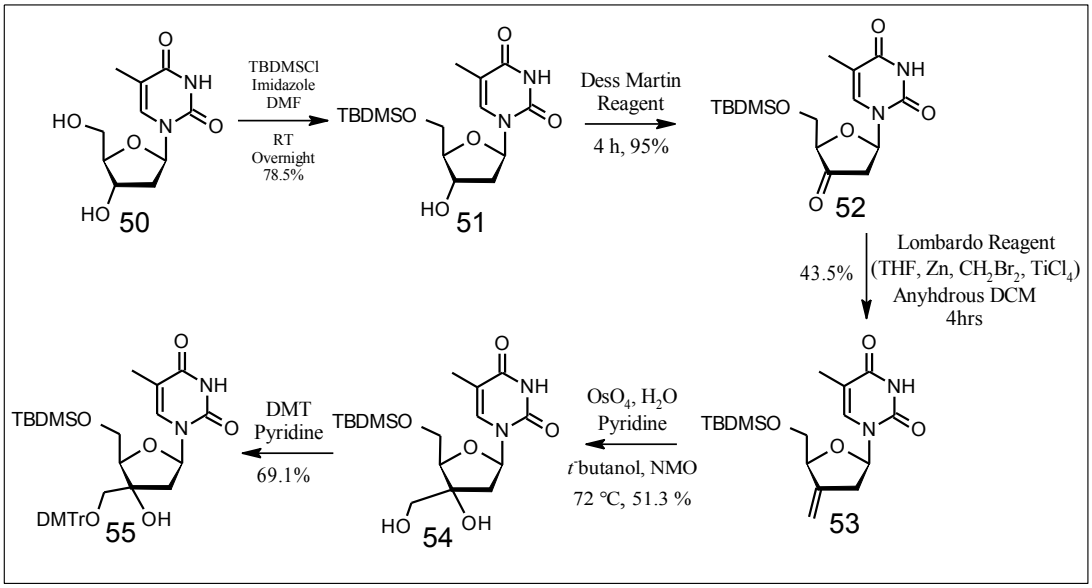

Scheme 3: Synthesis of 5′-*O*-(*t-butyl*-dimethylsilyl)-3′-C-((4,4′-dimethoxytrityl) oxymethyl)thymidine

The diol was then treated successively with dimethoxytrityl chloride (DMTrCl) and acetic anhydride to protect the primary and the tertiary alcohol at the 3′-carbon respectively. Finally tetra-*n*-butylammonium fluoride (TBAF) was used to remove the TBDMS protecting group to allow for phosphoramidite formation at the 5′-carbon. The synthesis of the phosphoramidite was accomplished by reaction with 2-cyanoethyl *N,N,N′,N′* tetraisopropylphosphoramidite (Scheme 4).

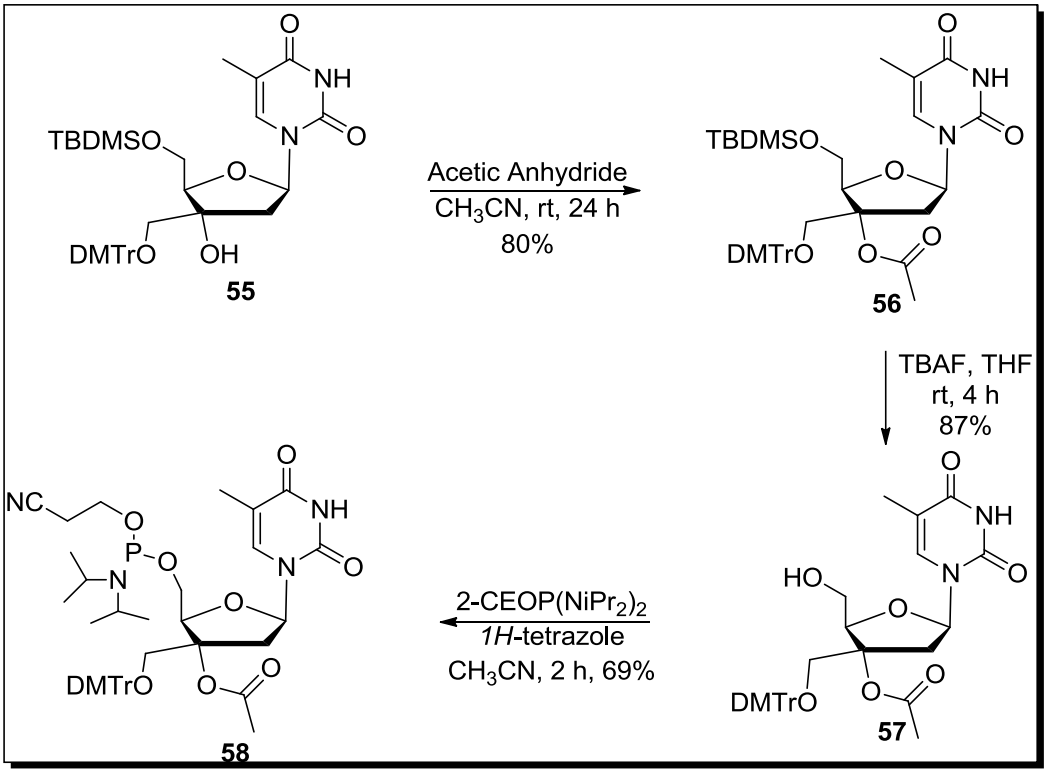

Scheme 4: Synthesis of the phosphoramidite precursor

3.2 Design and Synthesis of the phosphoramidite precursor

3.2.1 Synthesis of 5′-*O*-(*t*-butyldimethylsilyl)thymidine (**51**).

The first step in the synthesis of 3′-hydroxymethyl thymidine is the protection of the of the 5′-hydroxyl of thymidine with TBDMSCl.

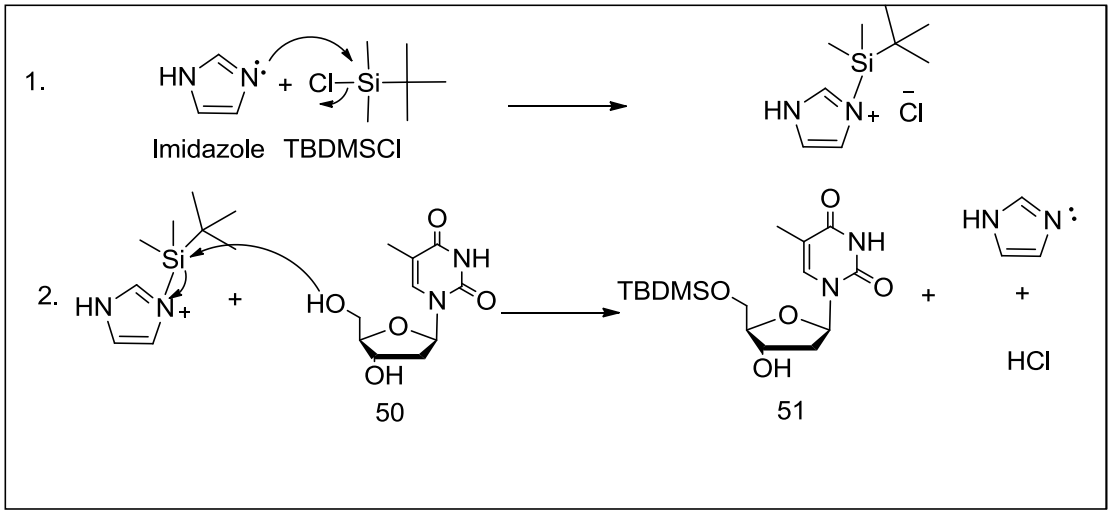

Scheme 5: The role of imidazole in TBMSCl protection of thymidine

Silyl ethers are routinely used in organic synthesis as protecting groups for carbohydrates. They are usually made up of a silicon atom, covalently bound to an alkoxy group with the general formula $R^1R^2R^3$-Si-O-R^4. The presence of the four R groups allows for a variety of silyl ethers suitable for diverse conditions. The four most common groups are triisopropylsilyl **(TIPS)**, trimethylsilyl **(TMS)**, *tert*-butyldiphenylsilyl (**TBDPS**) and tert-butyldimethylsilyl (**TBDMS**).[68] In our scheme, TBDMS group was selected for many reasons. It is more resistant to hydrolysis and exhibits excellent stability in alkaline environments. In addition, a primary TBDMS group can be

selectively introduced in the presence of a secondary hydroxyl group. In our case, we performed the silylation reaction in dry DMF with imidazole[69], or with dry pyridine at 0 ^{o}C (Scheme 5). The low temperature favors the formation of the 5′-TBDMS product as opposed to the 5′,3′-bis protected compound **60** which is observed as a side product (Figure 14).

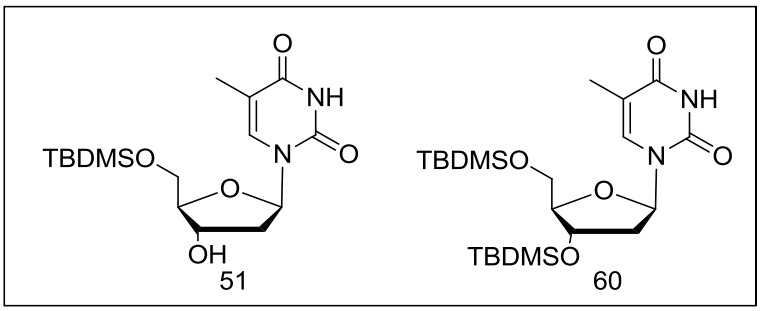

Figure 14: Products from the silylation of thymidine

The mixture of products was purified by column chromatography using either a ethyl acetate and hexane gradient or a methanol in DCM gradient. Yields of 80 % could be achieved in as little as one hour reaction time in the presence of anhydrous reagents.

3.2.2 Synthesis of 5′-*O*-(*t*-Butyldimethylsilyl)-3′-ketothymidine (**52**).

Following protection of the 5′-hydroxyl of thymidine, we proceeded to the conversion of the secondary 3′-hydroxyl to a ketone. Similar oxidations have been performed using pyridium dichromate (PCC) and dimethyl sulfoxide (DMSO) based oxidizing agents. We opted for the Dess-martin periodinane (Figure 15) because it allowed for shorter reaction times, milder conditions and a simplified work-up procedure.[66]

The Dess-Martin reagent was synthesized in two steps from 2-iodobenzoic acid. The 2-iodobenzoic acid was reacted with $KBrO_3$ in sulfuric acid to afford 2-iodoxybenzoic acid. The resulting 2-iodoxybenzoic acid was then heated in acetic anhydride and acetic acid at 100 ^{o}C for 40 min to afford the Dess Martin Periodinane.

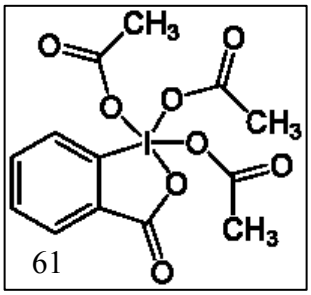

Figure 15: The Dess-Martin Reagent

Reactions of the Dess Martin periodinane with the 5′-TBDMS thymidine were performed under both inert and atmospheric conditions with similar success. The reactions were carried out in DCM at 0 ^{o}C with reactions time ranging from 1 to 4 hours depending on the age of the reagent (Scheme 6).

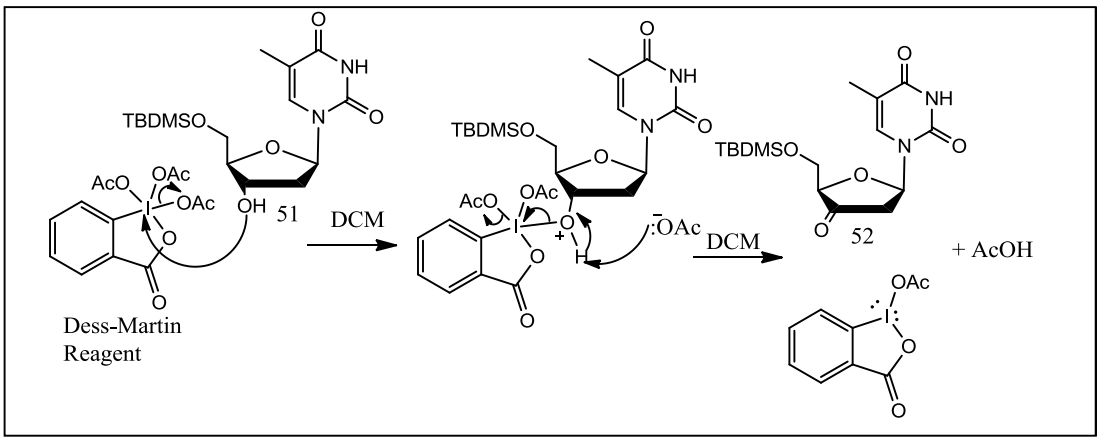

Scheme 6:Dess-Martin Reaction[66]

The 5′-*O*-(*t*-butyldimethylsilyl)-3′-ketothymidine was obtained in yields up to 99% yield by dissolving the reaction mixture in diethyl ether and performing washes with Sodium

thiosulfate, water and sodium bicarbonate. The product was obtained with high purity and did not require any chromatographic purification.

3.2.3 Synthesis of 5′-*O*-(*t*-Butyldimethylsilyl)-3′-deoxy-3′-*C*-methylenethymidine (**53**).

Upon completion of the oxidation reaction, our next step involved converting the 3′-ketone to an alkene. Wittig reagents are routinely used to convert ketones to alkenes with success. The conditions required for such reactions demand an alkaline environment that may not be suitable to the compound at hand. In an alkaline environment, 3′-ketonucleosides are believed to undergo degradation *via* base catalyzed elimination of the nucleobase. The hydrogen alpha to the 3′-ketone is relatively acidic and can participate in acid base reactions. Instead of using the Wittig reagent we selected the Lombardo reagent, an organotitanium reagent synthesized from activated zinc, dibromomethane and titanium chloride (see Scheme 7).

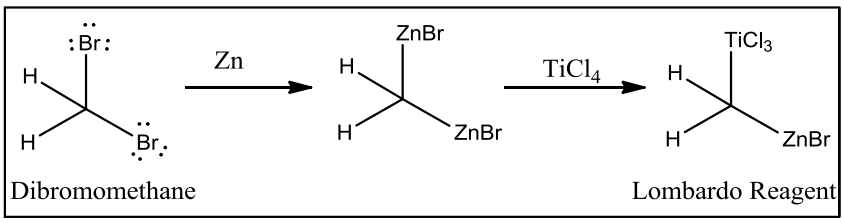

Scheme 7: Synthesis of the Lombardo reagent[67]

Similar to most organometallic reagents, the Lombardo reagent must be synthesized in inert conditions to guarantee its viability. A slurry of activated zinc, dibromomethane and $TiCl_4$ is stirred for 48-96 hours in a cold room before being used as a reagent in the synthesis of the 5′-*O*-(*t*-butyldimethylsilyl)-3′-deoxy-3′-*C*-methylenethymidine (Scheme 8).[67] The reagent reacts quickly and converts the ketone to an alkene with yields ranging from 25 to 30%.

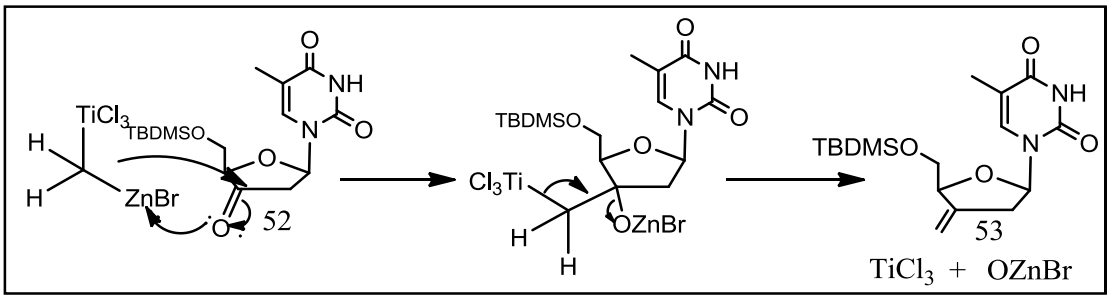

Scheme 8: The Lombardo Reaction

3.2.4 Synthesis of 5′-*O*-(*t*-butyldimethylsilyl)-3′-*C*-(hydroxymethyl)thymidine (**54**).

In order to convert the alkene to a vicinal diol, two possible reactions were considered. The first reaction would involve using potassium permanganate ($KMnO_4$) with sodium hydroxide at reduced temperature. The advantage of using $KMnO_4$ is that reaction completion is indicated by a simple color change.[70] An alternative reaction involves using osmium tetroxide (OsO_4) either in stoichiometric or catalytic amounts.[71]

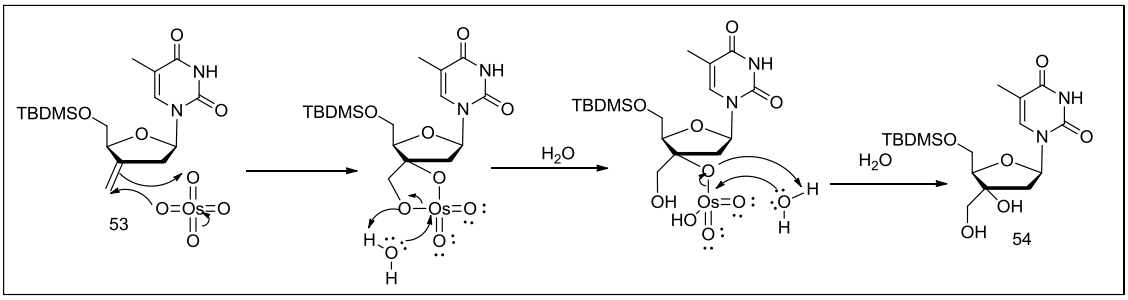

Scheme 9: Dihydroxylation with osmium tetroxide

Due to the high toxicity of OsO_4 vapors, the conversion to the cis diol was achieved through a dihydoxylation reaction using catalytic amounts of osmium tetroxide regenerated in the reaction by the presence of water and *N*-methylmorpholine oxide (Scheme 9). The nucleoside substrate contains two alkene functionalities on both the base and the sugar, each susceptible to undergoing a reaction with OsO_4. Although OsO_4 reacts primarily with the alkene on the sugar, dihydroxylation of the base becomes more of a concern as the amount of OsO_4 and the duration of the reaction increases. Theoretically, the OsO_4 reaction on the sugar moiety can take place on either the α-face or β-face of the molecule to produce a diastereomere. In our experience, the reaction occurs on the α-face, thus producing one major product in 48% yield after column chromatography with a 0-10% gradient of methanol in DCM.

3.2.5 Synthesis of 5′-*O*-(*t*-butyldimethylsilyl)-3′-*C*-((4,4′-dimethoxytrityl) oxymethyl)-thymidine **(55).**

Following the synthesis of 5′-*O*-(*t*-butyldimethylsilyl)-3′-*C*-(hydroxymethyl)-thymidine, it was necessary to protect both the hydroxyl groups of the cis-diol with groups suitable

for automated oligonucleotide synthesis. To protect the primary alcohol, the dimethoxytrityl group was used (Scheme 10). In this case it allows the efficient selective protection of the primary hydroxyl at room temperature under inert conditions. Purification by column chromatography with a gradient of methanol in DCM afforded the product in 80% yield.

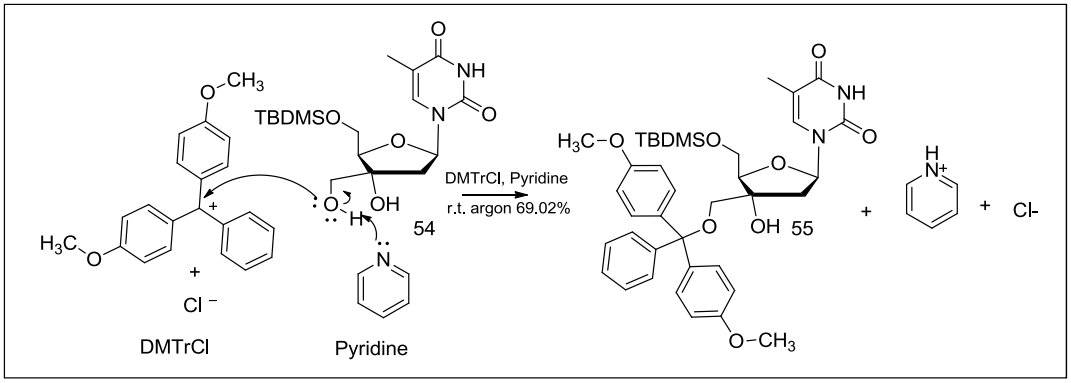

Scheme 10: Tritylation of the 5'-primary alcohol

3.2.6 Synthesis of 5′-*O*-(*t*-Butyldimethylsilyl)-3′-*C*-((4,4′-dimethoxytrityl)oxymethyl)-3′-*O*-acetyl-thymidine **(56)**.

The tertiary alcohol at the 3′-position is then acetylated using acetic anhydride in pyridine in the presence of 4-dimethylaminopyridine (DMAP). Although the acetylation reaction has proven to be lengthy due to the steric hindrance, yields of 80% have consistently been

achieved (Scheme 11).

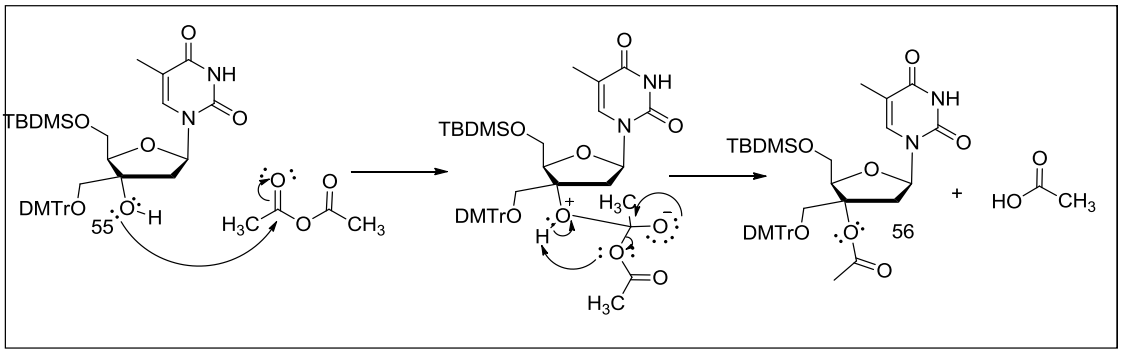

Scheme 11: Acetylation reaction

3.2.7 Synthesis of 3′-*C*-((4,4′-dimethoxytrityl)oxymethyl)-3′-*O*-acetyl-thymidine **(57)**.

Silyl protecting groups are easily removed with either acid or fluoride ions. In the presence of the very acid labile DMT protecting group, a reaction with TBAF was preferred. The strength of the Si-F bond (30 kcal) drives the high affinity that fluoride has for silicon and ensures a fast and efficient reaction. Removal of the TBDMS protecting group was performed at room temperature under inert conditions and afforded the 3′-*C*-((4,4′-dimethoxytrityl)-oxo-methyl)-3′-*O*-acetyl-thymidine in 69% yield.

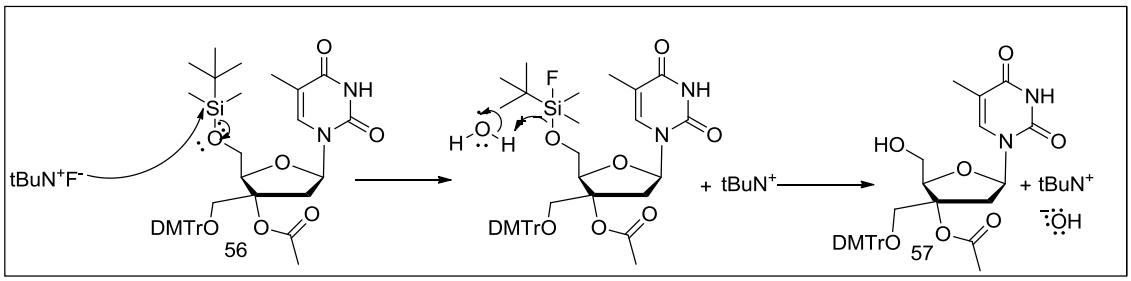

Scheme 12: TBAF deprotection

3.2.8 Synthesis of 5′-*O*-(2-cyanoethoxy(diisopropylaminophosphino))-3′-*C*-((4,4′-dimethoxytrityl)oxymethyl)-3′-O-acetyl-thymidine **(58).**

In order to incorporate the moiety into an oligonucleotide, it is necessary to insert a phosphate at the 5′-postion either using the H-phosphonate method or the phosphoramidite method followed by oxidation.[72,73] The phosphoramidite method was chosen, and the deprotected nucleoside was reacted with of 2- cyanoethyl *N,N,N′,N′* tetra-isopropyl phosphoramidite in acetonitrile. The phosphoramidite precursor was obtained in 69% yield after column chromatography purification.

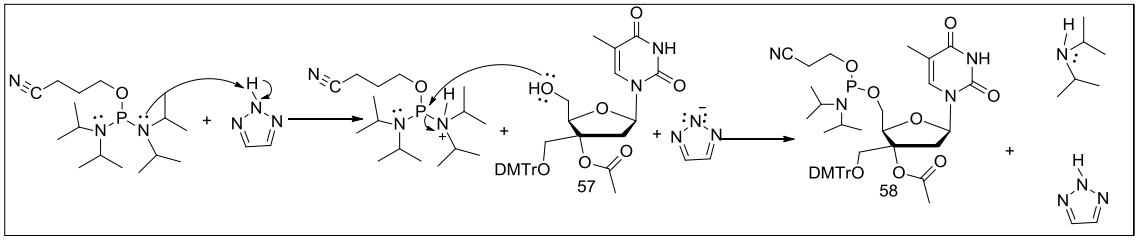

Scheme 13: Phosphoramidite synthesis

Chapter 4

4 Results and Discusions: Synthesis of oligonucleotides containing 3′-oxothymidine

Reactions of reactive oxygen species with the 2-deoxyribose of DNA usually involve the generation of reactive intermediates and very unstable damage products. In order to determine the biological contribution of each of the damaged products, it is imperative to synthesize them in a controlled environment for analysis. Such studies have been credited for the elucidation of reaction mechanisms involving ROS and DNA. Photolabile nucleosides with a phenylselenyl or acyl group are usually incorporated into oligos before being irradiated to generate the lesion of interest. As mentioned above, oxidative damage at the C-3′ can result in the generation of a cluster of products including a strand break terminated by a 3′-oxothymidine. As mentioned in chapter 1, the 3′-ketonucleoside lesion is believed to degrade to generate a 2-methylene-3-(2H)-furanone. The later compound can, in turn, interact with DNA and proteins *via* Michael addition to generate adducts. In order to determine the fate of the lesion and its degradation products, a 3′-hydroxymethyl thymidine moiety was synthesized with the aim to be inserted at the terminal end of an oligonucleotide. The 3′-oxonucleotide is then

generated through periodate cleavage. Automated DNA synthesis is employed in this process.

4.1 Overview of the oligonucleotide synthesis process

The oligonucleotides used in this study were synthesized using solid phase automated DNA synthesis. The process consisted of adding a nucleotide residue to a growing chain of an oligonucleotide to obtain a desired sequence. In solid phase synthesis the nucleosides are added to the 5′-end of the growing oligonucleotide chain. In the case of the synthesis of the 3′-ketonucleoside lesion, reverse automated DNA synthesis was employed because of the position of the lesion at the 3′-end of DNA. Both processes are essentially and sequentially the same. In both cases a tritylated solid support is used and the process consists of a deprotection step also called the detritylation step, a coupling step, a capping step and an oxidation step. The types of nucleoside building blocks employed in reverse DNA synthesis are different: they are tritylated at the 3′-position and have a phosphoramidite group at the 5′-end.

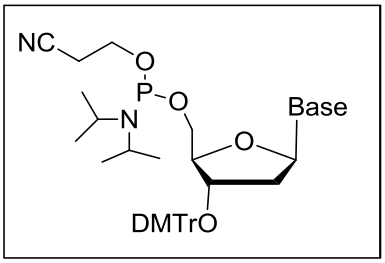

Figure 16: Nucleoside building blocks for reverse synthesis

4.1.1 Nucleoside building blocks for reverse synthesis.

The nucleoside building blocks used in reverse synthesis are 5′-*O*-*(N,N*, diisopropyl phosphoramidite analogs of the naturally occurring ones. They are protected on the 3′-hydroxyl end by a trityl group. The use of modified nucleosides allows improved reactivity relative to the naturally occurring ones. Other protecting groups are used to prevent side reactions to occur. Those protecting group are eventually removed post-synthetically.

4.1.2 Steps of the synthesis

Detritylation: In reverse synthesis, the nucleoside intended to be at the 5′-end is attached to the solid support *via* a linker while the 3′-end is protected by a trityl group. The first step of the synthesis is the removal of the trityl protecting group present at the 3′-end of the resin bound nucleoside. It is achieved by treating the resin bound nucleoside with 3%

tricloroacetic acid in dichloromethane. The efficiency of the reaction is assessed using a trityl monitor.

Coupling: Following detritylation, the coupling step occurs. It consists of the reaction of the free hydroxyl at the 3′-end of the resin bound nucleoside with an incoming 5′-phosphoramidite. An activator such as H-tetrazole is used to protonate the diisopropyl amine of the phosphoramidite rendering it an ideal leaving group. When the 3′-hydroxyl of the resin bound nucleoside attacks the phosphate of the incoming phosphoramidite, the protonated diisopropyl amine group is easily displaced. The reaction results in a phosphite triester.

Capping: At the end of the coupling reaction, any unreacted free hydroxyl group is blocked using a reaction with acetic anhydride and *N*-methyl imidazole. The reaction effectively acetylates the hydroxyl groups to prevent the accumulation of failure sequences. A small quantity of pyridine is added to avoid acidic pH conditions that could lead to premature de-protection of the trityl groups.

Oxidation step: The very reactive phosphite triester obtained in the coupling step is oxidized to a phosphotriester by reaction with iodine in the presence of pyridine and water. After the oxidation the cycle starts over with the detritylation step.

4.2 Synthesis of the 3′-modified ODNs

Oligonucleotides of two different sequences were synthesized using the automated synthesis process outlined above. **ODN 36a** and **36b** were synthesized on a 0.2 umol

scale incorporating the 3′-hydroxymethyl phosphoramidite precursor at the 3′-end of the growing oligo. Standard instrument conditions were used except that the coupling time was increased to 15 minutes to ensure completion of the reaction at the modified substrate.

At the end of the synthesis cycle, cleavage from the solid support and deprotection of the bases were achieved by incubating the DNA in 1.5 M NH_4OH for 18 hours. The oligonucleotides were then purified using OPC purification and quantified using UV-VIS. The samples were then analyzed using ion-exchange HPLC and the structures identified with MALDI-TOF MS.

Table 4.1: C3′-hydroxymethyl thymine containing ODNs (36)

	Sequence	Theoretical [M + H]	Experimental [M + H]
36a	GACTGAT(C3′-CH_2OH)	21**51**.5	2152.1
36b	ACGTTGACTACCGT(C3′-CH_2OH)	4269.8	4270.9

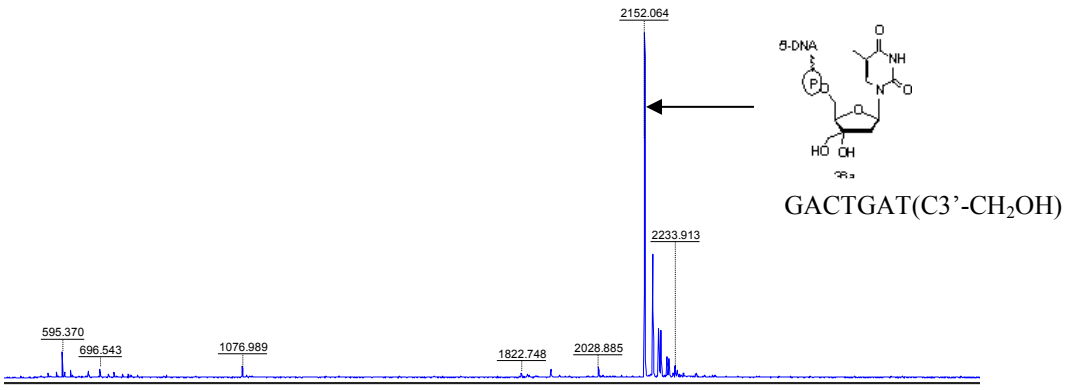

Figure 17: MALDI-TOF of 36a (m/z=2152.064)

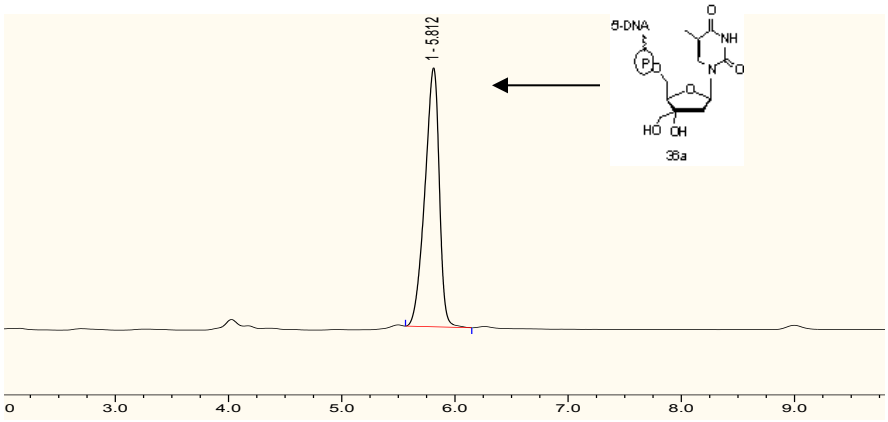

Figure 18: HPLC-of 36a

4.3 Synthesis of 3′-oxothymidine containing oligos

Upon successful completion of the synthesis of the 3′-hydroxymehtyl nucleoside, synthesis of 3′-oxothymidine oligos was achieved by reaction with sodium periodate in water at 20 ^{o} C. Initially the reaction was quenched using methionine and the

oligonucleotide was precipitated from the reaction mixture using ethanol. The oligonucleotide was then analyzed using ESI-MS.

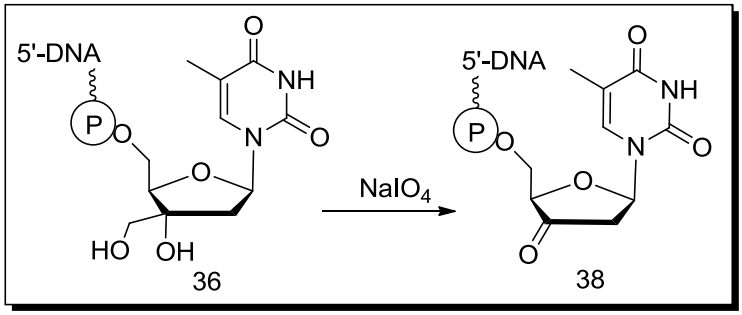

Scheme 14: Synthesis of 3′-oxothymidine

Analysis with ESI-MS only indicated the presence of a compound with a m/z 1898.1, corresponding to the 3′-phosphate which is one of the degradation products observed after base elimination of the 3′-oxothymidine.

In order to better monitor the reaction, aliquots of the mixture were taken, desalted using the ZIPTIP® desalting protocol and analyzed using MALDI-TOF MS. Through HPLC analysis of an independently obtained standard, one substance was determined to be 3′-phosphate **20**, which is obtained upon elimination of the diol containing nucleoside. Through MALDI-ToF analysis of the crude reaction mixture, we were able to identify the presence of ketone **38** as a minor constituent in the product mixture in addition to the base elimination product **41**. Due to the known instability of this fragment, we were not surprised to find that lesion **38** readily decomposed to 3′-phosphate **20** under the reaction conditions employed for this work.

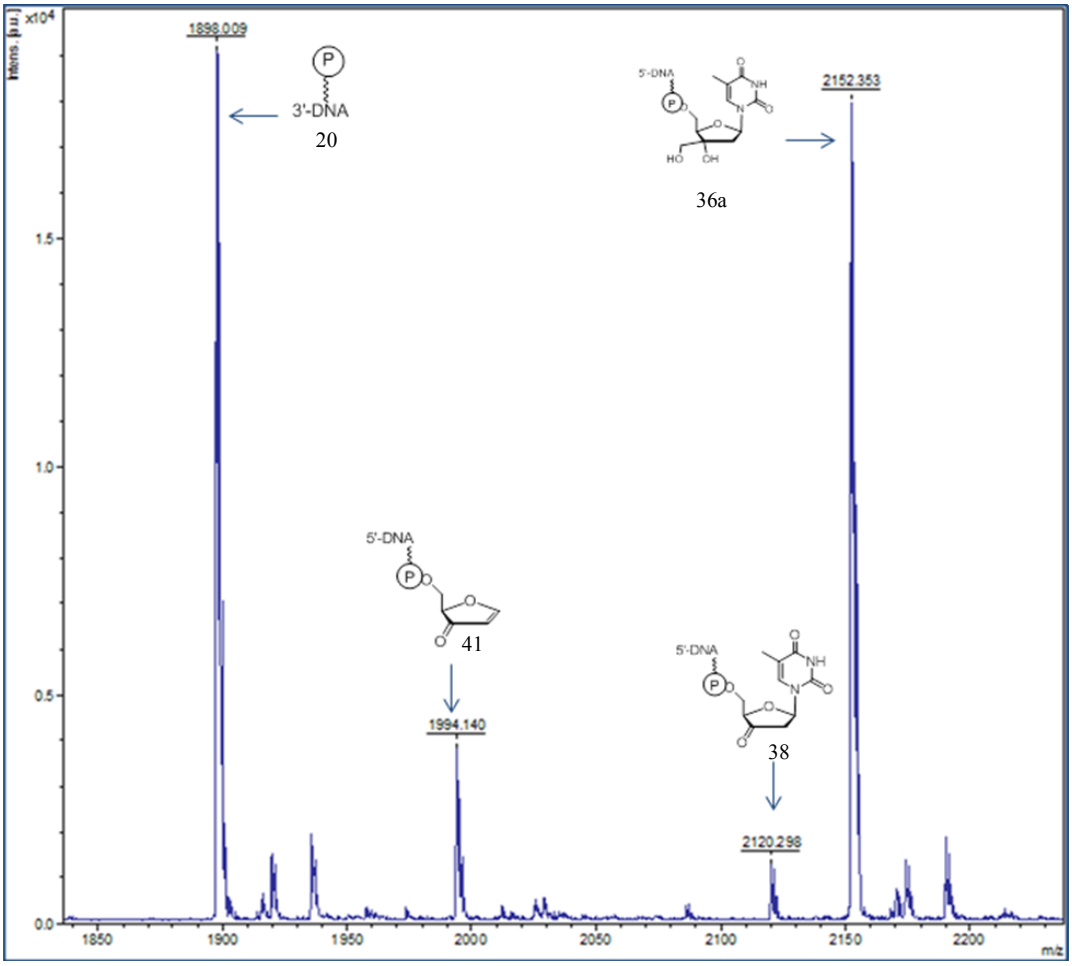

Figure 19: MALDI-ToF MS: Oxidative cleavage of 36a with $NaIO_4$

Monitoring the reaction over a period of two hours indicated that the 3′-oxothymidine underwent base elimination immediately upon formation.

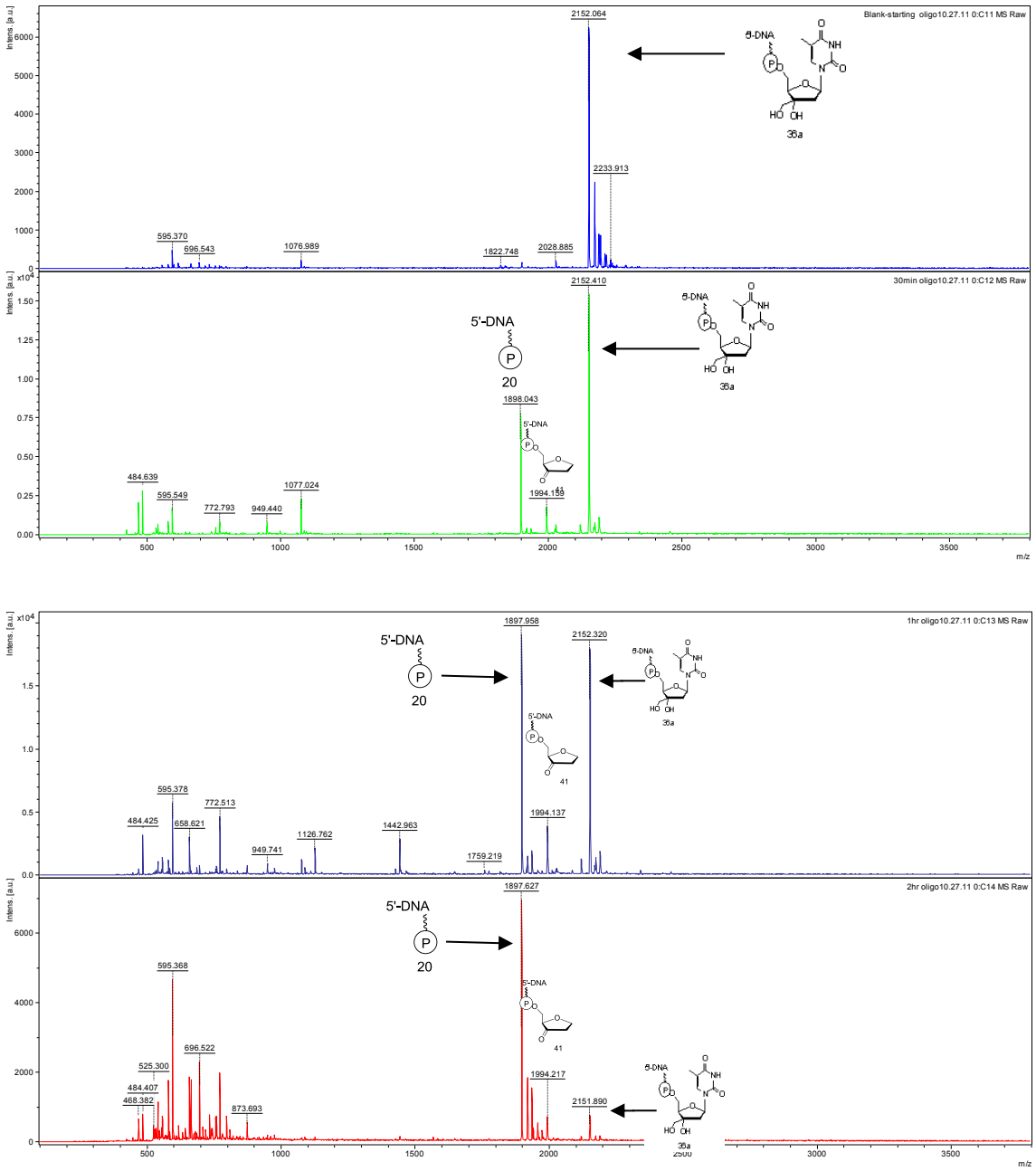

Figure 20: Reaction with $NaIO_4$ monitored over time

The presence of the 5′-phosphate implied that the 3′-ketonucleoside decomposed as expected to generate the very reactive 2-methylene-3-(2H)-furanone (Scheme 15).

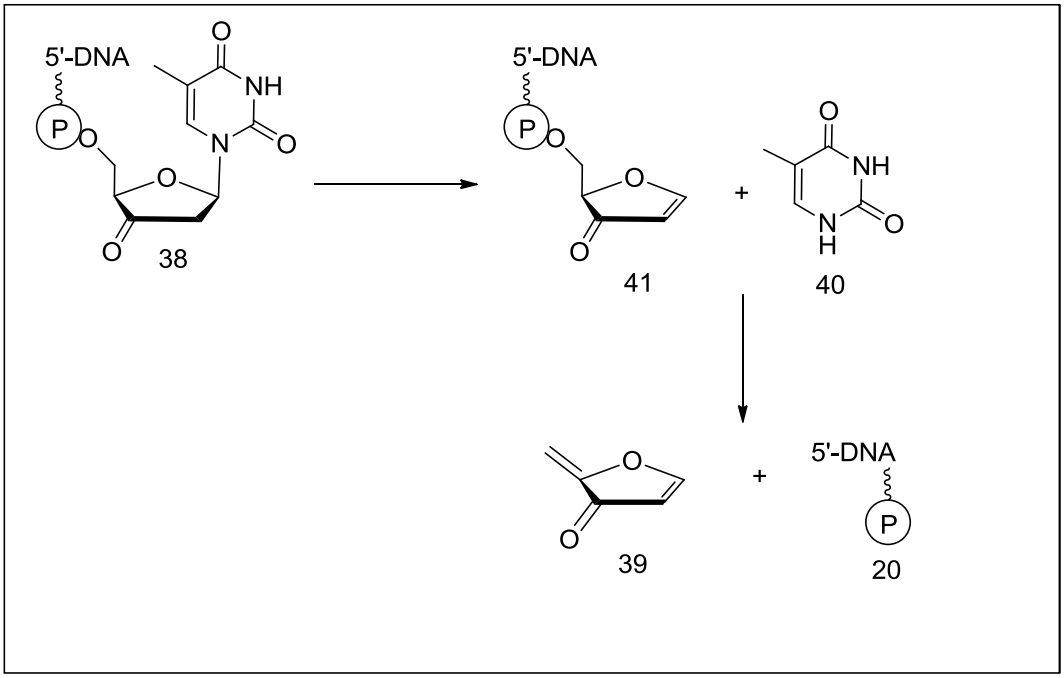

Scheme 15: Degradation of 3′-ketonucleoside 38

Due to the high instability of the latter, monomeric studies with analogs are warranted to determine possible relevant reactions with biological species.

Chapter 5

5 Conclusions and future works

5.1 Conclusions

Oxidative damage represents one of the most common types of injuries occurring to DNA *in vivo*. This type of damage has been linked to numerous diseases and conditions. One particular type of damage of interest is the oxidation of the 2-deoxyribose of DNA resulting in hydrogen abstraction. It has been demonstrated that once a hydrogen is extracted from the sugar portion of DNA, it sets in motion a series of reactions involving the generation of a carbocation. The very unstable DNA lesion can undergo molecular rearrangement or react with other macromolecules and cause further damage. Many reports have highlighted the practicality of undertaking the independent synthesis of oligonucleotide damage product to elucidate their stability and reactivity in a controlled environment. The result of such studies can precede *in vivo* studies to help anticipate the type of reactions the lesions are involved in *in vivo* and the possible adducts that can be generated.

5.1.1 Independent synthesis of the 3′-oxothymidine lesion

Independent generation of DNA lesions has been achieved for numerous DNA intermediates derived from hydrogen abstraction at each of the carbons of the 2-deoxyribose. One of the most common methods involves the generation of a photo labile precursor that can be incorporated into an oligonucleotide and photoactivated at will to generate the lesion. Such methods have been used extensively with considerable success. Another method involves the incorporation of a cis-diol at the position on the sugar where the damage is intended. Successful generation of aldehydes have been reported when the diol undergoes periodate cleavage to generate the lesion of interest.

Taking advantage of the later method, this work reports the synthesis of a phosphoramidite precursor to 3′-oxonucleotide, a lesion observed as a result of hydrogen abstraction at both the C-2′ and C-3′ position of the sugar. The precursor was successfully synthesized and incorporated in ODNs using reverse automated DNA synthesis

5.2 Future work

Considerable work remains to obtain a complete picture of the fate of the 3′-oxonucleotide lesion.

5.2.1 Optimization of synthesis conditions for ODN containing 3′-oxothymidine

Further studies are warranted to determine the best conditions for the isolation of lesion **38**. To this aim, the lesion can be generated in phosphate buffer with varying conditions

of pH and temperature to determine, which conditions are the best to maintain the stability of the lesion over time. Ethanol precipitation can be performed to isolate the lesion and ZIPTIP® filtration will still be required to desalt the lesion before analysis using MALDI-TOF, ion exchange and HPLC.

Once the synthesis of the oligonucleotides has been optimized as describe above, the lesion of interest can then be incorporated into other ODNs of varying lengths. The incorporation into a greater number of ODNs will validate our assumption that our lesion can be generated in a variety of sequence context. We expect the lesion to be very unstable under basic conditions, with stability improving with pH values between 7-7.5. The yield of the synthesis is expected to decrease as the lengths of the oligonucleotides increase.

5.2.2 Investigate the chemical and biological reactivity of 3′-ketothymidine in biological systems

Being able to identify adducts that are formed *in vitro* will be beneficial in studying the fate of the DNA lesion in cellular environments. The ODN containing 3′-oxothymidine is expected to be base labile and react in biological systems to form adducts. Identifying and characterizing these adducts in vitro will allow us to have specific biomarkers for our studies in a cellular environment.

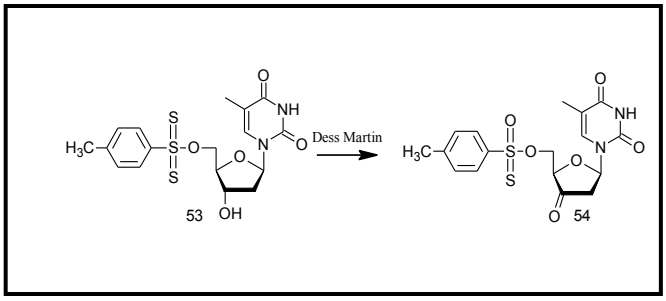

Figure 21: Synthesis of 5'-tosyl-3'-ketothymidine

For this purpose monomer studies can be undertaken by synthesizing ketonucleosides and manipulating them under acidic and basic conditions. These reactions will be monitored

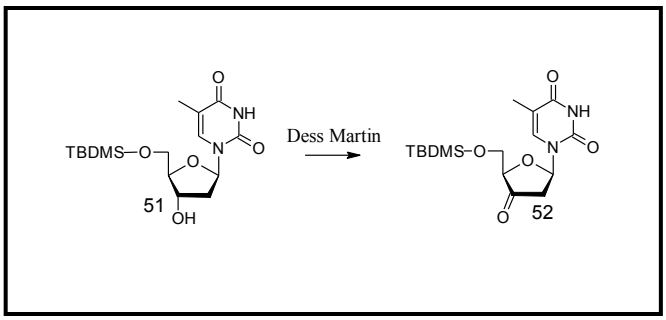

Figure 22: Monomer studies

to identify the products that are formed and elucidate the mechanisms of their formation.

Secondly, the ketonucleosides can be treated in the presence of glutathione to identify the types of adducts that can be formed. Ketonucleosides are known to be very labile under basic conditions. Our own initial studies have shown that once the ketonucleoside is formed in an oligonucleotide, it degrades very rapidly. Being able to identify adducts that are formed *in vitro* will be beneficial in proving the formation of the damaged product in cellular environments.

5.2.3 Comparative thermodynamic stability.

Efforts should be made to determine the effect that the 3′-oxothymidine has on the stability of binary and ternary DNA complexes as well as the stability of the lesion in these complexes**.** The use of melting assays in the study of the stability of oligonucleotides is precedented. The thermodynamic parameters obtained from the assays will allow us to determine the effect that 3′-ketothymidine may have on binary and ternary complexes.

The following DNA sequences will be synthesized *via* automated DNA synthesis and annealed (**50** mM sodium phosphate (pH 7.2) and 100 mM NaCl).

Table 5.1: Oligonucleotide sequences

Oligonucleotide sequences
5′-ACG-TTG-ACT-ACC-GT*-3′ 3′-TGC-AAC-TGA-TGG-CA -5′
5′-ACG-TTG-ACT-ACC-GT-3′ 3′-TGC-AAC-TGA-TGG-CA -5′
5′-ACG-TTG-ACT-ACC-GT* 3′-TGC-AAC-TGA-TGG-CA –TCC-GTC-TCA-GGC-5
5′-ACG-TTG-ACT-ACC-GT 3′-TGC-AAC-TGA-TGG-CA –TCC-GTC-TCA-GGC-5
14-mers 12-mers 5′-ACG-TTG-ACT-ACC-GT*P-AGG-CAG-AGT-CCG-3′ 3′-TGC-AAC-TGA-TGG-CA –TCC-GTC-TCA-GGC-5′
14-mers 12-mers 5′-ACG-TTG-ACT-ACC-GT-- AGG-CAG-AGT-CCG-3′ 3′-TGC-AAC-TGA-TGG-CA –TCC-GTC-TCA-GGC-5′

Thermal denaturation studies will then be performed using an ultraviolet-visible (UV-VIS) spectrophotometer equipped with a temperature controller. ODNs will be dissolved in 10 mM sodium phosphate (pH 7.2) and 100 mM NaCl. The temperature will be increased at a rate of 0.5 °C/min with absorbance readings recorded every 0.2 °C.

Thermodynamic parameters including the change in enthalpy, entropy and free energy derived from the melting assay will be used to draw conclusions on the comparative stability of the modified ODNs

Using the computational chemistry program Hyther®[74], we were able to predict the thermodynamic parameters for the following sequences below (see Table 5.2).

In order to perform our thermal denaturation studies, the duplex and ternary complexes will be annealed first. Then the 3′-end of the ODN containing the *cis*-diol will be cleaved using periodate cleavage.

We expect to successfully generate the duplex and ternary complexes above. Incorporation of a damaged lesion into DNA is expected to affect the stability of ODNs in both single strand and double strand architectures. In studies on the 5′ modified nucleoside, Greenberg and Kodama were able to indicate that the presence of a 5′-aldehyde in DNA greatly affected its stability.[16] We are expecting to observe similar changes in the stability of DNA containing our 3′-damaged lesion.

Table 5.2: Thermodynamic Parameters of Modified ODNs

5′-ACG-TTG-ACT-ACC-GT-3′ **3′-TGC-AAC-TGA-TGG-CA-5′**	In 1.0000 M NaCl and 0.0000 M $MgCl_2$: ΔH^o =-106.20 kcal/mol ΔS^o = -287.83 kcal/mol $\Delta G^o_{37.0}$ = -16.93 kcal/mol T_M = 73.8 ^oC
5′-ACG-TTG-ACT-ACC-GTAGG-CAG-AGT-CCG-3′ **3′-TGC-AAC-TGA-TGG-CATCC-GTC-TCA-GGC-5′**	In 1.0000 M NaCl and 0.0000 M $MgCl_2$: ΔH^o = -208.70 kcal/mol ΔS^o = -560.12 kcal/mol $\Delta G^o_{37.0}$ = -34.98 kcal/mol T_M = 87.7 ^oC

Conclusions

Our approach has allowed us to develop an efficient method for the site-specific generation of 3′-oxothymidine lesions into ODNs. Due to the availability of appropriately derivatized and highly stable amidite **38**, this lesion can be generated selectively using $NaIO_4$ in a variety of sequence context. Once the studies to determine appropriate conditions for the isolation of this lesion are elucidated and its chemical and biological reactivity determined, this lesion can serve as a tool for further studies.

The synthesis of longer ODNs containing our lesion of interest, possibly using polymerase chain reaction and their incorporation into cells could allow us to study their fate *in vivo*.

Chapter 6

6 Experimental procedures

Unless indicated, the organic reactions requiring inert conditions were performed under argon in oven dried glassware, using anhydrous solvents.

6.1 Materials

All reagents and anhydrous solvents were purchased from the following suppliers: Sigma Aldrich, Arcos Organic, Fisher Scientific and Pharmco-AAPER. The reagents were used as obtained, without further purification unless otherwise noted.

For reactions involving dry THF and dry diethyl ether, anhydrous solvents purchased from Arcos organic were further purified using a Pure Solv ^{TM} solvent purification system. Nano pure water was obtained from a PURELAB® Ultra Water Purification System. Deuteurated solvents were purchased from Cambridge Isotope Laboratories for NMR analysis and HPLC grade solvents were used for chromatographic separations.

The Dess-Martin reagent and the Lombardo reagent were both synthesized using published literature.[67,66]

6.2 Structural Analysis

NMR spectroscopy and mass spectroscopy were used to characterize all synthesized products.

6.2.1 NMR Analysis

6.2.1.1 ^{1}H-NMR

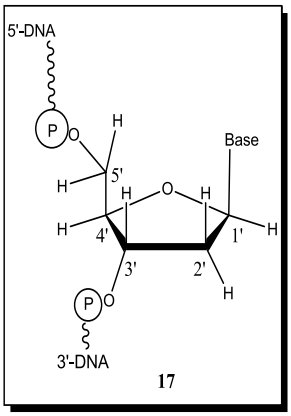

Figure 23: 2-deoxyribose hydrogens

^{1}H-NMR spectra were recorded on Varian VXRs 400, Varian Inova 600 or Bruker Avance 600 NMR spectrometers in $CDCl_3$ and CD_3CN. Chemical shifts were reported in ppm relative to tetramethylsilane (TMS) or CD_3CN as internal references. Coupling constants (J) are reported in hertz (Hz). Multiplicity is as follows: s = singlet, d = doublet, dd = doublet of doublet, t = triplet, q = quartet, m = multiplet. The protons of the carbons of the furanose ring are designated as shown in Figure 23.

6.2.1.2 ^{13}C-NMR

^{13}C-NMR spectra were recorded on Varian VXRs-400, Varian Inova 600 or Bruker Avance 600 NMR spectrometers in $CDCl_3$ and CD_3CN. Chemical shifts were reported in ppm using $CDCl_3$ and CD_3CN as internal references.

6.2.1.3 ^{31}P-NMR

^{31}P NMR data was obtained on a Varian VXRS-400 Nuclear Magnetic Resonance Spectrometer. Chemical shifts for phosphorus NMR were reported in ppm using 85% phosphoric acid as an external standard.

6.2.2 Mass Spectrometry

6.2.2.1 ESI-MS

Electrospray Ionization Mass spectrometry was performed using an Esquire Ion Trap Mass Spectrometer (Bruker Daltonics, Bremen, Germany) equipped with a quadrupole ion-trap mass analyzer. The mass spectrometer was operated in positive ion mode with methanol used as a solvent for most analytes. The $[M+H]^+$ or $[M+Na]^+$ ions signals were obtained.

6.2.2.2 MALDI-MS

MALDI-TOF mass spectra were recorded on a Bruker Daltonics Ultraflex Extreme spectrometer. The matrix consisted of 90% 3-hydroxypicolinic acid (**50** mg/mL in **50**% acetonitrile) and 10% ammonium citrate (**50** mg/mL in nanopure water). Samples were

desalted by solid phase extraction using C18 ZIPTIP^{TM}. The samples were mixed with the matrix solution and spotted on a 100 well stainless steel plate. The analytes were left in open air until complete dryness before the analysis. Alternatively 1 µL of the Matrix solution was spotted on the MALDI plate and left to dry. Then 1 µL of sample was spotted on top of the matrix and air dried. The mass range for measurements was 1000-5000 Da. The instrument was calibrated for each experiment using the Low Molecular weight and high molecular weight calibration mixtures from Bruker. The isotopic peaks and $[M+H]^+$ peaks were recorded.

To facilitate the analysis of small molecules, a matrix solution containing 2,5-dihydroxybenzoic acid (DHB) (20mg/ml in 30% acetonitrile: 0.11 TFA in H_2O) was used.

6.2.2.2.1 High Resolution Mass Spec

High resolution mass spec was obtained from the mass spectrometry and proteomics facility located at the Ohio State University. The analyses were performed on a Micromass Q ToF II mass spectrometer.

6.3 Chromatographic Methods

6.3.1 Thin Layer Chromatography (**TLC**)

We used both aluminum backed and glass backed silica gel plates to monitor the progress of our reactions and the content of our flash chromatography fractions. TLC spots were visualized using a UV lamp at 254 nm. Taking advantage of the presence of carbonyl

groups in our compounds, the plates were stained with a p-anisaldehyde dip and heated to facilitate spots visualization. The p-anisaldehyde dip was made of absolute ethanol, concentrated sulfuric acid and glacial acetic acid in a ratio of 18:1:0.2 with a few drops of p-anisaldehyde.

6.3.2 Flash Chromatography

For steps requiring chromatographic purification, flash chromatography was carried out on a Biotage SP4 flash chromatography system using Biotage Snap KP-SIL Flash cartridges. The solvents used for the purification were either gradients of methanol in DCM (0-10%) or varying ethyl acetate in hexane gradients. The order of elution of compounds was monitored using the instruments UV light and wavelength detector set at 254 nm and 260. Before fractions were concentrated, TLC was performed to confirm purity.

6.3.3 HPLC

Analytical ion exchange HPLC was performed on a Dionex instrument using a Biol C^{R} DNA PacR PA-100 (4 x 205 mm) anion exchange column from Dionex. The instrument was equipped with a dual wavelength UV detector set at 260 nm and 280 nm and Chromeleon software for analysis. Compounds were eluted using a NaCl gradient in sodium acetate buffer (pH 6) and 5% acetonitrile in 20 minutes. The solvent systems used were: solvent A: 25 mM sodium acetate in 5% acetonitrile, pH = 6.0 and Solvent B: 25 mM sodium acetate in 5% acetonitrile, pH = 6.0, 1 M NaCl.

6.4 Other Equipment and devices

Centrifuge - Thermo Electron Sorall Legend Micro21 centrifuge

High vacuum pump – Edwards RV3

Pipettes- Eppendorf Series 2100

pH meter – Fisher Accumet Basic AB15

Rotary evaporator – Heidolph Collegiate Brinkmann rotary evaporator

SpeedVac concentrator – Thermo Electron Savant DNA120

Solvent purification system – Innovative Technology PS-MD-2 Pure Solvent system

Thermal mixer – Eppendorf Thermomixer

Vortex mixer – Fisher Scientific

6.5 Synthesis of 5′-*O*-(2-cyanoethoxy(diisopropylaminophosphino))-3′-*C*-((4,4′-dimethoxytrityl)oxymethyl)-3′-*O*-acetyl-thymidine

6.5.1 5′-*O*-(*t*-Butyldimethylsilyl)thymidine. **(51)**

Thymidine **50** (5.03g, 20.77 mmol) was dissolved in DMF (35 ml). Imidazole (3.4 g, 49.9 mmol) was added in portions over a 25 min period. The reaction was stirred at room temperature overnight under argon atmosphere. At completion NH_3 (1 M, 17 mL) was added to the reaction flask. The organic layer is extracted with diethyl ether (3×100 mL), washed with saturated NaCl (100 mL), dried over $MgSO_4$ and concentrated. The product was purified with column chromatography (0-33% Ethyl acetate in hexane). Yield: 5.35g, 72.3%. ^{1}H NMR ($CDCl_3$) δ 8.27 (s, 1H), 7.51 (s, 1H), 6.38 (m, 1H), 5.31 (s, 1H), 4.48 (m, 1H), 4.04 (d, 1H, J = 2.6 Hz), 3.88 (m, 1H), 2.36 (m, 1H), 2.11 (m, 1H), 1.93 (d, 3H, J = 1.1 Hz), 0.93 (s, 9H) , 0.13 (d, 6H, J = 2.9 Hz)

6.5.2 5′-O-(t-Butyldimethylsilyl)-3′-ketothymidine. **(52)**

A solution of **51** (5.35 g, 15.00 mmoles) in CH_2Cl_2 (45.2 mL) was added to a solution of periodinane (9.64g, 22.59 mmoles) in CH_2Cl_2 (105.4 mL) at 0^o C. The mixture was stirred for 15 min before being brought gradually to room temperature. The reaction was left to run overnight. The mixture was diluted with 451 mL of ethyl ether and added to a cold solution of saturated of $NaHCO_3$/H_2 O (37.5g, 301 ml). The organic layer was washed with water and NaCl successively dried and then concentrated. Yield 4.12 g, 77.44% ^{1}H NMR ($CDCl_3$) δ 8.21 (s, 1H), 7.66 (s, 1H), 6.49 (dd, 1H, J = 8.4, 6.6 Hz),

5.31 (s, 1H), 4.14 (t, 1H, *J* = 1.8, 1.8 Hz), 4.00 (d, 2H, *J* = 2.2 Hz), 2.99 (dd, 1H, *J* = 18.3, 6.6 Hz), 2.43 (dd, 1H, *J* = 18.7, 8.4 Hz), 1.96 (d, 3H, *J* = 1.1 Hz), 0.9 (s, 9H) , 0.10 (d, 6H, *J* = 11.35 Hz)

6.5.3 5′-*O*-(*t*-Butyldimethylsilyl)-3′-deoxy-3′-*C*-methylenethymidine **(53)**

To a solution of **52** (4.12 g, 11.62 mmol) in CH_2Cl_2 (70.8 ml) at 0 ^{o}C was added 3 portions of Lombardo reagents (3×24 ml) in 10 min intervals. The reaction was left in an ice bath for 10 min then removed and stirred at room temperature. After two hours the mixture was poured onto an ice cold solution of $NaHCO_3$. $CHCl_3$ (589 mL) were added to the mixture with stirring. The mixture was filtered through a lower layer of sand and an upper layer of silica. The filtrate was washed with three portions of $CHCl_3$ (3×235 mL). The organic layer was dried over $MgSO_4$, filtered and concentrated. Purification with column chromatography (0-10% CH_3OH in CH_2Cl_2) yielded **53**. Yield: 1.99g, 48.6%. ^{1}H NMR ($CDCl_3$) δ 8.91 (s, 1H), 7.63 (s, 1H), 6.2 (dd, 1H, J = 7.3, 6.6 Hz), 5.11 (d, 1H *J* = 0.5 Hz), 4.51 (s, 1H), 3.88 (m, 3H), 3.01 (dd, 1H, J = 15.6, 5.7 Hz), 2.65-2.50 (m, 1H), 1.93 (s, 3H) , 0.91 (s, 9H), 0.09 (s, 6H).

6.5.4 5′-*O*-(*t*-Butyldimethylsilyl)-3′-*C*-(hydroxymethyl)-thymidine **(54)**

To a flask containing **53** (0.96 g, 2.48 mmol), was added *tert*-butanol (20 mL), pyridine (1 mL) and H_2O (1 mL), *N*-methylmorpholine *N*-oxide (2.11g, 18.1 mmol) and OsO_4 (0.1 ml, 9.8×10^{-3} mmol), were added to the flask with stirring. The flask was then placed in

an oil bath with the internal temperature of the flask was maintained at 76 ^{o}C. Upon completion the mixture was diluted with a 20% aqueous solution of sodium bisulfite (2.5 mL) and concentrated. The residue was then dissolved in NaCl (5 mL), extracted with ethyl acetate (3 × 20 mL) and dried over Na_2SO_4. The crude product was purified using column chromatography (1-3% methanol in DCM) Yield: 0.49 g, 46.5%.^{1}H NMR ($CDCl_3$) δ 8.63 (s, 1H), 7.41-7.39 (m, 3H), 6.29-6.26 (dd, 1H, J = 9.03, 5.37 Hz), 4.03-4.02 (m, 1H), 4.01 (m, 1H), 3.86 (m, 1H), 3.85 (d, 1H *J* = 1.2 Hz), 3.75 (d, 1H, *J* = 11.72 Hz), 2.36 (m, 1H), 1.96 (dd, 1H, *J*= 13.1, 9.2 Hz), 1.93 (s, 3H) , 0.93 (s, 9H), 0.15 (s, 6H).

6.5.5 5′-*O*-(*t*-Butyldimethylsilyl)-3′-*C*-((4,4′-dimethoxytrityl)oxymethyl)thymidine **(55)**

Compound **54** (0.425 g, 1.09 mmol) was dissolved in 12 mL of pyridine. 4,4'-dimethoxytrityl chloride (1.119 g, 3.3 mmol) was added to the reaction mixture. The reaction was left to stir overnight. At completion the reaction mixture was diluted with ethyl acetate (10 mL), washed with H_2O (3 × 10 mL), $NaHCO_3$ (3 × 10 mL), and NaCl (3 × 10 mL). The organic layer was dried over Na_2SO_4 and concentrated. The crude product was purified with column chromatography with a gradient of ethyl acetate and hexanes. The synthesis of known compound **55** was completed in five steps from commercially available thymidine *via* methods developed by Nielsen et al. The analytical data corresponds to the literature.[75]

^{1}H NMR (CD_3CN) δ 9.16 (s, 1H), 7.48-7.43 (m, 3H), 7.35-7.20 (m, 9 H), 6.89-6.82 (m, 5H), 6.16 (dd, 1H, *J* = 9.28 Hz, 5.13 Hz), 3.92 (m, 1H), 3.76 (s, 6H), 3.72-3.68 (m, 2H), 3.46 (dd, 1H, *J* = 11.7 , 4.39 Hz), 3.09 (d, 1H *J* = 9.3 Hz), 3.8 (d, 1H, *J* = 9.3 Hz), 2.42 (dd, 1H, *J* = 12.94, 5.13 Hz), 1.91 (dd, 1H, *J*= 12.9, 9.3 Hz), 1.79 (s, 3H) , 0.74 (s, 9H), -0.07 (s, 3H), -0.09 (s, 3H)^{13}C NMR (CD_3CN) δ 164.72, 159.66, 151.41, 146.09, 140.9, 136.76, 136.65, 136.56, 131.17, 131.14, 130.02, 129.05, 128.84, 128.64, 127.83, 127.79, 114.10, 114.05, 113.86, 110.57, 88.31, 86.98, 85.75, 81.52, 66.82, 63.35, 55.91, 55.88, 43.23, 26.36, 18.82, 12.63, -5.14, -5.19 HRMS: $C_{28}H_{48}N_2O_8SiNa$ Calc. 711.31, found 711.31

6.5.6 5′-*O*-(*t*-Butyldimethylsilyl)-3′-*C*-((4,4′-dimethoxytrityl)oxymethyl)-3′-*O*-acetyl-thymidine **(56)**

Compound **55** (0.53 g, 0.78 mmol) was coevaporated in pyridine (5 mL). Dry pyridine (5 mL) was then added to the flask followed by addition of acetic anhydride (0.88 mL, 9.76 mmol) and excess DMAP under argon. The mixture was allowed to stir overnight, then diluted with ethyl acetate (100 mL), washed with water (2 × 50 mL) and saturated NaCl (2 × 50 mL). The organic layer was dried over Na_2SO_4, concentrated and purified by column chromatography (0 - 10% methanol in DCM). Yield: 0.45 g, 80 %. ^{1}H NMR (CD_3CN) δ 9.15 (s, 1H), 7.42-7.37 (m, 3H), 7.31-7.20 (m, 7 H), 6.87-6.84 (m, 4H), 6.14 (dd, 1H, *J* = 9.2 Hz., 5.1 Hz), 4.36 (t, 1H, *J* = 3.67 Hz), 3.81 (dd, 1H, *J* = 11.7 Hz, 3.3 Hz), 3.77-3.74 (m, 7H), 3.6-3.55 (m, 2H), 2.85 (dd, 1H, *J* = 13.57 Hz, 5.1 Hz), 2.04 (s, 3H), 2.02 (dd, 1H, *J* = 13.9 Hz, 9.54 Hz), 1.8 (d, 3H, *J* = 1.47 Hz), 0.76 (s, 9H), -0.05 (s,

3H),-0.07 (s, 3H) ^{13}C NMR (CD_3CN) δ 171.28, 164.68, 159.63, 151.47, 146.12, 136.69, 136.65, 136.18, 131.14, 131.10, 128.98, 128.96, 127.97, 114.23, 114.19, 111.09, 89.75, 86.92, 85.25, 84.58, 63.12, 62.92, 55.99, 42.68, 26.41, 22.34, 18.90, 12.82, -5.13, -5.16 HRMS (M+Na): $C_{40}H_{50}N_2O_9Na$ calc. 753.32, found 753.32

6.5.7 3′-*C*-((4,4′-dimethoxytrityl)oxymethyl)-3′-*O*-acetyl-thymidine **(57)**

Tetra-n-butylammonium fluoride (TBAF) (4 mL, 4 mmol) was added to a solution of **56** (0.40 g, 0.57 mmol) in 5 mL THF under argon. The reaction was left to stir overnight. The mixture was then diluted with ethyl acetate (10 mL) and washed with water (3 × 5 mL) water. The organic layer was dried over Na_2SO_4 and concentrated. The residue was purified by column chromatography using 0-10 % methanol in DCM Yield: 0.27 g, 82% ^{1}H NMR δ 8.97 (s, 1H), 7.59 (d, 1H, *J* = 1.1 Hz), 7.42-7.39 (m, 2H), 7.33-7.21 (m, 7H), 6.89-6.85 (m, 4H), 6.15 (dd, 1H, *J* = 9.5 Hz, 5.5 Hz), 4.32 (t, 1H, *J* = 3.3 Hz), 4.06 (dd, 1H, *J* = 14.3 Hz, 6.97 Hz), 3.77 (s, 6H), 3.75 (s, 1H), 3.67 -3.62 (m, 2H), 3.50-3.46 (m, 1H), 3.15 (t, 1H, *J* = 4.77 Hz), 2.80-2.75 (dd, 1H, *J* = 13.9 Hz, 5.5 Hz), 2.07 (s, 3H), 2.0 (dd, 1H, *J* = 13.9 Hz, 9.5 Hz), 1.78 (d, 1H, *J* = 1.1 Hz) 1.20 (t, 1H, *J* = 7.3 Hz) ^{13}C NMR δ 171.35, 164.71, 159.68, 151.57, 145.85, 137.12, 136.55, 130.98, 128.81, 127.86, 118.30, 114.02, 111.14, 90.21, 86.94, 85.49, 84.69, 70.03, 62.76, 61.34, 55.86, 55.18, 41.40, 29.65, 22.32, 12.57. HRMS (M+Na): $C_{34}H_{36}N_2O_9Na$ calc. 639.23, found 639.23

6.5.8 5′-*O*-(2-cyanoethoxy(diisopropylaminophosphino))-3′-*C*-((4,4′-dimethoxytrityl)oxymethyl)-3′-O-acetyl-thymidine **(58)**

To a solution of **57** (0.24 g, 0.4 mmol) in tetrazole (0.47 mL, 0.21 mmol) was added 2-cyanoethyl tetraisopropylphosphoramidite in tetrazole (0.2 mL, 0.61 mmol). The reaction was stirred at room temperature for two hours. The mixture was then diluted with 2.8 mL of dichloromethane then washed twice with phosphate buffer (1.4 mL, pH 7). The aqueous phase was extracted twice with DCM (2× 2.8 mL). The organic layer was dried over Na_2SO_4 and concentrated. The substrate was purified by column chromatography (0-10% methanol in DCM). Yield: 0.22 g, 69%.^{1}H NMR δ 7.8 (s, 1H), 7.45-7.2 (m, 28H), 6.32-6.28 (m, 1H), 6.16-6.12 (m, 1H), 4.54-4.48 (m, 2H), 4.08-4.04 (m, 6H), 3.90-3.85 (m, 1H), 3.77-3.43 (m, 29H), 2.94-2.89 (m, 2H), 2.70-2.49 (m, 5H), 2.43-2.36 (s, 9H), 2.10 (s, 3H), 2.09-2.095 (m, 5H), 1.96 (s, 10H), 1.85-1.80 (m,6H), 1.29-1.23 (m, 6H), 1.22-1.19 (m, 11H), 1.16, (d, 6H, *J* = 7.0 Hz), 1.13, (d, 5H, *J* = 6.6 Hz), 1.07, (d, 6H, *J*=7.0 Hz), 0.98 (d, 5H, *J* = 7 Hz), 0.92 (t, *J* = 14.67, 7.34 Hz) ^{13}CNMR δ 171.79, 171.39, 171.29, 165.06, 159.81, 159.78, 151.83, 151.60, 145.97, 136.91, 136.61, 136.52, 136.39, 131.21, 131.08, 128.96, 128.01, 122.04, 120.08, 119.46, 119.29, 118.38, 114.19, 111.11, 90.23, 89.58, 87.07, 84.98, 84.49, 64.90, 63.43, 61.06, 60.03, 59.62, 55.99, 46.78, 46.53, 46.49, 43.93, 43.91, 42.21, 41.36, 32.96, 31.50, 29.96, 26.64, 25.11, 24.98, 24.93, 22.37, 21.25, 21.08, 19.89, 15.85, 14.62, 12.76. ESI-MS (M+Na): $C_{43}H_{53}N_4O_{10}PNa$ calc. 839.34, found 839.40

6.6 Oligonucleotides Synthesis

6.6.1 General methods

Oligonucleotides were synthesized on an Applied Biosystems DNA/RNA Synthesizer ABI 391 and ABI 394 using standard conditions on a 0.2 umol scale using controlled pore glass columns (3′-dimethoxytrityl-N-benzoyl-2′-deoxyribose nucleotides, 5′-succinoyl-long chain alkylamino-CPG column). All reagents for automated synthesis were purchased from Glen Research and used without further purification. The synthesis of the modified nucleotides proceeded from the 5′ to 3′ direction with standard phosphoramidite chemistry. The coupling time for the incorporation of the modification was 15 minutes and standard instrument conditions were used. Trichloroacetic acid (3% in DCM) was used for detritylation of the solid support. The activator for the coupling steps was 5-ethylthio-1H-tetrazole in acetonitrile. Acetic anhydride in THF/pyridine and 1-methylimidazole in THF were used for the capping step. Oxidation was achieved with 0.02 M I_2 in pyridine/THF/H_2O.

6.6.2 Synthesis of modified oligonucleotides **36**

ODN 36a and **36b** were synthesized on a 0.2 umol scale with the phosphoramidite precursor **58** at the 3′-end. The coupling time was 15 minutes and standard instrument conditions were used. Cleavage from the solid support and deprotection of the bases were achieved by incubating the DNA in 1.5 M NH_4OH for 18 hours. The sequences were then purified using OPC purification and quantified using UV-VIS. The samples were then

analyzed for purity using ion-exchange HPLC and the structures identified with MALDI-TOF MS.

6.6.3 Cleavage from solid support and deprotection

At the end of the synthesis, the oligonucleotides were cleaved from the solid support by treatment with 1 ml concentrated ammonium hydroxide (28-30%). The resin was left on the thermomixer for 18 hours at 55 ^{0}C.

6.6.4 Oligonucleotides Purification

The oligonucleotides synthesized with a trityl group at the 5′-end were purified using oligonucleotide purification cartridges (OPC) with Glen Pak Column purchased from Glen Research.

Following cleavage from the solid support, the solution of concentrated ammonia containing the oligonucleotide is diluted to 4 ml with deionized water. Using a polypropylene syringe, the OPC cartridge is activated by flushing the column with 5 ml acetonitrile. A 5 mL solution of 2 M TEAA buffer is then passed through the column drop wisely. The oligo is then loaded onto the column at the rate of one drop per second. This allows the tritylated oligo to bind to the column while other byproducts are flushed through. The column is then flushed with a 5 mL solution of 1.5 M concentrated ammonium hydroxide followed by a flush with deionized water. Detritylation of the oligonucleotide is accomplished through slowly pushing through 5 mL solution of 2%

TFA. The column is then flushed again with deionized water before the oligonucleotide is eluted by slowly running a 20% solution of acetonitrile in water solution.

For oligonucleotides synthesized using the trityl-off method, purification was accomplished using ion exchange HPLC as described above.

6.6.5 Oligonucleotide quantification

The oligonucleotides were quantified using UV-VIS. UV spectra were recorded on an Aligent 8453 UV/Visible spectrometer at the wavelengths of 260 nm using standardized quantification methods. The extinction coefficient for **36a** and **36b** were 81 and 149.12 $M^{-1}.cm^{-1}$.

6.7 Generation of 38a *via* oxidative cleavage with NaIO4

To a solution of **ODN 36a** in water (100 uL, 4.7 nmoles), was added 4.7 mmoles of $NaIO_4$ from a 0.2 M stock solution. The reaction mixture was stirred at 20° C. The reaction progress was monitored with MALDI-TOF MS, and HPLC at 30 min, 1 hr, 2 hr and 4 hr: 10 uL of the reaction mixture was desalted using C18 ZIPTIP® and the crude reaction mixture analyzed with MALDI-TOF MS and ion-exchange HPLC.

References

1. Lodish H, B. A., Zipursky SL, et al. , Structure of Nucleic Acids. . In *Molecular Cell Biology.*, 4th ed.; W. H. Freeman: New York: , 2000.

2. Berg JM, T. J., Stryer L. , DNA Can Assume a Variety of Structural Forms. In *Biochemistry*, 5th edition ed.; Freeman, W. H., Ed. New York, 2002.

3. Alberts B, J. A., Lewis J, et al. , *Molecular Biology of the Cell:The Structure and Function of DNA*. 4th ed.; Garland Science: New York, 2002.

4. Alvarez-Salas, L. M., Nucleic acids as therapeutic agents. *Current topics in medicinal chemistry* **2008,** *8* (15), 1379-404.

5. Wright, K., AIDS therapy: First tentative signs of therapeutic promise. *Nature* **1986,** *323* (6086), 283-283.

6. Krieg, A. M.; Yi, A.-K.; Matson, S.; Waldschmidt, T. J.; Bishop, G. A.; Teasdale, R.; Koretzky, G. A.; Klinman, D. M., CpG motifs in bacterial DNA trigger direct B-cell activation. *Nature* **1995,** *374* (6522), 546-549.

7. Klinman, D. M., Immunotherapeutic uses of CpG oligodeoxynucleotides. *Nat Rev Immunol* **2004,** *4* (4), 249-259.

8. Ames, B. N.; Shigenaga, M. K.; Hagen, T. M., Oxidants, antioxidants, and the degenerative diseases of aging. *Proceedings of the National Academy of Sciences of the United States of America* **1993,** *90* (17), 7915-22.

9. Huang, H.; Greenberg, M. M., Synthesis and analysis of oligonucleotides containing abasic site analogues. *J Org Chem* **2008,** *73* (7), 2695-703.

10. Mattes, W. B.; Hartley, J. A.; Kohn, K. W., DNA sequence selectivity of guanine-N7 alkylation by nitrogen mustards. *Nucleic acids research* **1986,** *14* (7), 2971-2987.

11. Talhout, R.; Schulz, T.; Florek, E.; van Benthem, J.; Wester, P.; Opperhuizen, A., Hazardous Compounds in Tobacco Smoke. *International Journal of Environmental Research and Public Health* **2011,** *8* (2), 613-628.

12. Cheung-Ong, K.; Giaever, G.; Nislow, C., DNA-Damaging Agents in Cancer Chemotherapy: Serendipity and Chemical Biology. *Chemistry & Biology 20* (5), 648-659.

13. Brunaud, L.; Alberto, J. M.; Ayav, A.; Gerard, P.; Namour, F.; Antunes, L.; Braun, M.; Bronowicki, J. P.; Bresler, L.; Gueant, J. L., Effects of vitamin B12 and folate deficiencies on DNA methylation and carcinogenesis in rat liver. *Clinical chemistry and laboratory medicine : CCLM / FESCC* **2003,** *41* (8), 1012-9.

14. Winterbourn, C. C., Toxicity of iron and hydrogen peroxide: the Fenton reaction. *Toxicology letters* **1995,** *82-83*, 969-74.

15. Schroeder, G. K.; Lad, C.; Wyman, P.; Williams, N. H.; Wolfenden, R., The time required for water attack at the phosphorus atom of simple phosphodiesters and of DNA. *Proceedings of the National Academy of Sciences of the United States of America* **2006,** *103* (11), 4052-4055.

16. Shapiro R, D. M., Acidic hydrolysis of deoxycytidine and deoxyuridine derivatives. The general mechanism of deoxyribonucleoside hydrolysis. *Biochemistry.* **1972;,** *11*, 23–29.

17. Shapiro R, K. R., The deamination of cytidine and cytosine by acidic buffer solutions. Mutagenic implications. *Biochemistry* **1966,** (5), 2358–2362.

18. Karran P, L. T., Hypoxanthine in deoxyribonucleic acid: generation of heat-induced hydrolysis of adenine residues and release in free form by a deoxyribonucleic acid glycosylase in calf thymus. *Biochemistry* **1980,** *19*, 6005–601.

19. Shen JC, R. W., Jones PA. , The rate of hydrolytic deamination of 5-methylcytosine in double-stranded DNA. . *Nucleic Acids Res.* **1994;,** *22* (6), 972–976.

20. Lindahl T, N. B., Rate of depurination of native deoxyribonucleic acid. *Biochemistry* **1972,** *11*, 3610–3618.

21. Lindahl T, K. O., Heat-induced depyrimidination of deoxyribonucleic acid in neutral solution.. *Biochemistry* **1973,** *12* (25), 5151-5154.

22. Auerbach P, B. R., Bailey EA, Krokan HE, Demple B, Mutagenic specificity of endogenously generated abasic sites in Saccharomyces cerevisiae chromosomal DNA. *Proc Natl Acad Sci U S A.* **2005,** *102* (49), 17711-6.

23. Lindahl T, A. A., Rate of chain breakage at apurinic sites in double-stranded deoxyribonucleic acid. *Biochemistry* **1972** *11* (19), 3618-23.

24. Rydberg, B.; Lindahl, T., NON-ENZYMATIC METHYLATION OF DNA BY THE INTRACELLULAR METHYL-GROUP DONOR S-ADENOSYL-L-METHIONINE IS A POTENTIALLY MUTAGENIC REACTION. *Embo J.* **1982,** *1* (2), 211-216.

25. Lindahl, T., DNA-REPAIR ENZYMES. *Annu. Rev. Biochem.* **1982,** *51*, 61-87.

26. Abbott, P. J.; Saffhill, R., DNA synthesis with methylated poly(dC-dG) templates. Evidence for a competitive nature to miscoding by O(6)-methylguanine. *Biochimica et biophysica acta* **1979,** *562* (1), 51-61.

27. Jackson, A. L.; Loeb, L. A., The contribution of endogenous sources of DNA damage to the multiple mutations in cancer. *Mutation Research/Fundamental and Molecular Mechanisms of Mutagenesis* **2001,** *477* (1–2), 7-21.

28. Michiels, C.; Raes, M.; Toussaint, O.; Remacle, J., Importance of Se-glutathione peroxidase, catalase, and Cu/Zn-SOD for cell survival against oxidative stress. *Free radical biology & medicine* **1994,** *17* (3), 235-48.

29. Kohen, R.; Nyska, A., Oxidation of biological systems: oxidative stress phenomena, antioxidants, redox reactions, and methods for their quantification. *Toxicologic pathology* **2002,** *30* (6), 620-50.

30. Higuchi, Y.; Linn, S., Purification of All Forms of HeLa Cell Mitochondrial DNA and Assessment of Damage to It Caused by Hydrogen Peroxide Treatment of Mitochondria or Cells. *Journal of Biological Chemistry* **1995,** *270* (14), 7950-7956.

31. Wagner, J. R.; Hu, C. C.; Ames, B. N., Endogenous oxidative damage of deoxycytidine in DNA. *Proceedings of the National Academy of Sciences* **1992,** *89* (8), 3380-3384.

32. Burcham, P. C., Internal hazards: baseline DNA damage by endogenous products of normal metabolism. *Mutat. Res. Genet. Toxicol. Environ. Mutagen.* **1999,** *443* (1-2), 11-36.

33. (a) Dedon, P. C., The chemical toxicology of 2-deoxyribose oxidation in DNA. *Chemical research in toxicology* **2008,** *21* (1), 206-19; (b) Greenberg, M. M., Elucidating DNA damage and repair processes by independently generating reactive and metastable intermediates. *Organic & biomolecular chemistry* **2007,** *5* (1), 18-30; (c) Gates, K. S., An overview of chemical processes that damage cellular DNA: spontaneous hydrolysis, alkylation, and reactions with radicals. *Chemical research in toxicology* **2009,** *22* (11),

1747-60; (d) Greenberg, M. M., Investigating nucleic acid damage processes via independent generation of reactive intermediates. *Chemical research in toxicology* **1998,** *11* (11), 1235-48.

34. (a) Balasubramanian, B.; Pogozelski, W. K.; Tullius, T. D., DNA strand breaking by the hydroxyl radical is governed by the accessible surface areas of the hydrogen atoms of the DNA backbone. *Proceedings of the National Academy of Sciences of the United States of America* **1998,** *95* (17), 9738-43; (b) Pogozelski, W. K.; Tullius, T. D., Oxidative Strand Scission of Nucleic Acids: Routes Initiated by Hydrogen Abstraction from the Sugar Moiety. *Chemical reviews* **1998,** *98* (3), 1089-1108.

35. (a) Pardo, L.; Banfelder, J. R.; Osman, R., Theoretical studies of the kinetics, thermochemistry, and mechanism of hydrogen-abstraction from methanol and ethanol. *Journal of the American Chemical Society* **1992,** *114* (7), 2382-2390; (b) Miaskiewicz, K.; Osman, R., Theoretical study on the deoxyribose radicals formed by hydrogen abstraction. *Journal of the American Chemical Society* **1994,** *116* (1), 232-238.

36. Chen, B.; Vu, C. C.; Byrns, M. C.; Dedon, P. C.; Peterson, L. A., Formation of 1,4-Dioxo-2-butene-Derived Adducts of 2‘-Deoxyadenosine and 2‘-Deoxycytidine in Oxidized DNA. *Chemical research in toxicology* **2006,** *19* (8), 982-985.

37. Nicolaou, K. C.; Smith, A. L.; Yue, E. W., Chemistry and biology of natural and designed enediynes. *Proceedings of the National Academy of Sciences* **1993,** *90* (13), 5881-5888.

38. Dedon, P. C.; Goldberg, I. H., Free-radical mechanisms involved in the formation of sequence-dependent bistranded DNA lesions by the antitumor antibiotics bleomycin, neocarzinostatin, and calicheamicin. *Chemical research in toxicology* **1992,** *5* (3), 311-32.

39. Chen, B.; Bohnert, T.; Zhou, X.; Dedon, P. C., 5‘-(2-Phosphoryl-1,4-dioxobutane) as a Product of 5‘-Oxidation of Deoxyribose in DNA: Elimination as trans-1,4-Dioxo-2-butene and Approaches to Analysis. *Chemical research in toxicology* **2004,** *17* (11), 1406-1413.

40. Kodama, T.; Greenberg, M. M., Preparation and Analysis of Oligonucleotides Containing Lesions Resulting from C5‘-Oxidation. *The Journal of Organic Chemistry* **2005,** *70* (24), 9916-9924.

41. Guan, L.; Greenberg, M. M., An Oxidized Abasic Lesion as an Intramolecular Source of DNA Adducts. *Australian journal of chemistry* **2011,** *64* (4), 438-442.

42. Manetto, A.; Georganakis, D.; Leondiadis, L.; Gimisis, T.; Mayer, P.; Carell, T.; Chatgilialoglu, C., Independent Generation of C5‘-Nucleosidyl Radicals in Thymidine and 2‘-Deoxyguanosine. *The Journal of Organic Chemistry* **2007,** *72* (10), 3659-3666.

43. Giloni, L.; Takeshita, M.; Johnson, F.; Iden, C.; Grollman, A. P., Bleomycin-induced strand-scission of DNA. Mechanism of deoxyribose cleavage. *The Journal of biological chemistry* **1981,** *256* (16), 8608-15.

44. Giese, B.; Beyrich-Graf, X.; Erdmann, P.; Petretta, M.; Schwitter, U., The chemistry of single-stranded 4'-DNA radicals: influence of the radical precursor on anaerobic and aerobic strand cleavage. *Chem Biol* **1995,** *2* (6), 367-75.

45. Povirk, L. F., DNA damage and mutagenesis by radiomimetic DNA-cleaving agents: bleomycin, neocarzinostatin and other enediynes. *Mutation research* **1996,** *355* (1-2), 71-89.

46. (a) Marx, A.; Amacker, M.; Stucki, M.; Hubscher, U.; Bickle, T. A.; Giese, B., 4'-Acylated thymidine 5'-triphosphates: a tool to increase selectivity towards HIV-1 reverse transcriptase. *Nucleic acids research* **1998,** *26* (17), 4063-7; (b) Giese, B.; Erdmann, P.; Schäfer, T.; Schwitter, U., Synthesis of a 4′-Selenated 2-Deoxyadenosine Derivative: A Novel Precursor suitable for the Preparation of Modified Oligonucleotides. *Synthesis* **1994,** *1994* (12), 1310-1312.

47. Kim, J.; Kreller, C. R.; Greenberg, M. M., Preparation and analysis of oligonucleotides containing the c4'-oxidized abasic site and related mechanistic probes. *J Org Chem* **2005,** *70* (20), 8122-9.

48. Colson, A.; Sevilla, M., Elucidation of primary radiation damage in DNA through application of ab initio molecular orbital theory. *International journal of radiation biology* **1995,** *67* (6), 627-645.

49. Sitlani, A.; Long, E. C.; Pyle, A. M.; Barton, J. K., DNA photocleavage by phenanthrenequinone diimine complexes of rhodium(III): shape-selective recognition and reaction. *Journal of the American Chemical Society* **1992,** *114* (7), 2303-2312.

50. Collins, C.; Zhou, X.; Wang, R.; Barth, M. C.; Jiang, T.; Coderre, J. A.; Dedon, P. C., Differential oxidation of deoxyribose in DNA by gamma and alpha-particle radiation. *Radiation research* **2005,** *163* (6), 654-62.

51. Stubbe, J.; Kozarich, J. W., Mechanisms of bleomycin-induced DNA degradation. *Chemical reviews* **1987,** *87* (5), 1107-1136.

52. Awada, M.; Dedon, P. C., Formation of the 1,N2-glyoxal adduct of deoxyguanosine by phosphoglycolaldehyde, a product of 3'-deoxyribose oxidation in DNA. *Chemical research in toxicology* **2001,** *14* (9), 1247-53.

53. Lahoud, G. A.; Hitt, A. L.; Bryant-Friedrich, A. C., Aerobic Fate of the C-3'-Thymidinyl Radical in Single-Stranded DNA. *Chemical research in toxicology* **2006,** *19* (12), 1630-1636.

54. Kim, J.; Weledji, Y. N.; Greenberg, M. M., Independent Generation and Characterization of a C2'-Oxidized Abasic Site in Chemically Synthesized Oligonucleotides. *The Journal of Organic Chemistry* **2004,** *69* (18), 6100-6104.

55. Sugiyama, H.; Tsutsumi, Y.; Fujimoto, K.; Saito, I., Photoinduced deoxyribose C2' oxidation in DNA. Alkali-dependent cleavage of erythrose-containing sites via a retroaldol reaction. *Journal of the American Chemical Society* **1993,** *115* (11), 4443-4448.

56. Pitie, M.; Bernadou, J.; Meunier, B., Oxidation at Carbon-1' of DNA Deoxyriboses by the Mn-TMPyP/KHSO5 System Results from a Cytochrome P-450-type Hydroxylation Reaction. *Journal of the American Chemical Society* **1995,** *117* (10), 2935-2936.

57. Neyhart, G. A.; Cheng, C.-C.; Thorp, H. H., Kinetics and Mechanism of the Oxidation of Sugars and Nucleotides by Oxoruthenium(IV): Model Studies for Predicting Cleavage Patterns in Polymeric DNA and RNA. *Journal of the American Chemical Society* **1995,** *117* (5), 1463-1471.

58. Urata, H.; Akagi, M., Photo-induced formation of the 2-deoxyribonolactone-containing nucleotide for d(ApCpA); effects of neighboring bases and modification of deoxycytidine. *Nucleic acids research* **1991,** *19* (8), 1773-1778.

59. Kow, Y. W.; Bao, G.; Minesinger, B.; Jinks-Robertson, S.; Siede, W.; Jiang, Y. L.; Greenberg, M. M., Mutagenic effects of abasic and oxidized abasic lesions in Saccharomyces cerevisiae. *Nucleic acids research* **2005,** *33* (19), 6196-202.

60. Hashimoto, M.; Greenberg, M. M.; Kow, Y. W.; Hwang, J.-T.; Cunningham, R. P., The 2-Deoxyribonolactone Lesion Produced in DNA by Neocarzinostatin and Other Damaging Agents Forms Cross-links with the Base-Excision Repair Enzyme Endonuclease III. *Journal of the American Chemical Society* **2001,** *123* (13), 3161-3162.

61. Kroeger, K. M.; Jiang, Y. L.; Kow, Y. W.; Goodman, M. F.; Greenberg, M. M., Mutagenic effects of 2-deoxyribonolactone in Escherichia coli. An abasic lesion that disobeys the A-rule. *Biochemistry* **2004,** *43* (21), 6723-33.

62. Sugiyama, H.; Fujimoto, K.; Saito, I., Stereospecific 1,2-Hydride Shift in Ribonolactone Formation in the Photoreaction of 2'-Iododeoxyuridine. *Journal of the American Chemical Society* **1995,** *117* (10), 2945-2946.

63. (a) Cook, G. P.; Greenberg, M. M., A Novel Mechanism for the Formation of Direct Strand Breaks upon Anaerobic Photolysis of Duplex DNA Containing 5-Bromodeoxyuridine. *Journal of the American Chemical Society* **1996,** *118* (42), 10025-10030; (b) Cook, G. P.; Chen, T.; Koppisch, A. T.; Greenberg, M. M., The effects of secondary structure and O2 on the formation of direct strand breaks upon UV irradiation of 5-bromodeoxy-uridine-containing oligonucleotides. *Chemistry & Biology* **1999,** *6* (7), 451-459.

64. (a) Urata, H. A., Masao A convenient synthesis of oligonucleotides with a 3′-phosphoglycolate and 3′-phosphoglycaldehyde terminus.

Tetrahedron Letters **1993,** *34*, 4015-4018; (b) Karino, N.; Ueno, Y.; Matsuda, A., Synthesis and properties of oligonucleotides containing 5-formyl-2'-deoxycytidine: in vitro DNA polymerase reactions on DNA templates containing 5-formyl-2'-deoxycytidine. *Nucleic acids research* **2001,** *29* (12), 2456-63.

65. Kim, J.; Weledji, Y. N.; Greenberg, M. M., Independent generation and characterization of a C2'-oxidized abasic site in chemically synthesized oligonucleotides. *J Org Chem* **2004,** *69* (18), 6100-4.

66. Dess, D. B.; Martin, J. C., Readily accessible 12-I-5 oxidant for the conversion of primary and secondary alcohols to aldehydes and ketones. *The Journal of Organic Chemistry* **1983,** *48* (22), 4155-4156.

67. Lombardo, L., Methylenation of carbonyl compounds with Zn · CH2Br2 · TiCl4. Application to gibberellins. *Tetrahedron Letters* **1982,** *23* (41), 4293-4296.

68. Greene, T. W. W., P. G. M., Protecting Groups in Organic Chemistry. John Wiley & Sons: New York, 1999.

69. Corey, E. J.; Venkateswarlu, A., Protection of hydroxyl groups as tert-butyldimethylsilyl derivatives. *Journal of the American Chemical Society* **1972,** *94* (17), 6190-6191.

70. Wiberg, K. B.; Saegebarth, K. A., The Mechanisms of Permanganate Oxidation. IV. Hydroxylation of Olefins and Related Reactions. *Journal of the American Chemical Society* **1957,** *79* (11), 2822-2824.

71. Schroeder, M., Osmium tetraoxide cis hydroxylation of unsaturated substrates. *Chemical reviews* **1980,** *80* (2), 187-213.

72. Sobkowski, M.; Kraszewski, A.; Stawinski, J., Recent Advances in H-Phosphonate Chemistry. Part 2. Synthesis of C-Phosphonate Derivatives. *Topics in current chemistry* **2014**.

73. Reese, C. B., Oligo- and poly-nucleotides: 50 years of chemical synthesis. *Organic & biomolecular chemistry* **2005,** *3* (21), 3851-3868.

74. SantaLucia, J. Hyther.

75. Wengel, J.; Svendsen, M. L.; J∅rgensen, P. N.; Nielsen, C., Synthesis of Novel 3′-C-(Hydroxymethyl)thymidines and Oligodeoxynucleotide Analogues Containing Compressed 3′-C-Hydroxymethyl-Linked Phosphodiester Backbones. *Nucleosides and Nucleotides* **1995,** *14* (7), 1465-1479.

Appendix A

Supplemental information

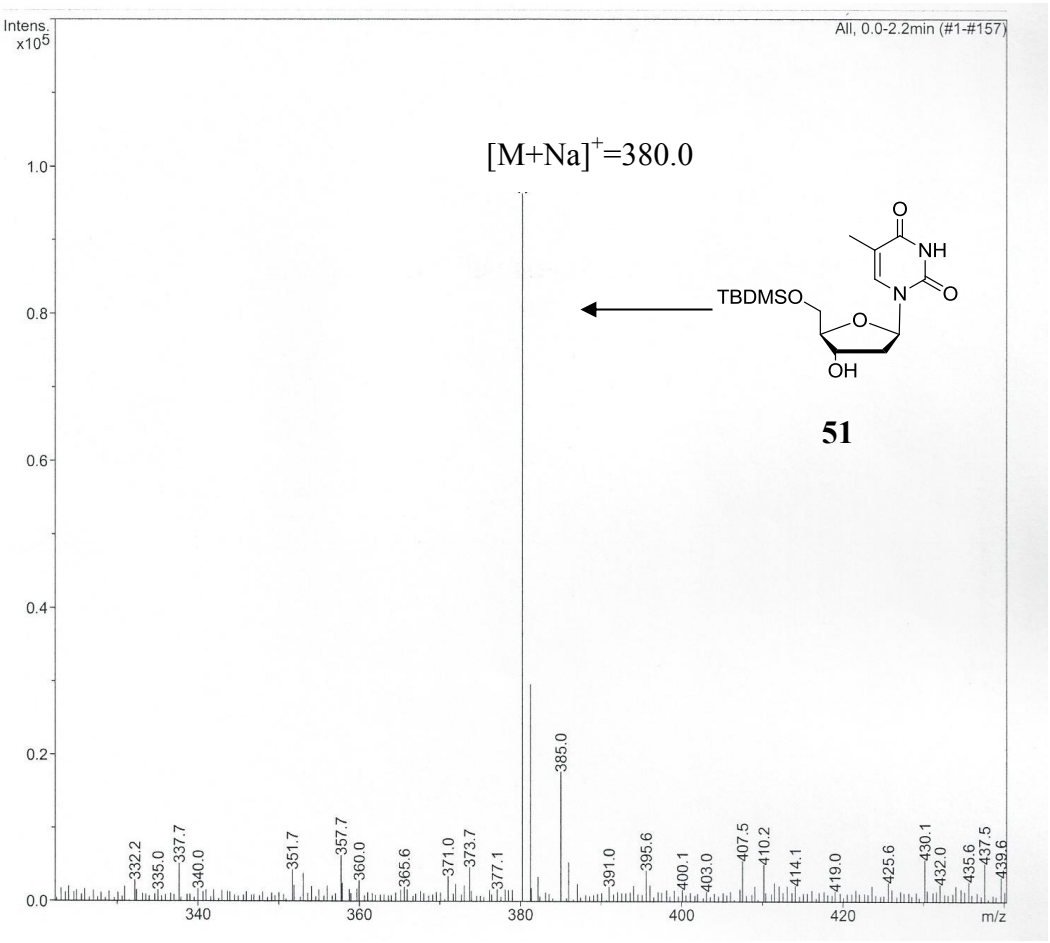

Figure 24: ESI-MS of Compound 51

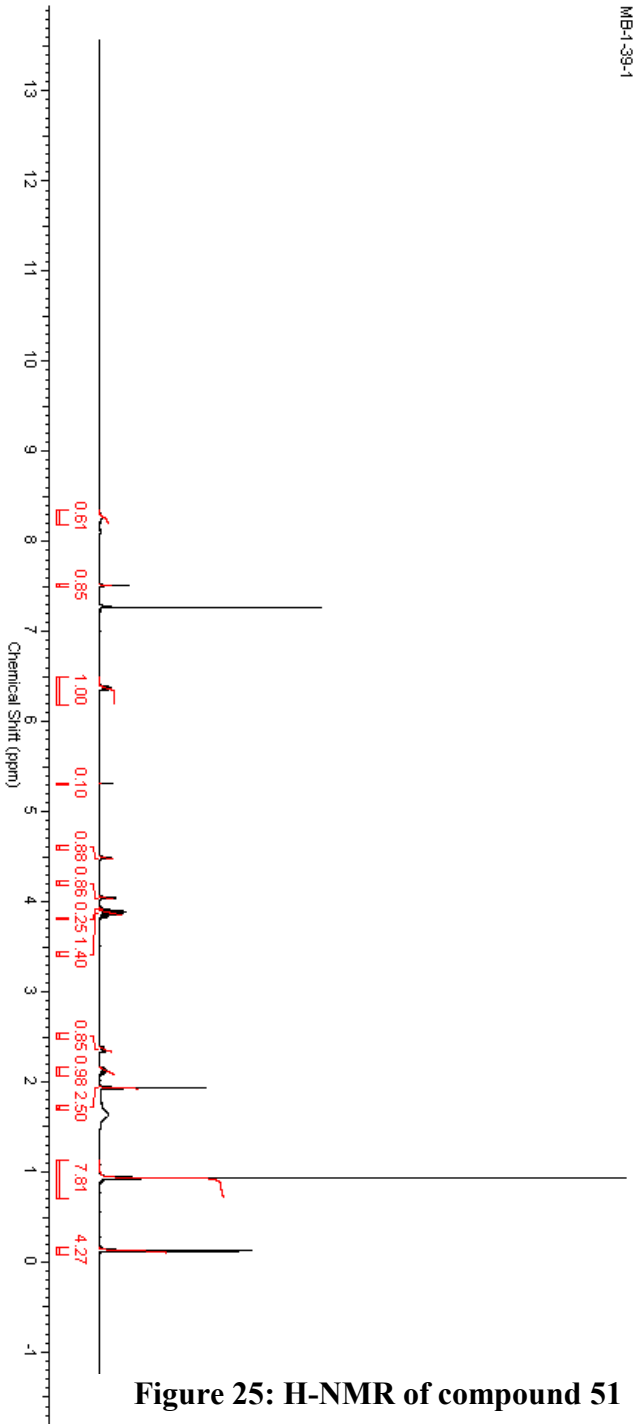

Figure 25: H-NMR of compound 51

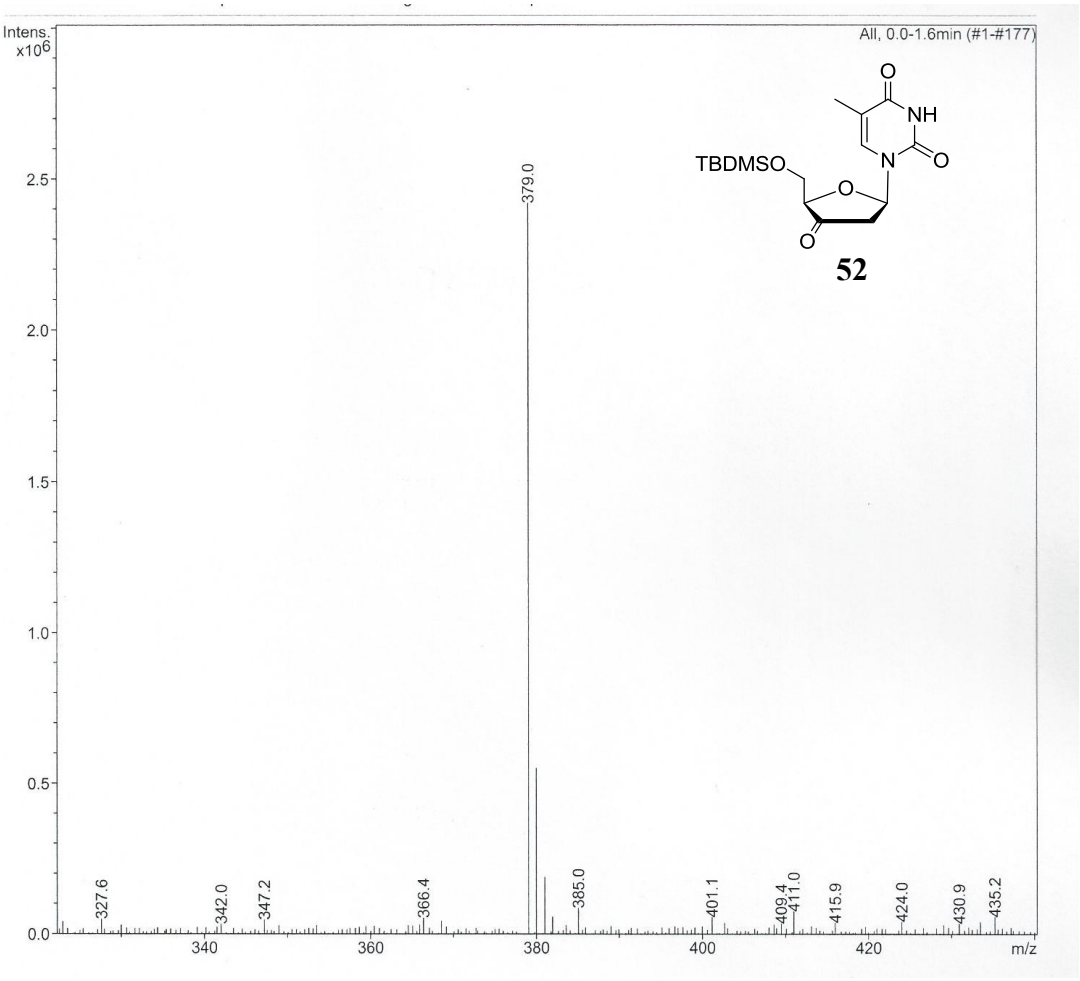

Figure 26: ESI-MS of Compound 52

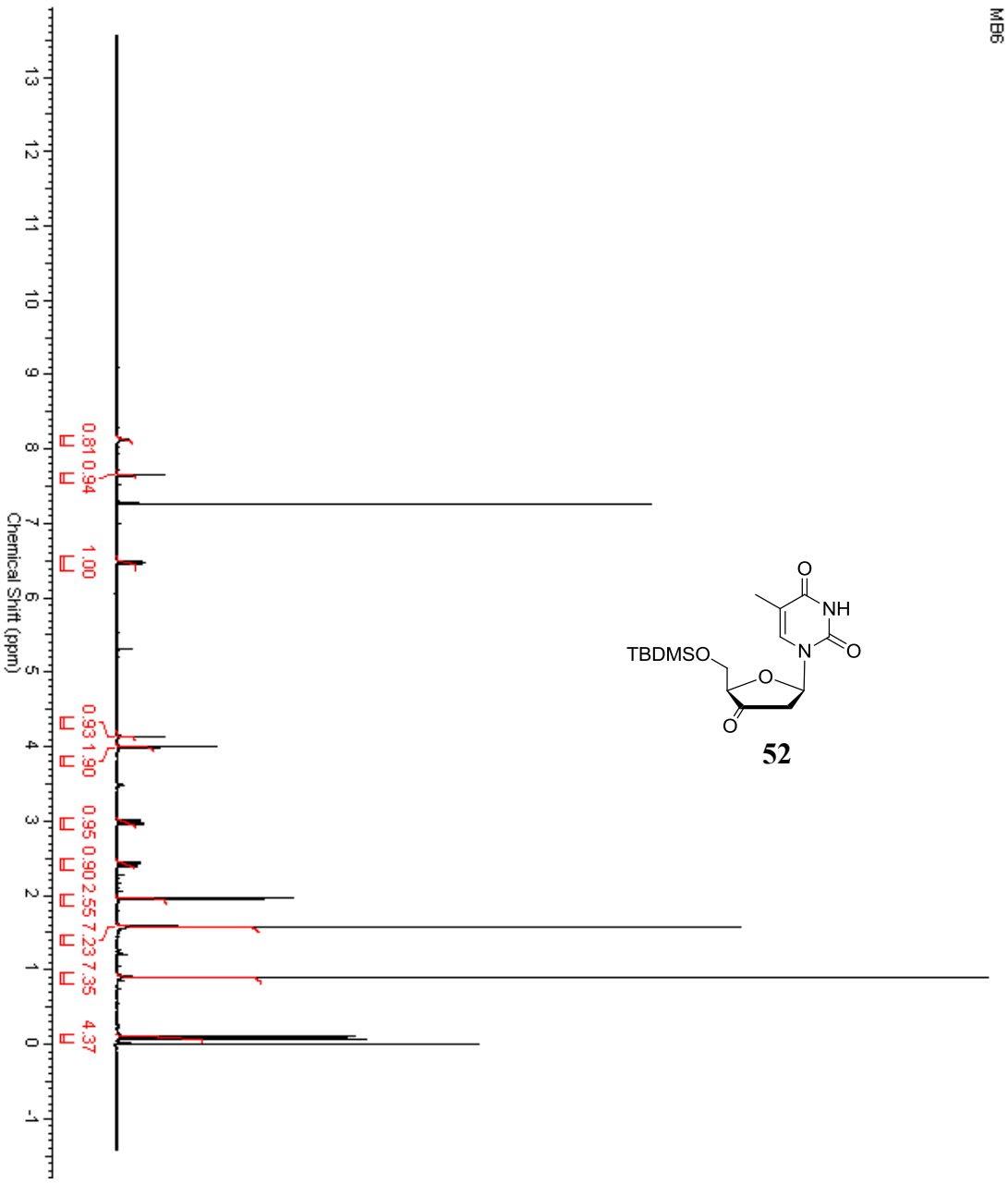

52

Figure 27: H-NMR of compound 52

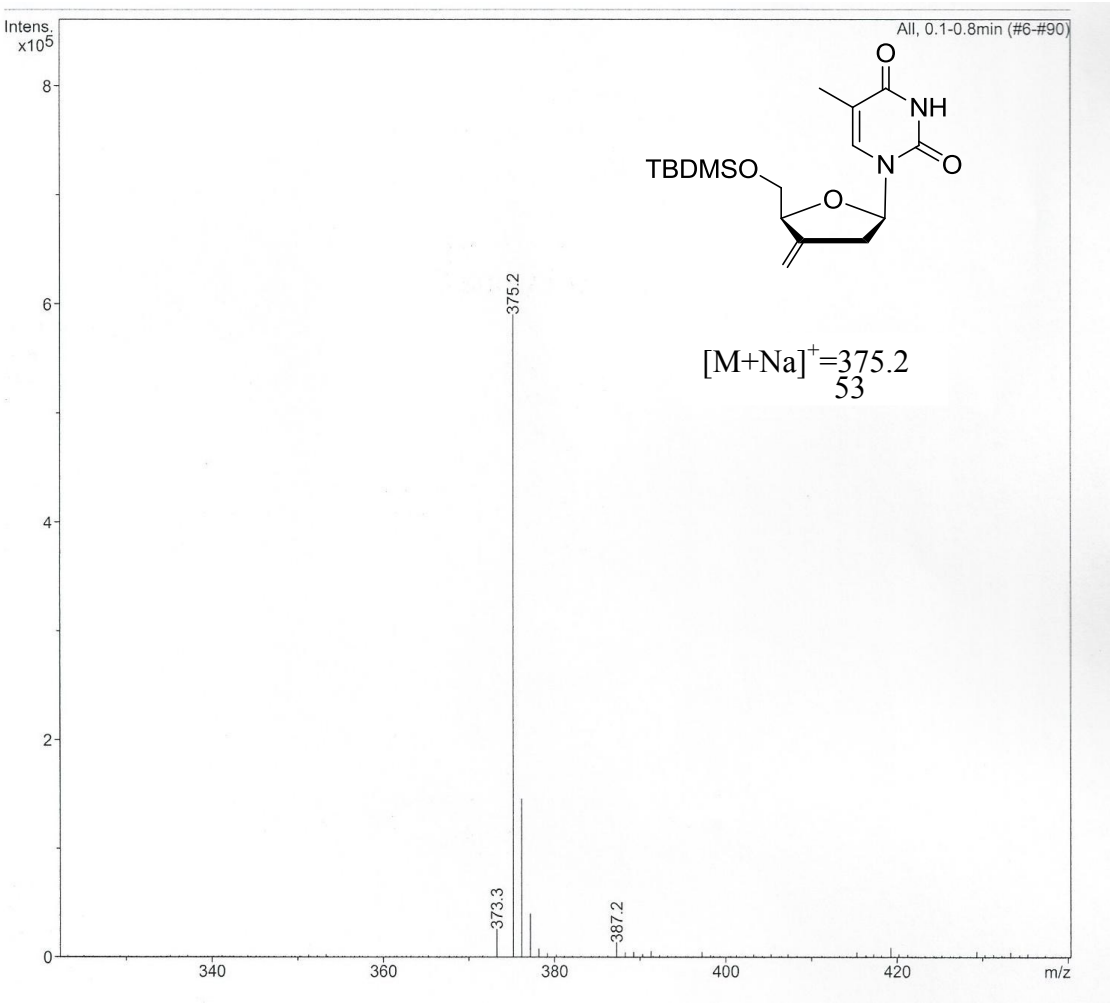

Figure 28: ESI-MS of compound 53

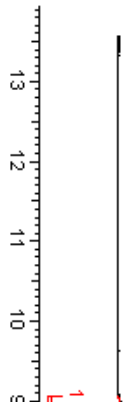

Figure 29: H-NMR of compound 53

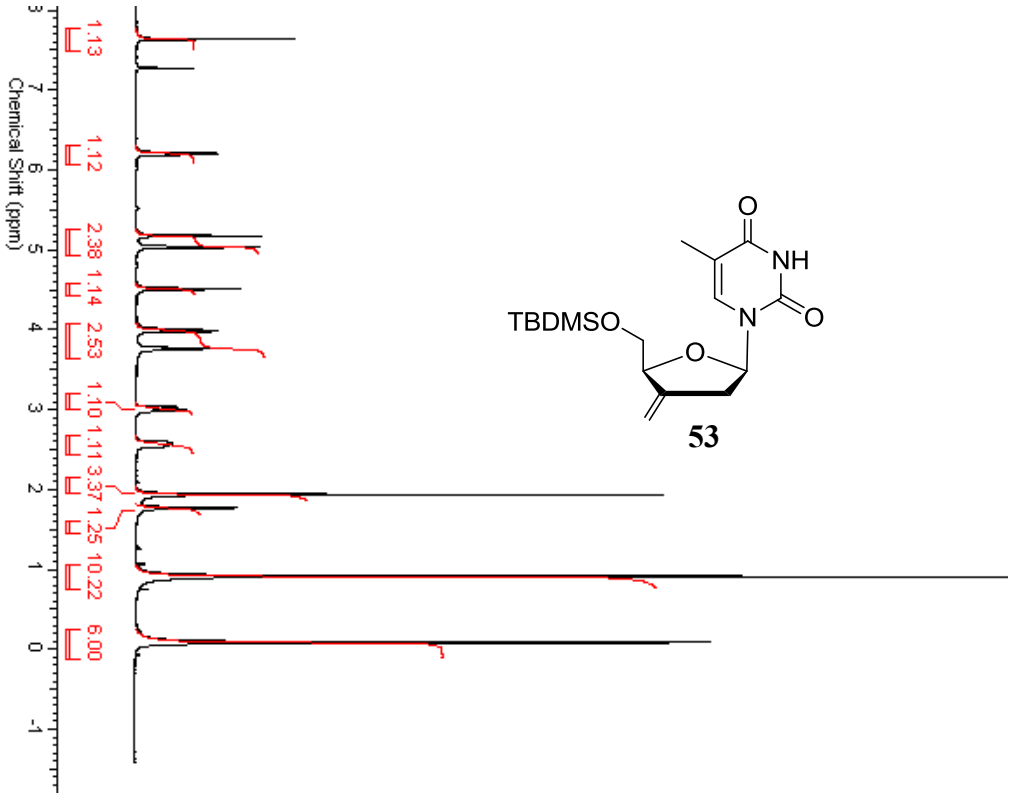

53

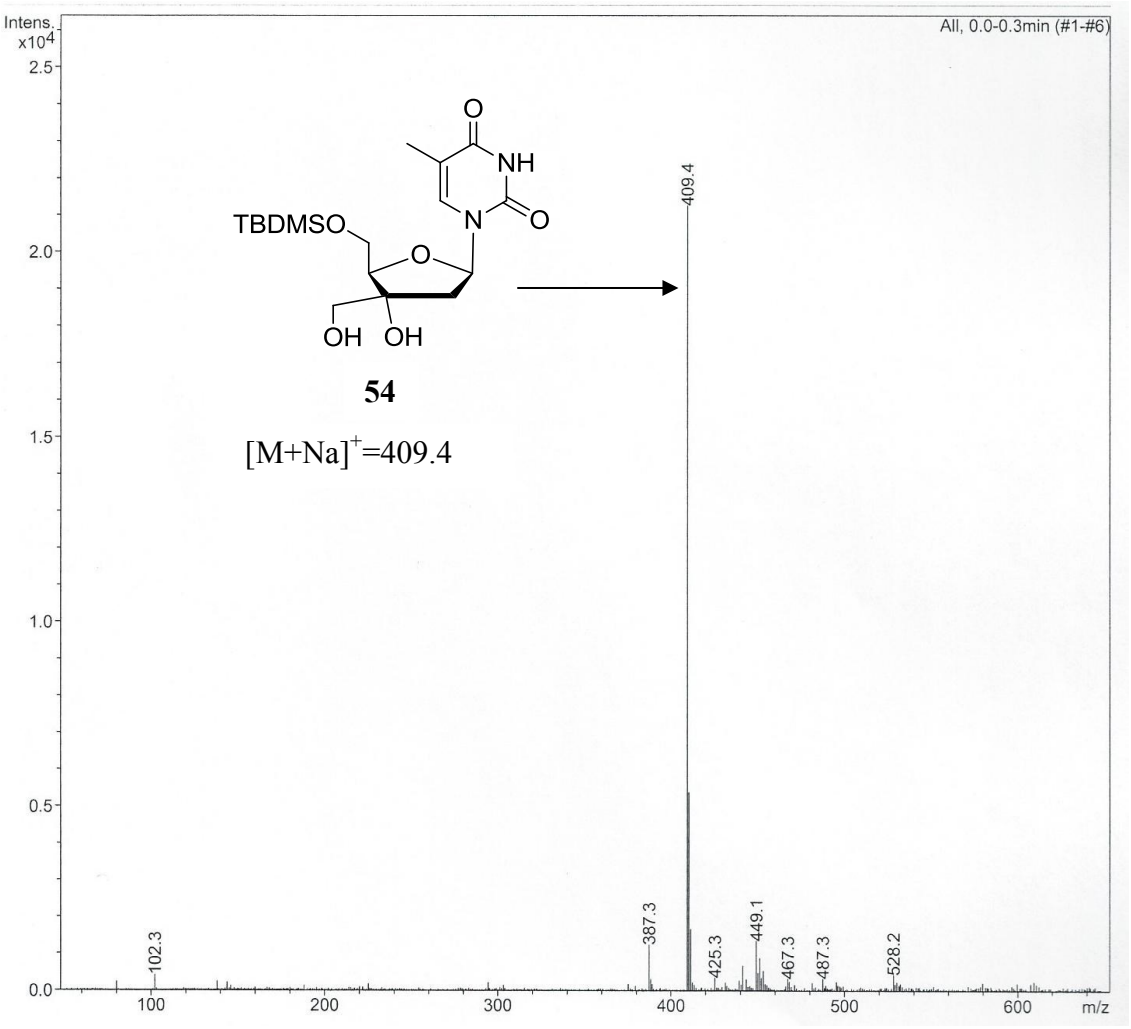

Figure 30: ESI-MS of compound 54

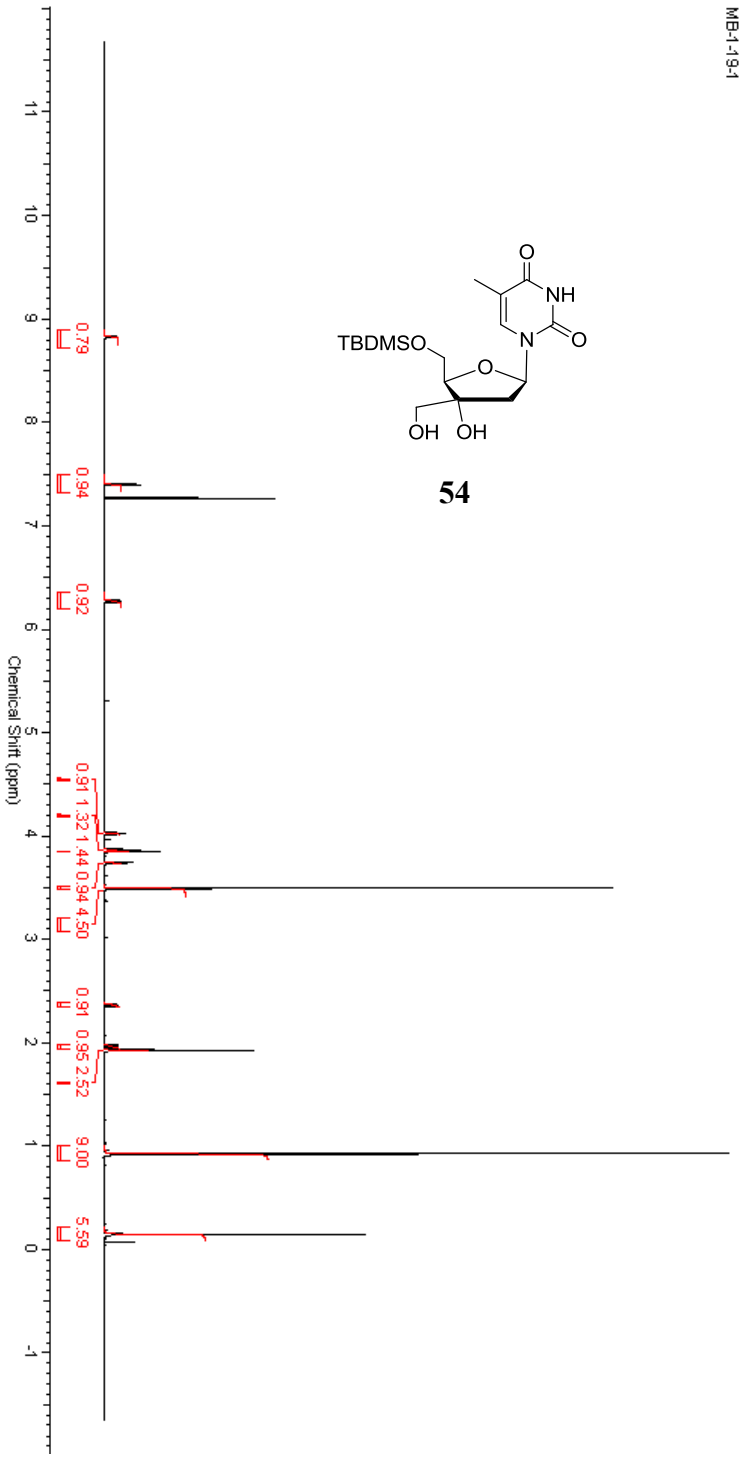

54

Figure 31: H-NMR of compound 54

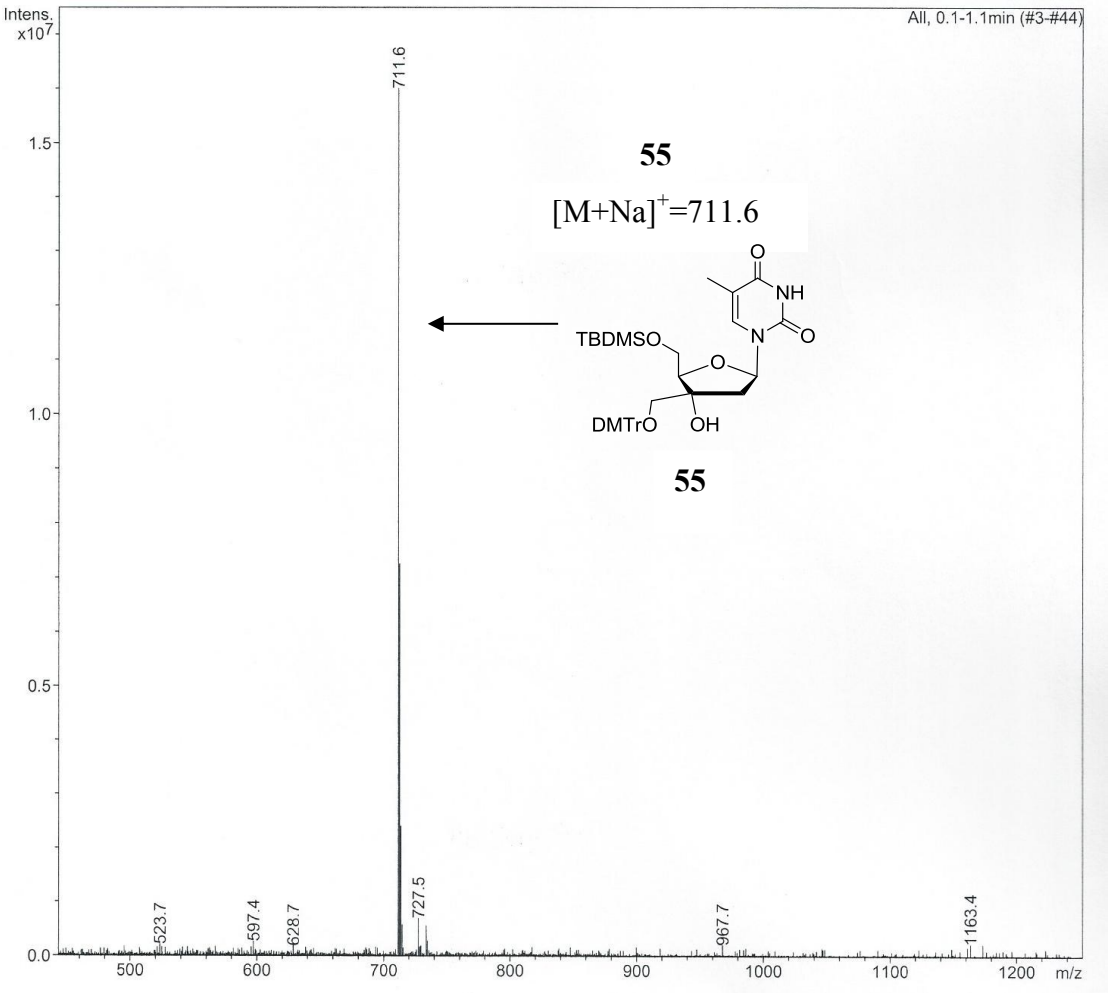

Figure 32: ESI-MS of compound 55

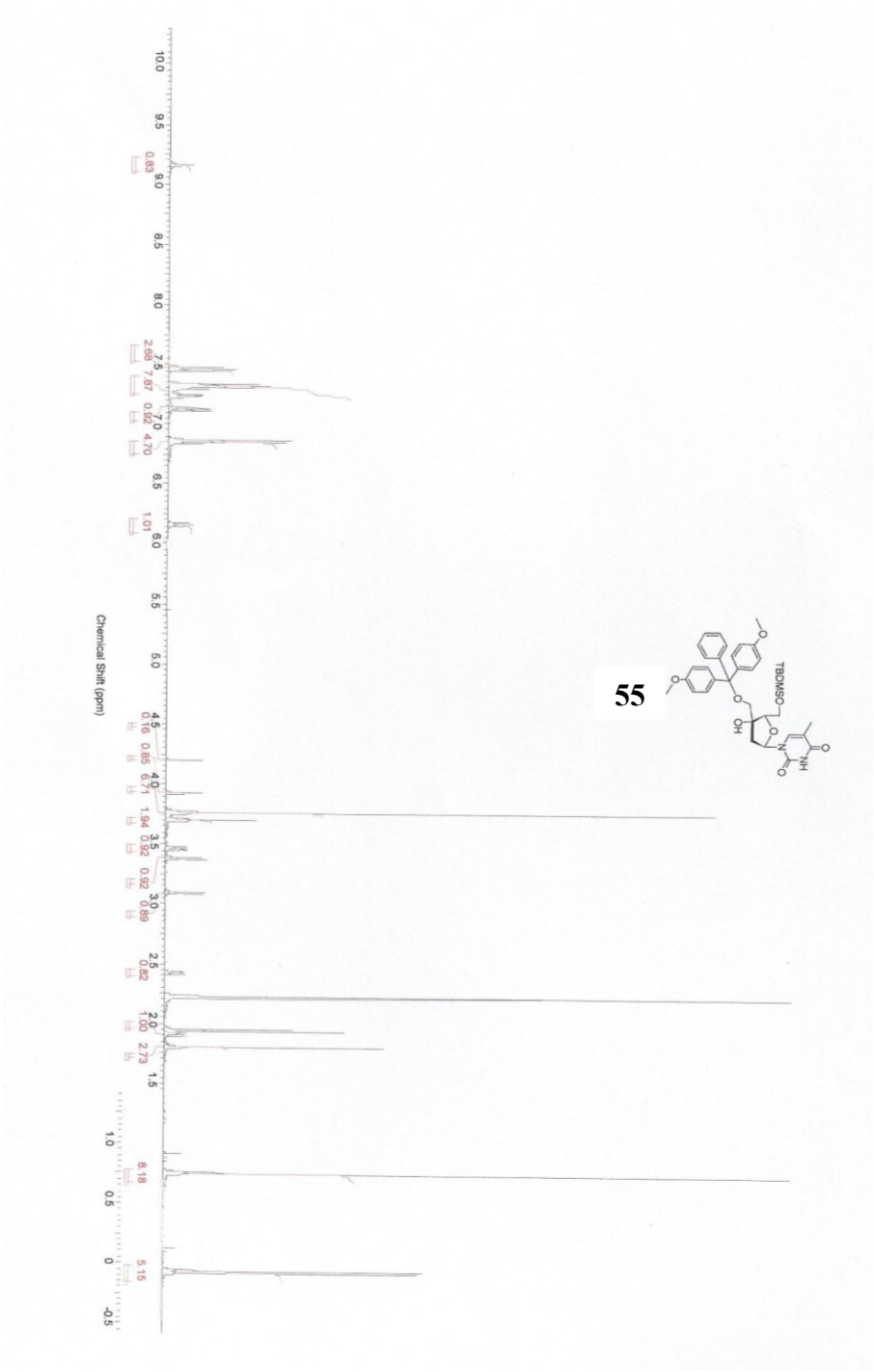

Figure 33: H-NMR of compound 55

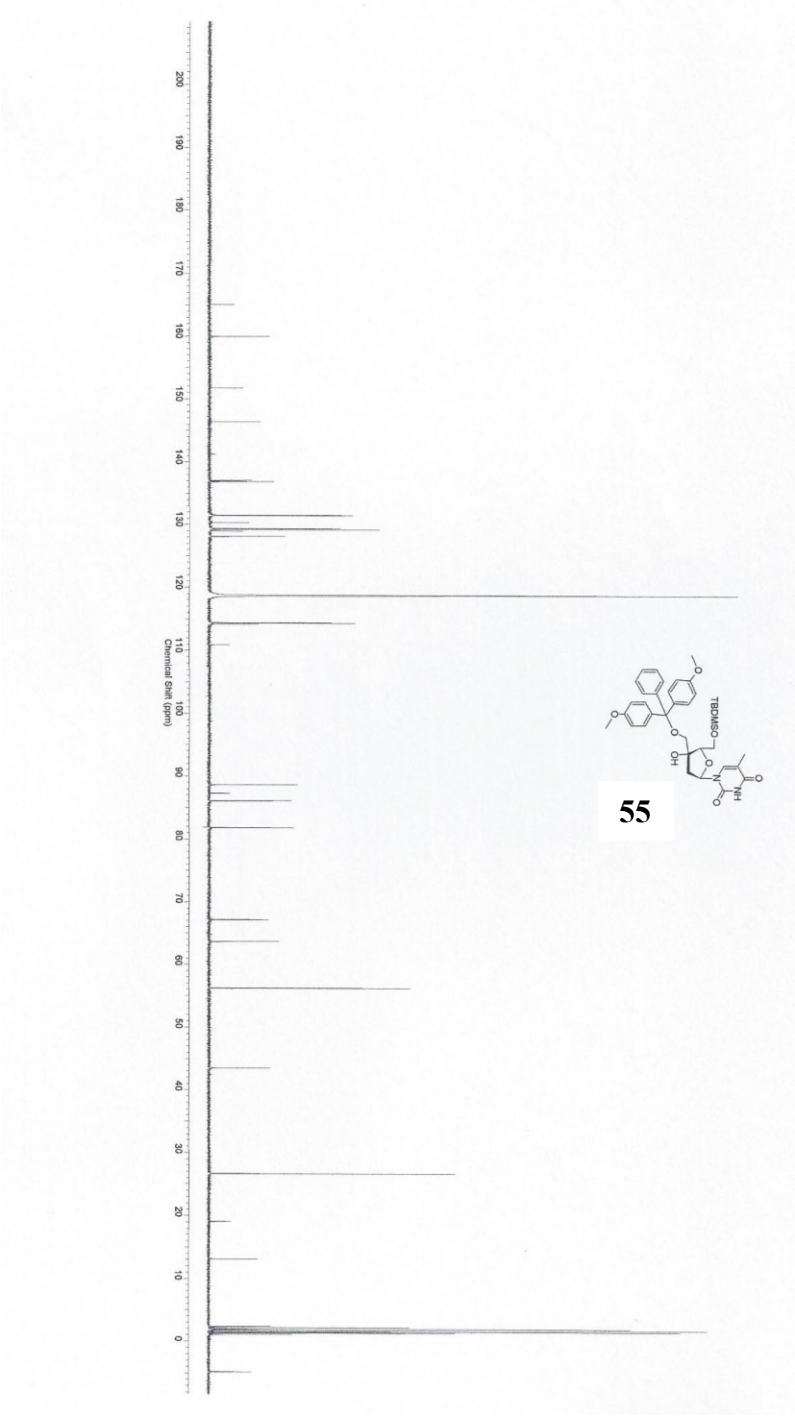

Figure 34: C-13 NMR of compound 55

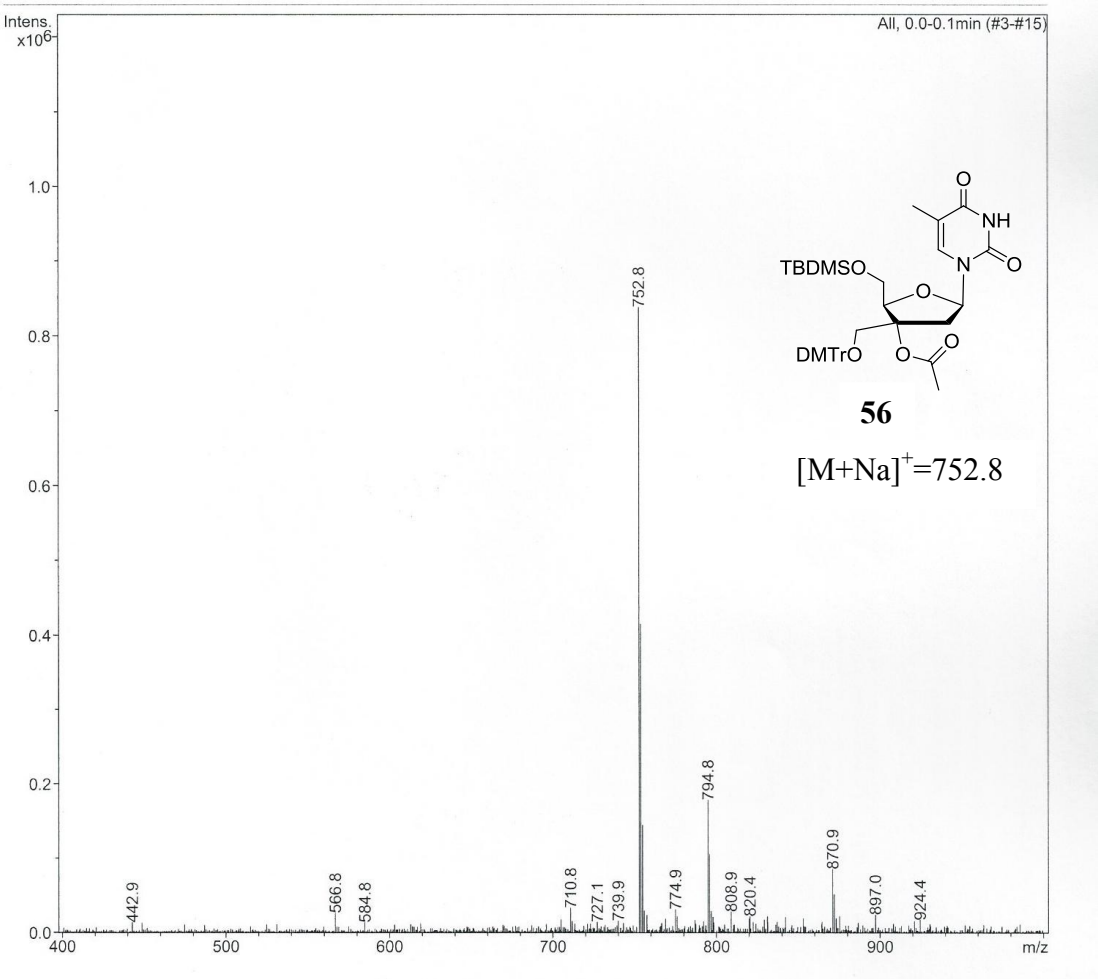

Figure 35: ESI-MS of compound 56

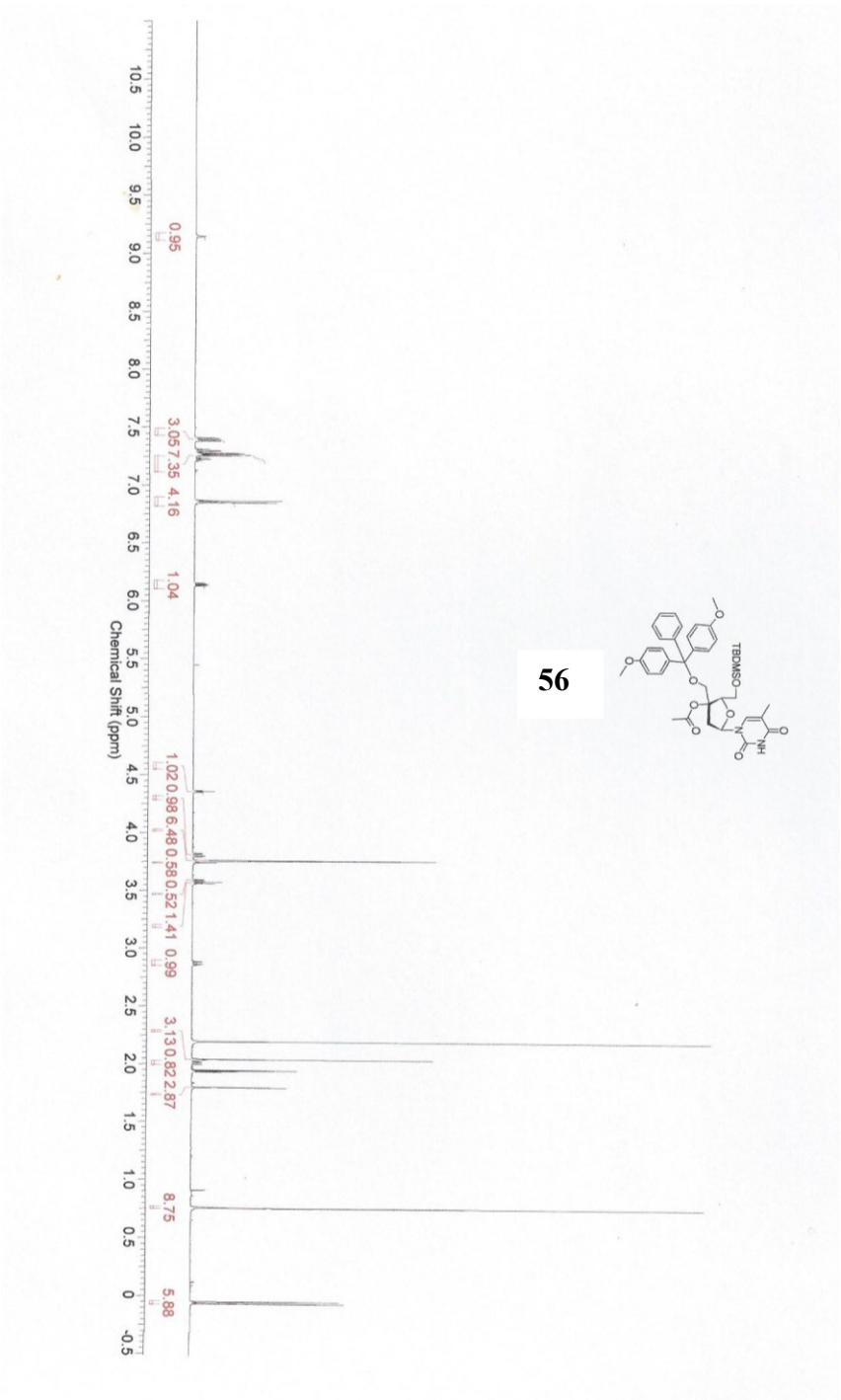

Figure 36: H-NMR of compound 56

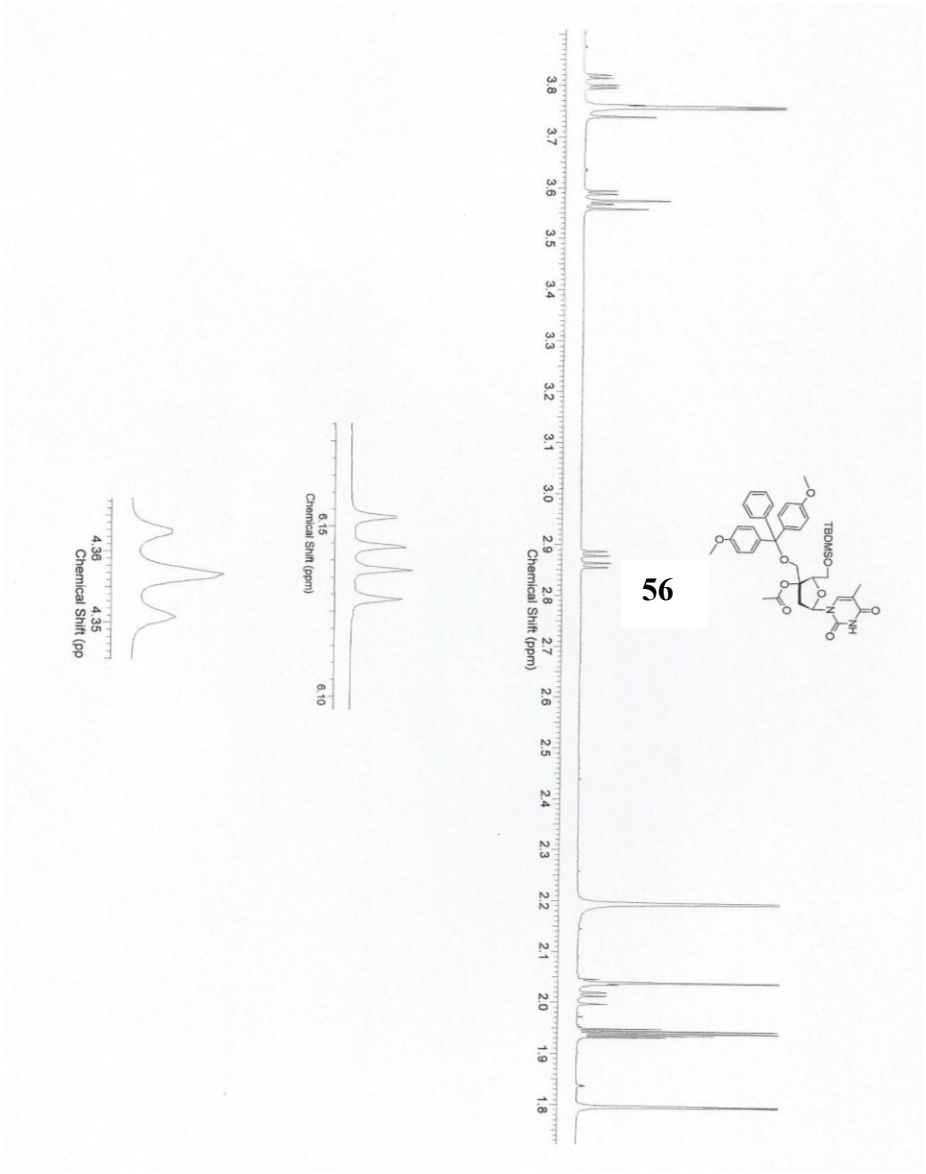

Figure 37: H-NMR of compound 56, expanded regions

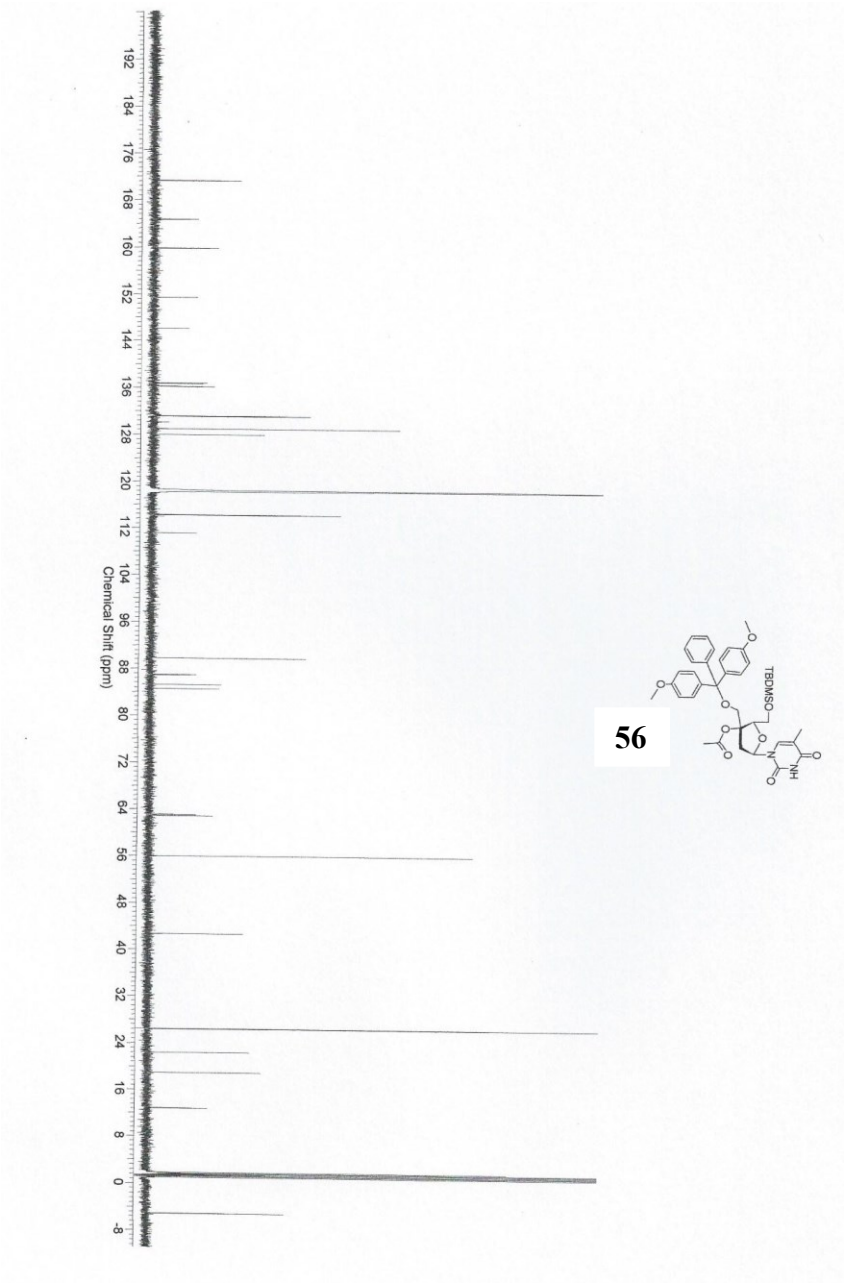

Figure 38: C-13 NMR of compound 56

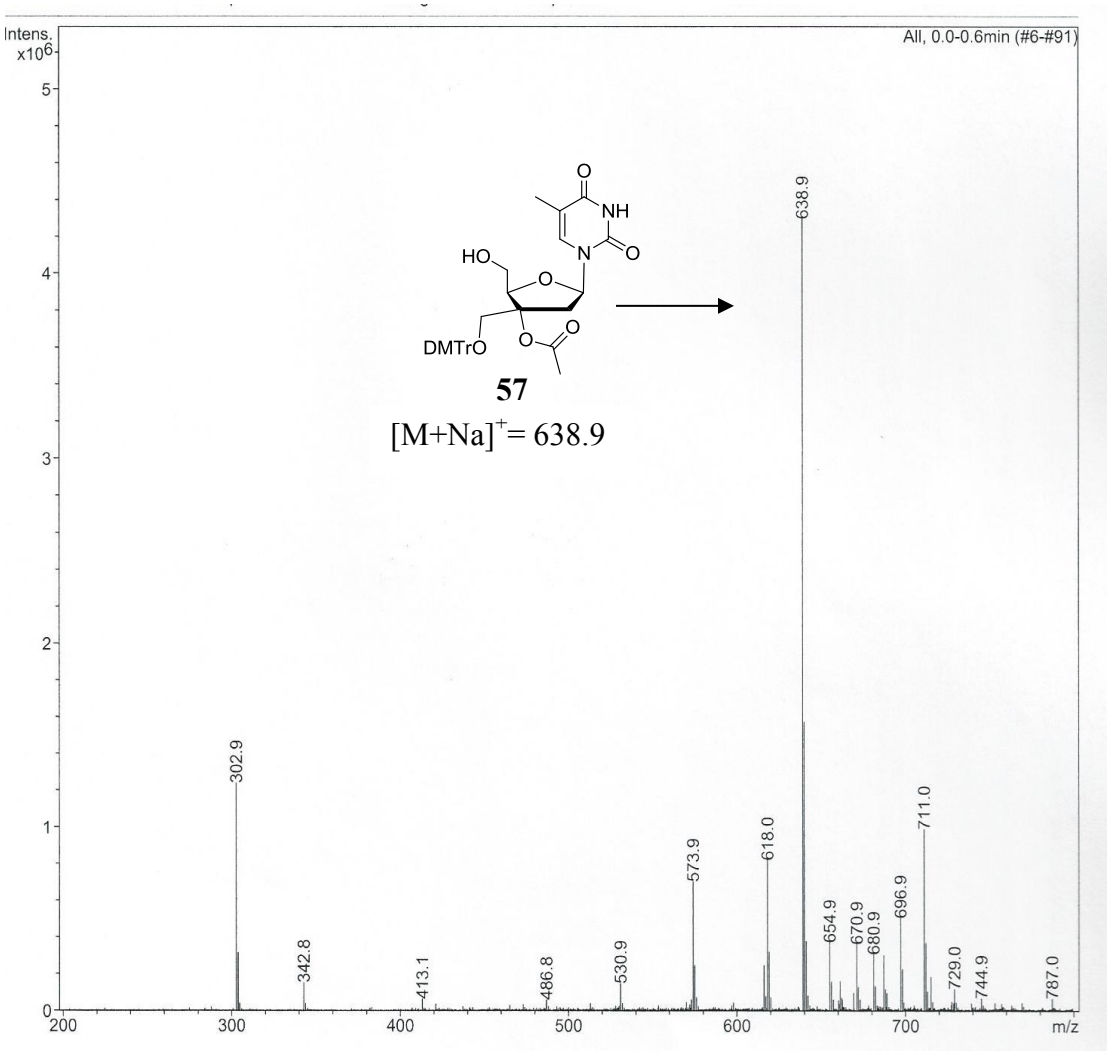

57

$[M+Na]^+ = 638.9$

Figure 39: ESI-MS of compound 57

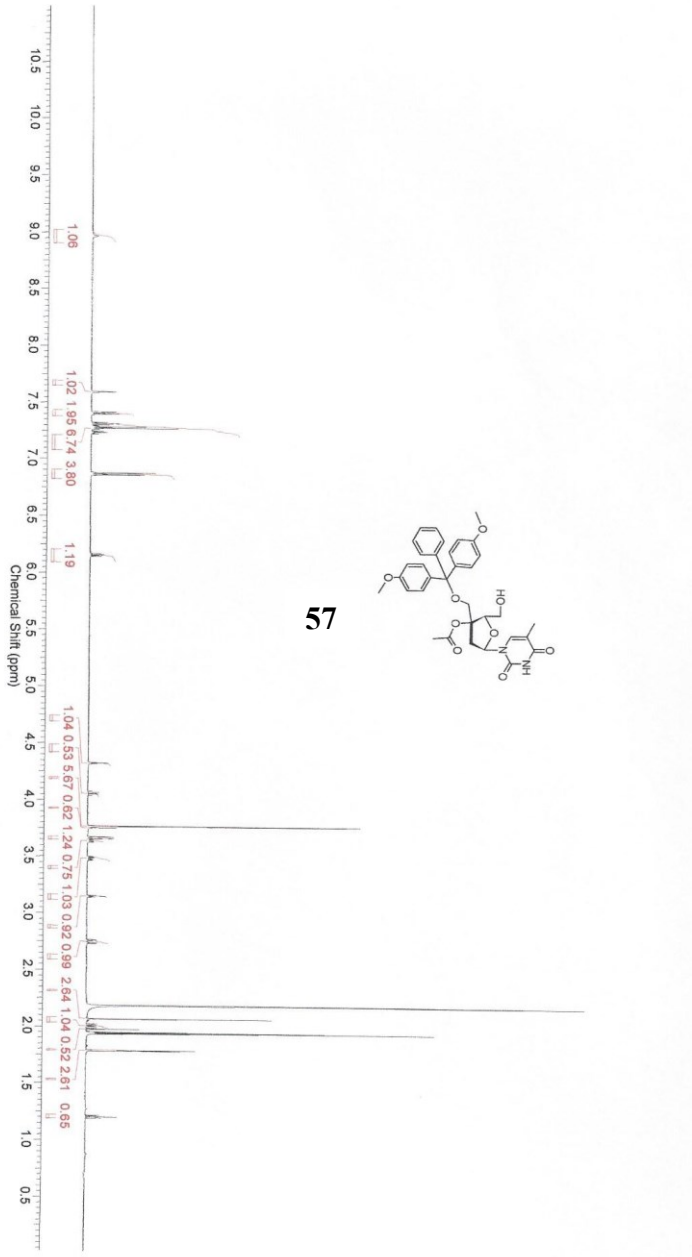

57

Figure 40: H-NMR of compound 57

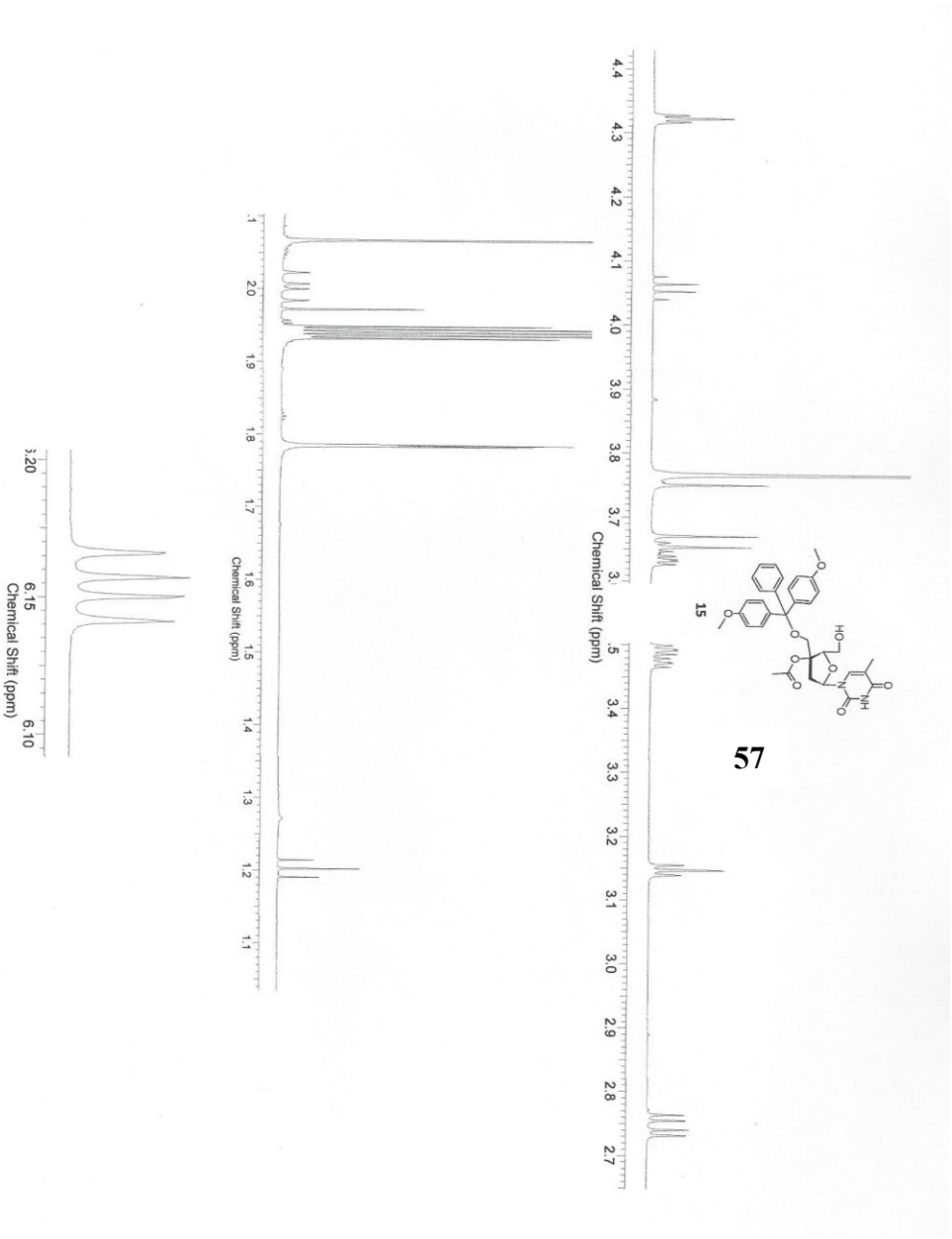

Figure 41: H-NMR of compound 57, expanded regions

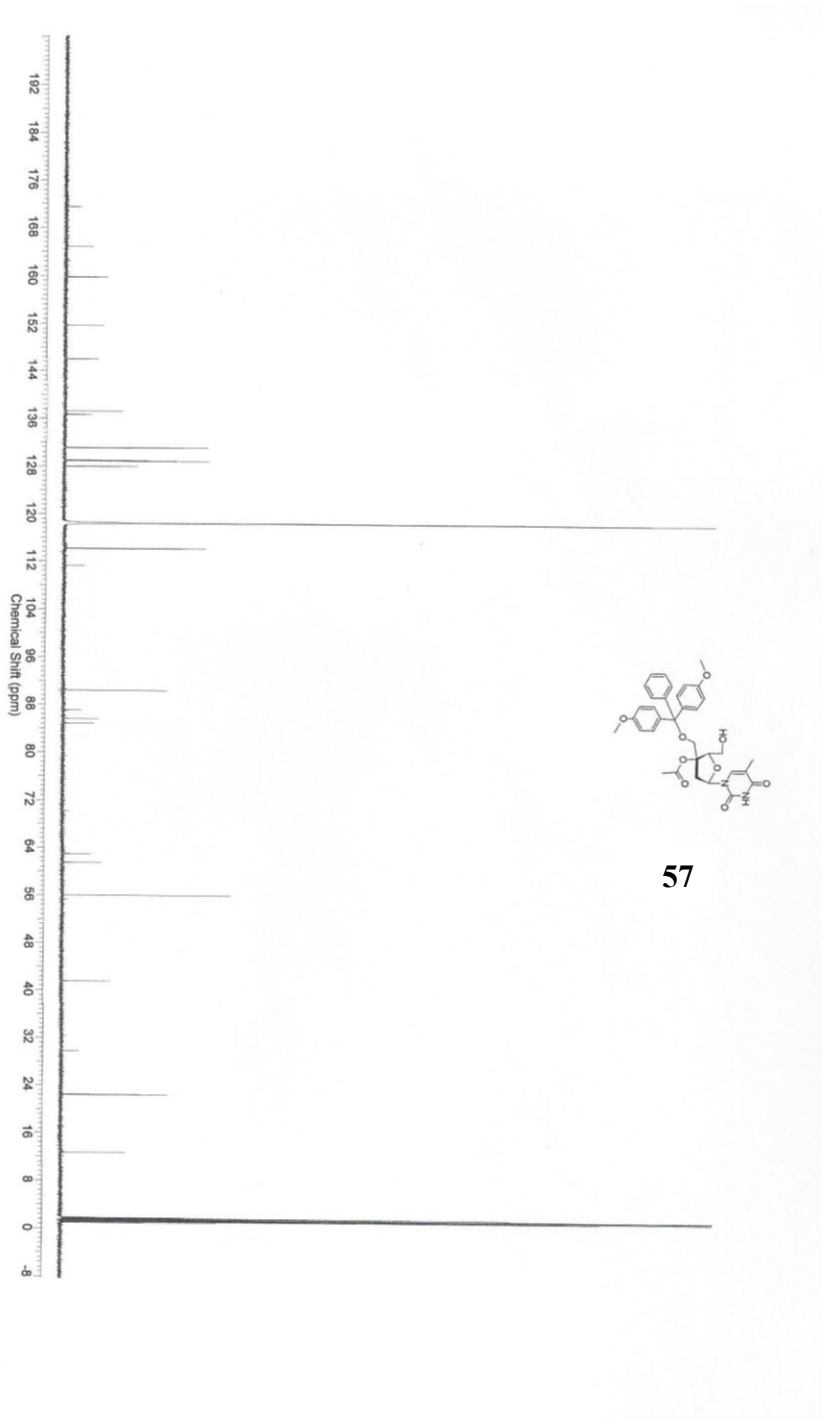

57

Figure 42: C-13 NMR of compound 57

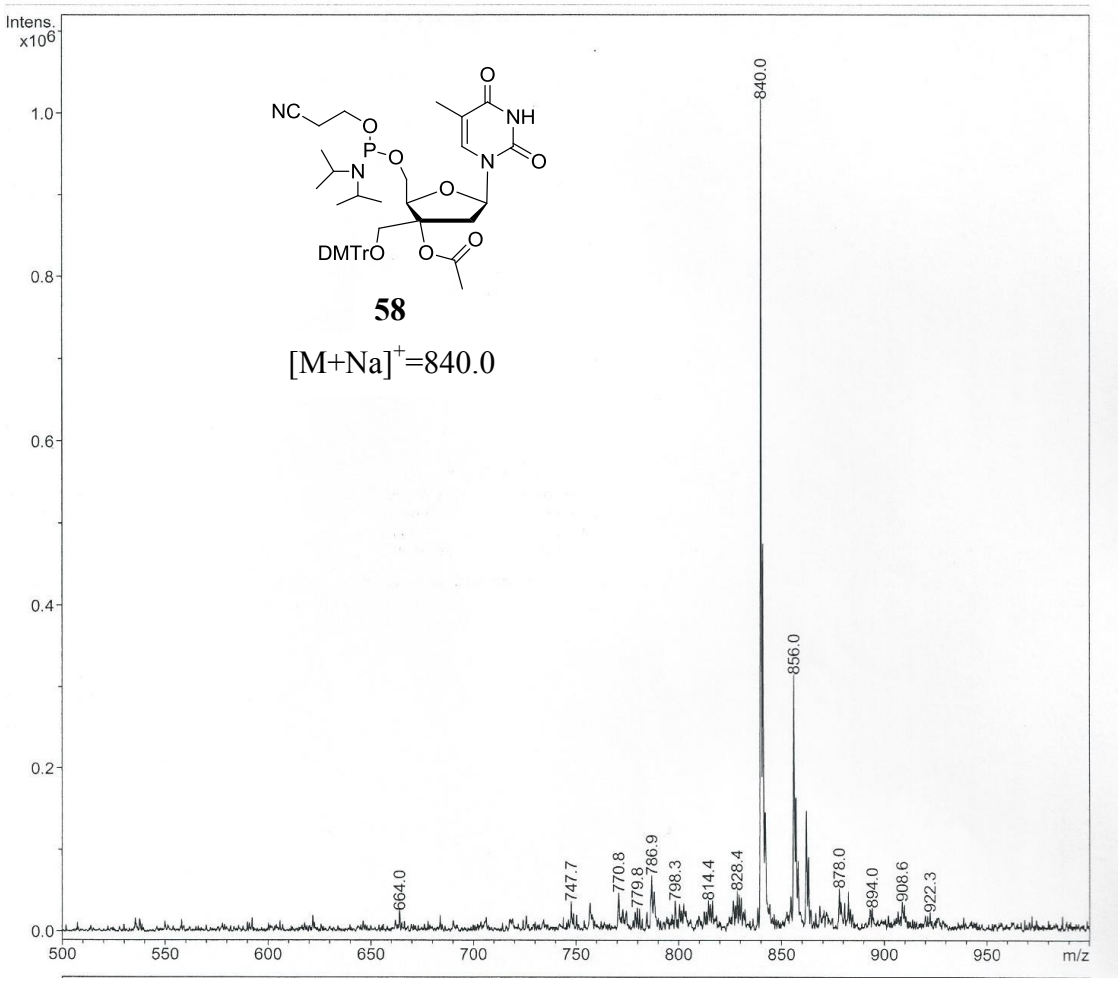

Figure 43: ESI-MS of compound 58

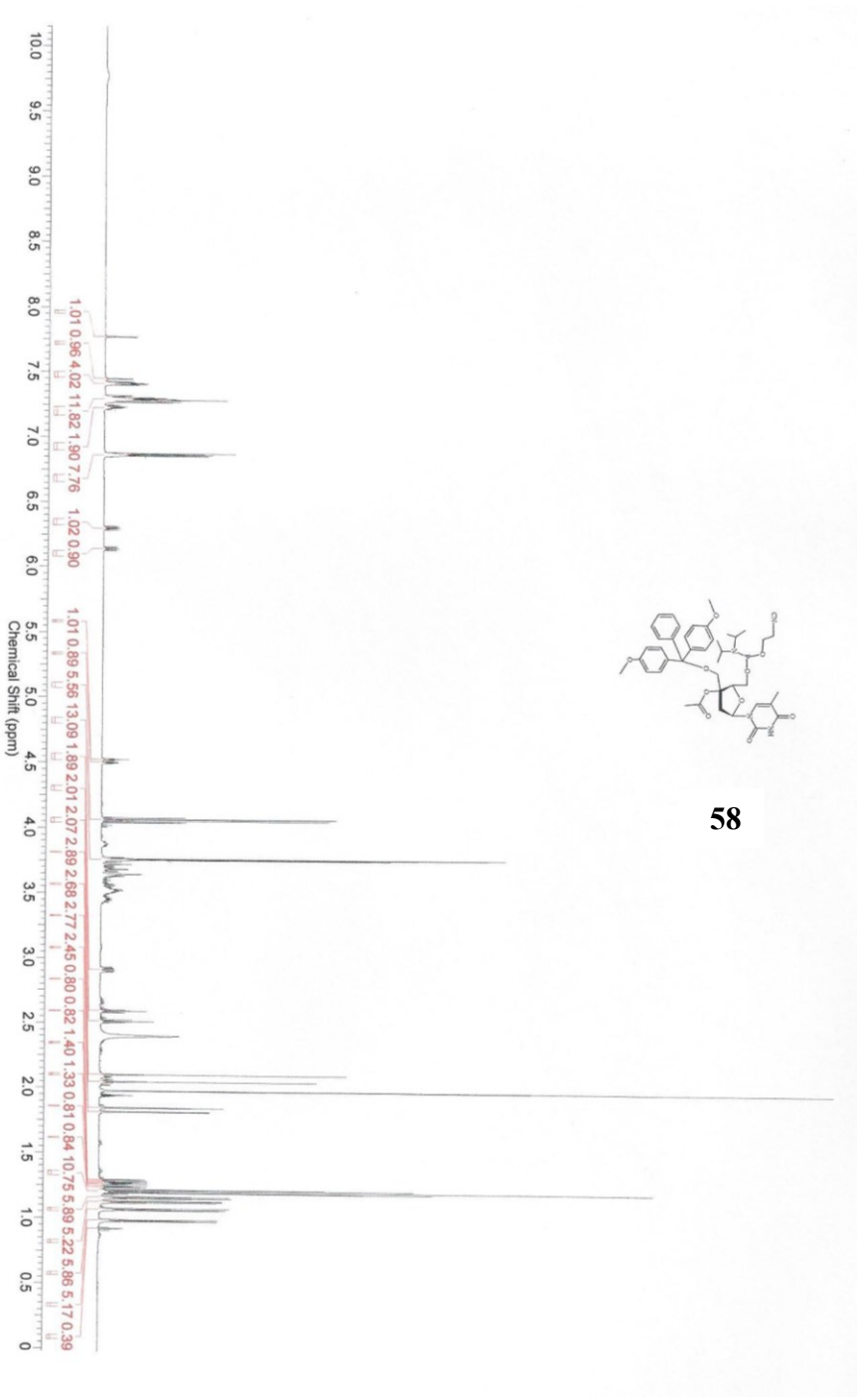

Figure 44: H-NMR of compound 58

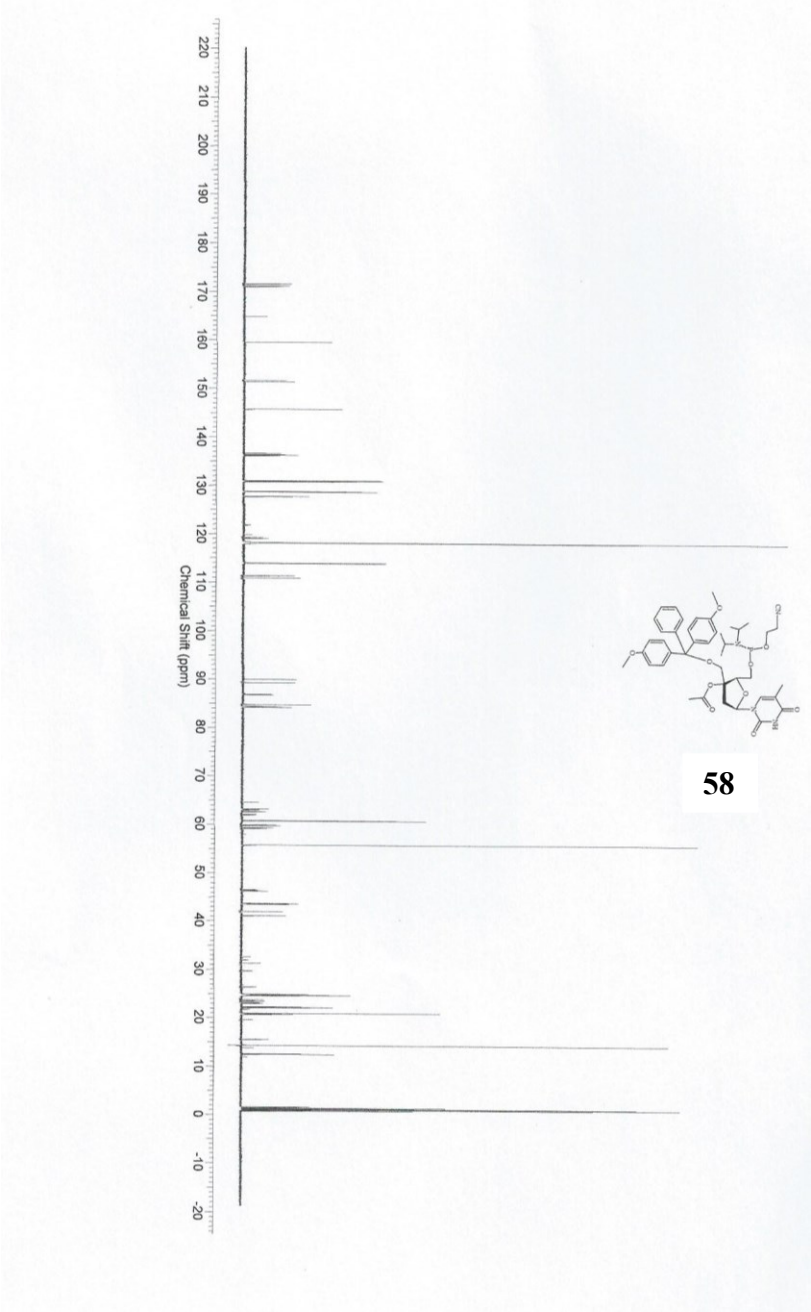

Figure 45: C-13 NMR of compound 58

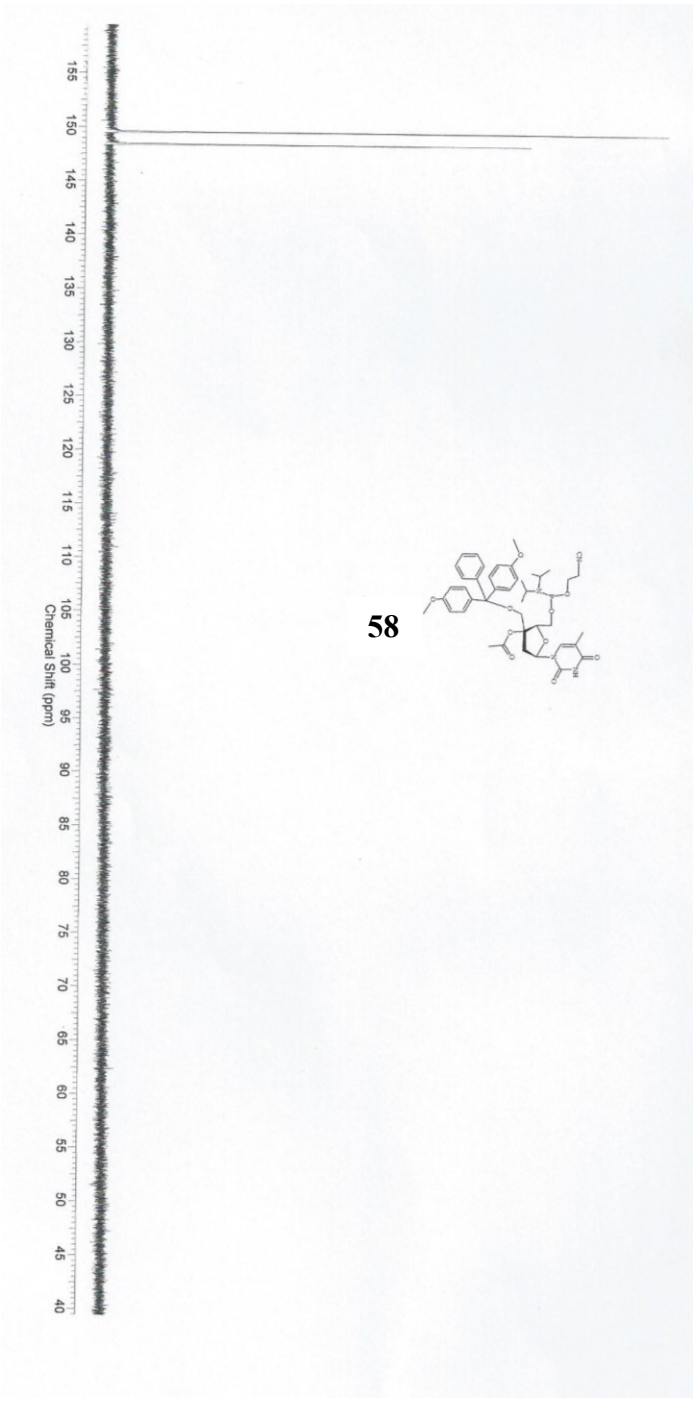

58

Figure 46: Phosphorus NMR of compound 58